Towards extending the luminescence dating range of quartz: exploring the 375 °C quartz TL peak

Dissertation

der Mathematisch-Naturwissenschaftlichen Fakultät

der Eberhard Karls Universität Tübingen

zur Erlangung des Grades eines

Doktors der Naturwissenschaften

(Dr. rer. nat.)

vorgelegt von

Neda Rahimzadeh

aus Babolsar, Iran

Tübingen

2023

Gedruckt mit Genehmigung der Mathematisch-Naturwissenschaftlichen
Fakultät der Eberhard Karls Universität Tübingen.

Tag der mündlichen Qualifikation:	17.07.2024
Dekan:	Prof. Dr. Thilo Stehle
1. Berichterstatterin:	Prof. Dr. Sumiko Tsukamoto
2. Berichterstatterin:	Prof. Dr. Kathryn Fitzsimmons

Abstract

Optically stimulated luminescence (OSL) dating of quartz is widely used to establish an absolute chronology for Quaternary sedimentary deposits. However, its applicability is in general limited to the last ~ 100-150 ka. Therefore extending the range of quartz luminescence dating beyond this limitation is a key challenge. In the quest for extending this limit, other luminescence signals from quartz have been proposed, among which violet stimulated luminescence (VSL) is a promising signal. It is based on the use of a violet stimulation (405 nm) to measure trap deeper than those accessible by blue light.

The overall objective of this thesis is to develop and test the applicability of VSL dating to extend the quartz dating range. Attempts to establish an optimised single aliquot regenerative dose (SAR) protocol for VSL dating on four coarse-grained quartz samples from the coastal environment of Sardinia have not all been successful. It is found that the range of the applicability of the SAR VSL protocol is dependent on the natural dose size; using the SAR method for VSL dating remains challenging for samples with large natural doses (i.e. ~250 Gy).

Subsequently, the multiple aliquot regenerative dose (MAR) protocol is, for the first time, tested on fine-grained quartz samples from a Chinese loess-palaeosol sequence in Luochuan with reference ages up to ~1400 ka. The natural VSL dose response curve (DRC) saturates at about 900 Gy, which would potentially allow dating at the Luochuan section using VSL up to ca. 300 ka. However, the application of the MAR protocol showed significant age underestimation for samples older than ~100 ka. This MAR VSL age underestimation can clearly be attributed to the different shapes of natural and laboratory DRCs; the natural signal progressively deviate from the laboratory signal beyond ~250 Gy. These observations are, however, contradicting the previous research in the same region, which showed

that the MAR DRC using coarse-grained quartz samples from the Luochuan section can reproduce the shape of the natural DRC. It can therefore be concluded that the grain size plays an important role in obtaining reliable ages. A direct comparison of fine- (4-11 μm) and coarse-grained (63-100 μm) quartz VSL data from nine samples from a loess section in southern Germany further confirm these observations. It is shown that there is a systematic tendency for the fine-grained VSL ages towards underestimation with increasing age. The fine-grained MAR DRC starts to deviate from the natural DRC at ~300 Gy and therefore tends to underestimate the reference ages beyond ~100 ka.

In addition to the VSL signal, the physical characteristics and applicability of the multiple aliquot methods (MAR and multiple aliquot additive dose (MAAD)) of the quartz isothermal thermoluminescence (ITL) signal measured at 330 °C (ITL_{330}) is systematically investigated by using nine fine-grained quartz samples from the Luochuan section. The natural ITL_{330} shows that the signal has a theoretical dating range up to ~800 Gy, equivalent to ~230 ka. The comparison of the natural and laboratory DRCs using MAR and MAAD protocols indicates that they start to diverge in shape beyond ~200 Gy, setting an upper limit for reliable ITL_{330} dating of ~70 ka. However, application of pulsed-irradiation (PI) for the MAAD protocol reveals that the shape of the natural DRC can mostly be reproduced with the PI-MAAD protocol and thus it can provide reliable ages up to natural saturation at ~230 ka.

Based on the observations summarised in this doctoral thesis it can be concluded that the natural VSL and ITL_{330} signals have an extended growth, and the main limitation is the deviation between natural and laboratory generated DRCs beyond a certain dose, which caused a progressive age underestimation. Application of pulsed irradiation increase the reproduction of the extended VSL and ITL_{330} natural growth. While further investigations will be needed, it appears that this method can be a promising step forward in our attempts to extend the quartz luminescence dating age range.

Zusammenfassung

Optisch stimulierte Lumineszenz (OSL) von Quarz ist eine häufig genutzte Datierungsmethode für die Erstellung absoluter Chronologien für quartäre Sedimentablagerungen. Die Anwendbarkeit dieser Methode ist jedoch im Allgemeinen auf die letzten ~100-150 ka beschränkt. Daher ist die Erweiterung der Datierungsgrenze der OSL-Datierung eine bedeutsame Herausforderung. In dem Bestreben, diese Grenze zu erweitern, wurden in dieser Arbeit weitere Lumineszenzsignale von Quarz herangezogen. Ein vielversprechendes Signal ist hierbei das violett stimulierte Lumineszenzsignal (VSL), das auf der Verwendung einer violetten Stimulation (405 nm) basiert. Hierbei werden Elektronenfallen erreicht, die tiefer liegen als diejenigen, die mit blauem Licht zugänglich sind.

Das übergeordnete Ziel dieser Arbeit ist es, eine allgemeine Anwendbarkeit der VSL-Datierung zu entwickeln und zu testen, mit dem Ziel, die Datierungsgrenze von Quarz zu erweitern. Die Versuche, ein optimiertes „single aliquot regenerative dose" (SAR)-Protokoll für die VSL-Datierung an vier grobkörnigen Quarzproben aus der Küstenumgebung Sardiniens zu erstellen, waren alle nicht erfolgreich. Es wurde festgestellt, dass der Anwendungsbereich des SAR VSL Protokolls von der Größe der natürlichen Dosis abhängt; die Anwendung eines SAR-Protokollsfür die VSL-Datierung bleibt eine Herausforderung für Proben mit natürlicher Dosis >250 Gy.

Darauf aufbauend wurde ein MAR-Protokoll (multiple aliquot regenerative dose) erstmals an feinkörnigen Quarzproben aus einer Löss-Paläosol-Sequenz in Luochuan, China, mit Referenzaltern bis ~1400 ka getestet. Die natürliche VSL-

dose response curve (DRC) sättigt bei ca. 900 Gy, was theoretisch eine Datierung in Luochuan mit VSL bis ca. 300 ka ermöglichen würde. Die Anwendung des MAR-Protokolls ergab jedoch eine erhebliche Unterschätzung des Alters für Proben, die älter als ~100 ka sind. Diese Unterschätzung des MAR VSL-Alters kann eindeutig auf die unterschiedlichen Formen der natürlichen und der Labor-DRCs zurückgeführt werden; das natürliche Signal weicht jenseits von ~250 Gy zunehmend vom Laborsignal ab. Dieses Ergebnis steht jedoch im Widerspruch zu früheren Untersuchungen in derselben Region, die gezeigt haben, dass die MAR-DRC bei grobkörnigen Quarzproben die Form der natürlichen DRC reproduzieren kann. Diese Beobachtung lässt den Schluss zu, dass die Korngröße eine wichtige Rolle bei der Ermittlung zuverlässiger Altersangaben spielt. Eine direkte Vergleichsstudie an neun fein- (4-11 μm) und grobkörnigen (63-100 μm) Quarzproben aus einem Lössabschnitt in Süddeutschland bestätigt diese Beobachtungen. Es wird gezeigt, dass die feinkörnigen VSL-Alter bei zunehmendem Alter das tatsächliche Alter systematisch unterschätzen. Die feinkörnige MAR-DRC beginnt bei ~300 Gy von der natürlichen DRC abzuweichen und neigt daher dazu, die Referenzalter über ~100 ka hinaus zu unterschätzen.

Zusätzlich zum VSL-Signal wurden die physikalischen Eigenschaften und die Anwendbarkeit der Multiple-Aliquot-Methoden (MAR und Multiple-Aliquot-Additive-Dose (MAAD)) des bei 330 °C an Quarz gemessenem -isothermalen Thermolumineszenz (ITL)-Signals (ITL_{330}) anhand von neun feinkörnigen Quarzproben aus einem Profil in Luochuan systematisch untersucht. Das natürliche ITL_{330}-Signal hat einen theoretischen Datierungsbereich bis zu ~800 Gy, was ~230 ka entspricht. Der Vergleich der natürlichen und Labor-DRCs unter Verwendung von MAR- und MAAD-Protokollen zeigt, dass sie jenseits von ~200 Gy zu divergieren beginnen, was zu einer oberen Anwendbarkeitsgrenze für eine zuverlässige ITL_{330}-Datierung von ~70 ka führt. Die Anwendung der gepulsten Bestrahlung (PI) für das MAAD-Protokoll zeigt jedoch, dass die Form der natürlichen DRC mit dem PI-MAAD-Protokoll größtenteils reproduziert werden kann und somit zuverlässige Altersangaben bis zur natürlichen Sättigung bei ~230 ka möglich sind.

Die in dieser Arbeit durchgeführten Untersuchungen zeigen, dass die natürlichen VSL- und ITL_{330}-Signale ein höheres Wachstum aufweisen. Die größte Einschränkung liegt jedoch in der Abweichung zwischen den natürlichen und im Labor erzeugten DRCs nach einer bestimmten Dosis, wodurch die Altersunterbestimmung mit steigender Dosis zunimmt. Die Anwendung der gepulsten Bestrahlung scheint jedoch ein vielversprechender Ansatz zu sein, um das natürliche Wachstum von VSL und ITL_{330} zu reproduzieren. Obwohl weitere Untersuchungen erforderlich sind, deutet diese Methode auf einen vielversprechenden Fortschritt hin, um den Altersbereich der Quarzlumineszenzdatierung zu erweitern.

Acknowledgments

Here I would like to thank everyone who has been part of this journey, making the travel enjoyable and the end achievable.

First of all, I would like to thank my main supervisor Prof. Dr. Sumiko Tsukamoto for her encouragement, scientific insights, and academic advice. Sumiko, your supervision began long before the start of this PhD journey, from the very first sequence I have measured in my life. I consider myself incredibly fortunate to have had you as my supervisor, always available with insightful answers and brilliant ideas to address any challenges that arose.

I would also like to thank Prof. Dr. Manfred Frechen for warmly welcoming me to the luminescence laboratory of LIAG in 2017, and later offering me the great opportunity to pursue my PhD research in Germany. Manfred, your support and encouragement instilled in me the confidence I needed as a young researcher. Looking back after several years, I am grateful for your guidance and for pushing me close to, and sometimes even beyond, my personal limits.

I am very grateful to Dr. Christine Thiel for initiating the junior research group "Middle Pleistocene Surface Processes" at LIAG, which gave me the great opportunity to contribute to this excellent project. Furthermore, I'd like to thank Christine for generously sharing her time and knowledge, her constant support, and her help in structuring my thoughts.

I am very grateful to Dr. Junjie Zhang for always being available whenever and wherever I encountered challenges in my work, and never got tired of answering my questions, which never seemed to end.

Special thanks are also extended to my thesis committee members, Prof. Dr. Kathryn Fitzsimmons, and Prof. Dr. Thomas Scholten for their constructive comments and for dedicating their time to thoroughly review the dissertation.

Dr. Hao Long and his colleagues in China are sincerely thanked for their invaluable assistance during the fieldwork and sample collection in China, as well as for their support in shipping the samples to Germany.

I am grateful to the whole team of Section 3 at the LIAG for their generous help not only in my research but also in daily life since the day I arrived in Germany. I received immense support from Sonja Riemenschneider, Sabine Mogwitz, Gudrun Drewes, Petra Posimowski, Dr. Astrid Techmer, Frank Oppermann, and Karsten Vollmer. A special thanks to Sabine for all the time spent in the lab, instructing and checking on me, and Sonja for her generous help from her international office!

I want to mention particularly my officemates Gwynlyn Buchanan (Gwyn), Valentina Argante, Junjie Zhang, Marcus Richter, and Erick Giovanni Prince Gutierrez (office mate for a few months per year but always a pleasure), who share not only the office space with me but also their friendship and knowledge. Together, you all made Room A48 a joyful place for me. A special thanks to Gwyn, my PhD twin, so happy to have landed on this adventure with you.

A heartfelt thank you goes out to my family for their unwavering support over the years and for always believing in me. And last but certainly not least, there is Navid, who has been by my side through both the peaks and valleys of this journey. Thank you for your love and for being my best friend.

Statement of collaborative work

The candidate's contributions along with those of the co-authors are outlined at the onset of each chapter. These contributions are categorised under Conceptualization, Investigation, Visualization, Formal analysis, Writing (original draft), and Writing (review and editing). These categories are customised to align with the unique research focus of each chapter. Within each category, authors are listed in accordance with their relative contribution to the assigned task.

Table of Contents

List of Figures

List of Tables

CHAPTER 1

Introduction

1.1 The Quaternary record and the importance of reliable chronology

The Quaternary period is the most recent geological time period (the last 2.6 Ma of Earth history), which is characterised by repeated glacial and interglacial cycles. During this period, the Earth's climate has gone through significant fluctuation. During the relatively long cold periods (i.e. glacial stages), temperature reduction and precipitation increase lead to expansion of continental ice sheets. These glacial stages alternated with shorter episodes during which the temperatures in the mid- and high altitude regions were similar to (or even higher than) those of present the day (i.e. interglacial stages). The last interglacial-glacial cycle (~120-11.5 ka) is of great importance for the Quaternary scientists because the full spectrum of glacial and interglacial, as well as shorter climatic fluctuations (i.e. stadials and interstadials), did happen during this period. In addition, considerable amount of palaeclimate proxies (e.g. oxygen isotope records, pollen) are available, which can offer a means of understanding past environmental changes and also predicting future climatically-driven land surface changes.

These climatic oscillations between glacial and interglacial conditions have produced important geological archives, such as ice cores (e.g. Kawamura et al., 2007), deep sea sediments (e.g. Lisiecki and Raymo, 2005) and terrestrial sediments, such as loess (e.g. Heller and Liu, 1982) that can provide valuable information on the environmental conditions at a specific time. While ice and marine cores, which are the most continuous Quaternary records, establish a general chronological framework of climate change at the global scale, terrestrial sediments, which are less continuous, reflect climate change and palaeoenvironmental conditions on regional and local scales. To establish a framework for regional or supra-regional correlation, integrate with the astronomically tuned oceanic $\delta^{18}O$ record, and subsequently reconstruct the Quaternary climate change, an accurate and reliable chronology of terrestrial archives is essential.

There is a wide variety of different dating methods available to quantitatively and qualitatively estimate the age of the Quaternary deposits. These dating techniques have their advantages and limitations, related to the physics principles on which these methods are based, and/or the datable materials. For example, radiocarbon dating, which is widely used in Quaternary research, is mostly limited to last ~50 ka, and only applicable to suitable not-reworked organic material (e.g. peat, wood or shells). Other dating methods such as Ar-Ar and K-Ar require the

presence of minerals (e.g. sanidine, anorthoclase, plagioclase, and biotite) derived from volcanic material found within tephra layers intercalated in the sediments.

1.2 Luminescence dating

Over the past few decades, optically stimulated luminescence (OSL) dating has been successfully applied widely to different terrestrial sedimentary sequences (e.g. aeolian: Roberts, 2008; Shallow marine: Jacob, 2008; fluvial: Rittenour, 2008; glacial: Lüthgens et al., 2010). This method enables the determination of the time elapsed since the last exposure of mineral grains to sunlight, i.e. the deposition age (Aitken, 1998), and has the potential to provide numerical ages from a few years to, theoretically, several hundred thousand years (e.g. Rhodes, 2011; Murray et al., 2021), far beyond the upper limit of radiocarbon dating. Furthermore, the main material used for OSL dating is quartz and feldspar, which are dominant in the most geological settings. Therefore, OSL dating is a powerful chronological tool for establishing an accurate and reliable chronological constraint.

The quartz OSL signal presents some advantages over the feldspar infrared stimulated luminescence (IRSL) signal, e.g. stable luminescence signal over time and faster bleachability under natural light conditions (Murray et al., 2012; Colarossi et al., 2015), which insure the full resetting of luminescence signal before the last burial event. However, the applicability of blue stimulated OSL, which is most commonly used for dating, is commonly limited to the last 100-150 ka (Wintle and Murray, 2006). In this thesis, other luminescence signals from quartz (i.e. violet stimulated luminescence (VSL) and isothermal thermoluminescence (ITL)) are thoroughly investigated and applied on the coastal and shallow marine sediments from Sardinia and loess sections from southern Germany and Chinese Loess Plateau with the aim to extend the upper age limit of quartz dating. Before discussing the aim of this thesis in more detail, we first introduce the basic principles of luminescence dating.

1.2.1 Principles of luminescence dating

The mechanism responsible for the luminescence process is best described by the energy level diagram for insulating solids (Aitken, 1998). During burial, surrounding radiation (mainly from natural radioactive nuclides of elements, such as ^{40}K, ^{232}Th, ^{238}U, and partly from cosmic radiation) will cause the excitation of electrons within the crystal lattices. The excited electrons will be lifted to higher energy levels (Conduction band; Fig. 1.1a) and producing a hole or electron vacancy. While most of the electrons will instantaneously drop back to a stable

level (i.e. valence band), some electrons will be trapped in crystal defects (traps) during their diffusion, leaving a hole due to the charge deficit called a recombination centre. In order to release the electrons from the traps, energy is required, with the amount of energy related to the depth of the trap below the conduction band. Stimulation with light or heat, releases the electrons from these traps, and they are either trapped again or recombine with the hole at luminescence centres. The recombination process is accompanied by the release of a portion of the stored energy in the form of light (Fig. 1.1c).

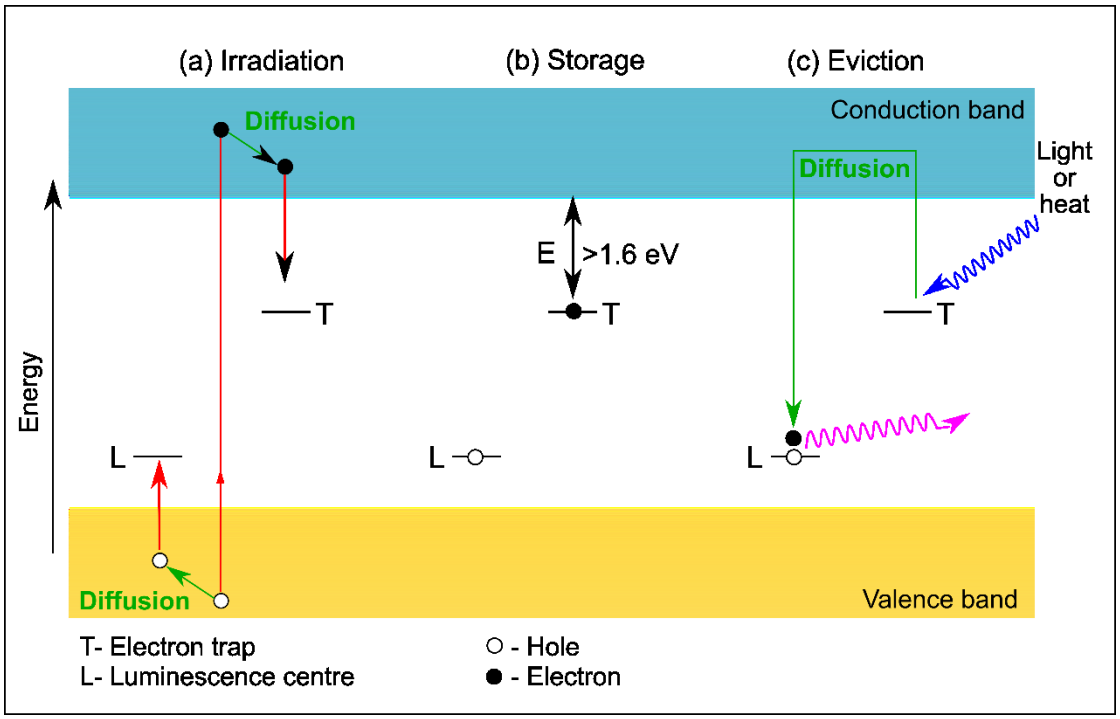

Figure 1.1: Schematic energy level diagram of luminescence process (modified from Aitken, 1998).

Luminescence dating is based on the principle that minerals, such as quartz or feldspar, can act as a natural dosimeter and chronometer, and accumulate luminescence signal from ionising radiation. When sediments are transported and exposed to natural light (e.g. during weathering and erosion), the accumulated signal will be released (bleaching; Fig. 1.2). When sediments are re-deposited and buried, the luminescence signal will accumulate again. For dating, artificial laboratory light stimulation of samples collected under dark conditions allows the release and measurement of the latent luminescence signal accumulated within the grains.

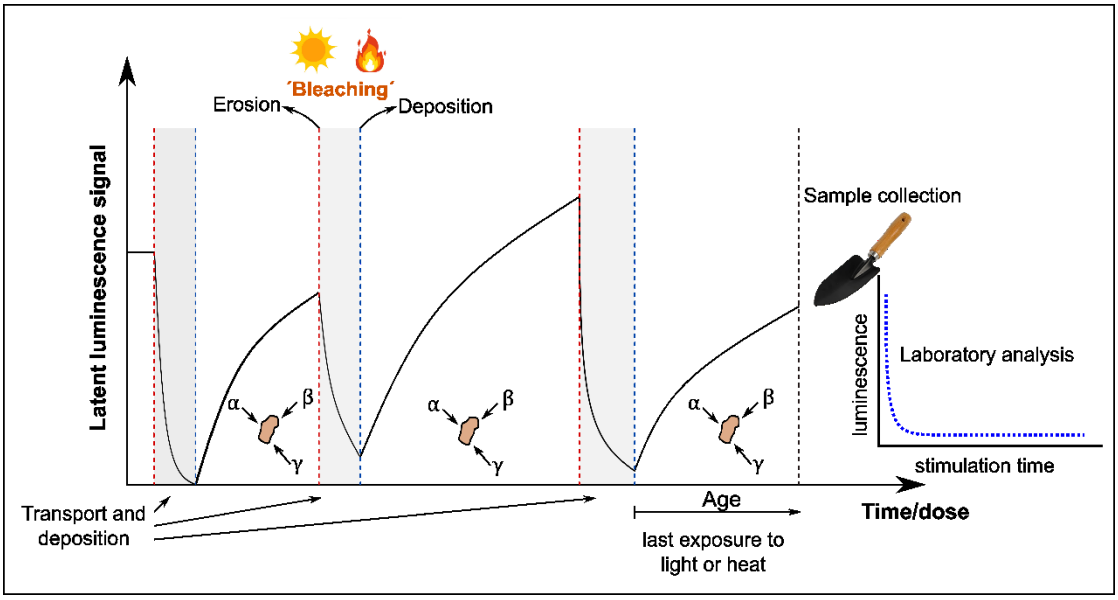

Figure 1.2: A schematic diagram illustrates the concept behind the luminescence dating technique (modified from Murray et al., 2021). Once sediment is buried, luminescence signal accumulates within grains due to exposure to ionising radiation from the surrounding environment. During sediment transport and exposure to light (or heat), the accumulated luminescence signal is released (i.e. bleaching process). The measured luminescence signal in the laboratory is related to the time since last exposure to light (or heat) and the environmental radioactivity.

The latent signal is proportional to the amount of dose received (equivalent dose; D_e) during burial. Dividing the equivalent dose (in Gy) by the local dose rate ($\dot{D}$), which corresponds to the surrounding radiation acting on the sediment during its burial over a time period (in Gy ka^{-1}), allows to determine the time elapsed since sediments have been deposited (equation 1.1).

$$Age\ (ka) = \frac{Equivalent\ dose\ (Gy)}{Dose\ rate\ (Gy\ ka^{-1})} = \frac{De\ (Gy)}{\dot{D}\ (Gy\ ka^{-1})} \qquad (1.1)$$

The dose rate can be determined by either measuring directly the natural radionuclides (U, Th, and K) or analyzing their concentration in the sediments. This is most commonly done by gamma spectrometry or neutron activation analysis. The measured concentrations have to be converted into the individual contribution of alpha, beta, and gamma dose rate using conversion factors (e.g. Adamiec and Aitken, 1998; Guérin et al., 2011; Liritzis et al., 2013). The cosmic dose rate can be calculated according to the geographical position, elevation, and burial depth (Prescott and Stephan, 1982). Another factor that should be considered is water content, as water attenuates ionising radiation. In general, the dose rate is normally considered to be remained constant over time, and therefore

the measured dose rate in the laboratory can be applied throughout the burial time. Although this assumption might not always be valid, the accurate determination of equivalent dose has been the main challenge in luminescence dating.

1.3 Measurement procedures for equivalent dose

In general, there are two different approaches for measuring the D_e: additive dose and regenerative dose (Fig. 1.3) methods. In both methods, the so-called dose response curve (DRC) is constructed reflecting the evolution of the luminescence signal according to the given dose. In the additive dose method, the natural aliquots are first irradiated (Fig 1.3a), while in the regenerative dose method the natural luminescence signal is first zeroed and the aliquots are then irradiated (Fig 1.3b). Of these, the regenerative dose method is the most frequently used technique. The advantage of this method is that no extrapolation of DRC is needed; the extrapolation can cause significant uncertainties, especially where the data are scattered or for old samples. The main disadvantage of the regenerative dose method is related to removing the natural signal prior to irradiation, which can cause luminescence sensitivity change.

In general, the determination of equivalent dose includes irradiation, preheating, and measurement of luminescence, regardless of the method applied. Irradiation is performed to induce a latent luminescence signal in the grains and is carried out by using either beta or gamma sources. Light sensitive shallow traps which are filled during laboratory irradiation and therefore can make an unwanted contribution to the luminescence signal are removed by preheating. Once the preheating of the sample has been applied, the luminescence signal is measured by stimulating the sample with either heat or light.

1.3.1 Multiple aliquot methods

The most common method in the 1980s and 1990s to determine D_e values was the multiple aliquot technique. In this method, several separate subsamples (i.e. aliquot) of same sample were used for luminescence measurement (both natural and laboratory induced). The major advantage of this method is that each aliquot is used only once, therefore there is no drastic sensitivity change induced by repeated treatments on the same aliquot. However, the main disadvantage of this technique is that each aliquot often behaves differently, and subsequently causing large scatter in the data. As a result, a relatively large uncertainty is often associated with mathematical fitting of DRC.

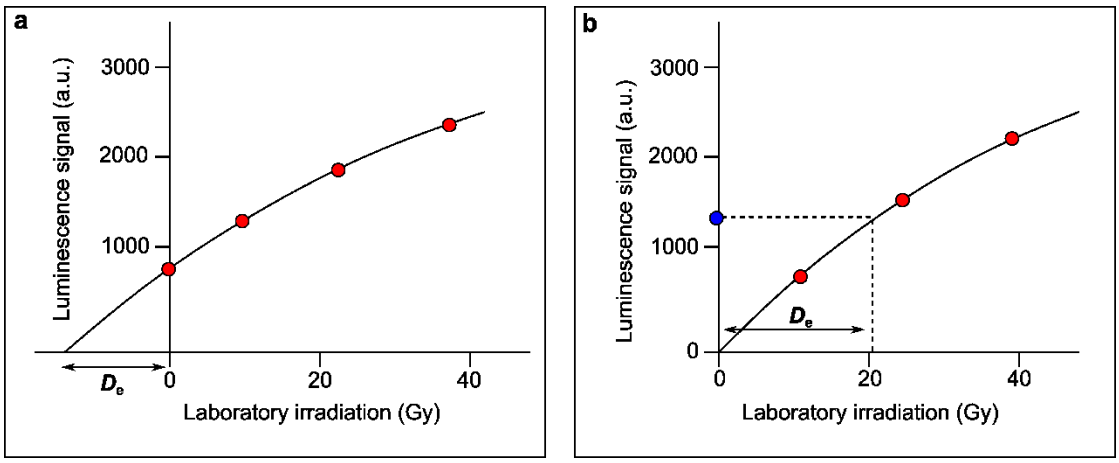

Figure 1.3: (a) additive dose and (b) regenerative dose response curves. In the additive dose method, different laboratory doses are given on top of the natural signal, causing the luminescence signal to increase, the D_e is obtained by extrapolation of the DRC to the x-axis. In the regenerative dose method, once the intensity of the natural signal has been measured (blue circle), the natural luminescence signal is erased by either light or heat, and then different laboratory radiation doses are given. The luminescence response to laboratory irradiation is used to construct the DRC, the D_e is calculated by interpolating the value of the natural intensity of the luminescence signal onto the DRC.

1.3.2 Single aliquot methods

Research over the last few decades (e.g. Duller, 1991; Mejdahl and Bøtter-Jensen, 1994; Murray and Roberts, 1997) have helped overcome the problem of individual luminescence properties of grains from different aliquots by allowing the possibility of repeated measurement on the same aliquots. A major breakthrough is the development of the single aliquot regenerative (SAR) protocol (Murray and Wintle, 2000).

The idea behind the SAR procedure is to use a regenerative dose technique and also to correct any sensitivity change which may be induced by measurement treatment (i.e. laboratory irradiation, preheating, and stimulation). To carry out the sensitivity correction, a fixed radiation dose (the test dose) is measured after each regenerative dose. The luminescence intensity resulting from each regenerative dose (L_x) is normalised by the luminescence intensity of the following test dose (T_x) and the sensitivity corrected luminescence signal (L_x/T_x) is used to construct a dose response curve. To obtain the D_e, the sensitivity corrected natural luminescence signal (L_n/T_n) is interpolated on the sensitivity corrected DRC.

However, since the number of traps is finite, the luminescence signal that corresponded to the number of trapped electron cannot increase indefinitely and will reach to saturation. Therefore, in the simplest instance, the generated DRC can be described by an exponential function:

$$I = I_{max}\left(1 - e^{\frac{-D}{D_0}}\right) \quad (1.2)$$

where I is the intensity of the luminescence signal for a given dose, I_{max} is the luminescence signal at saturation, and D_0 is the characteristic saturation dose of DRC. A pragmatic value of $2D_0$ has been suggested as an upper limit for reliable determination of D_e (Wintle and Murray, 2006).

1.4 Main dosimeters in luminescence dating

Luminescence dating is primarily applied to quartz and feldspar due to their abundance in sediments at most geological settings and also their sensitivity to environmental radiation, which generates the necessary signal for dating purposes. The luminescence signal of feldspar offers a number of advantages over the quartz signal. Firstly, the feldspar IRSL signal is generally much brighter than the quartz OSL signal, and a much larger proportion of grains are sensitive (~5% for quartz and >50% for feldspar, Duller, 2008). Another advantage of feldspar, especially for dating old sediments, is that the IRSL signal of feldspar grows to larger dose than the OSL signal of quartz and thus offers a higher saturation dose limit, by a factor of 4-5 compared to OSL of quartz. However the main disadvantage of regular IRSL protocol is anomalous fading (Spooner, 1994), which is caused by quantum mechanical tunnelling (Jain and Ankjærgaard, 2011) and can lead to age underestimation. This problem can be accounted for by using IR signals less affected by fading, the so-called post-IR IRSL (Thomsen et al., 2008; Thiel et al., 2011), multiple-elevated-temperature IRSL (MET-IRSL; Li and Li, 2011), pulsed IRSL (Tsukamoto et al., 2017), infrared-photoluminescence (IR-PL; Prasad et al., 2017), post-isothermal IRSL (Lamothe et al., 2020), and post-measurement fading correction models (e.g. Huntley and Lamothe, 2001; Lamothe et al., 2003; Wallinga et al., 2007; Kars et al., 2008).

Due to anomalous fading and the associated age underestimation, quartz has become the favoured dosimeter in luminescence dating despite its mentioned disadvantages. It is therefore of great interest to extend the quartz age range. Below is a brief review of different quartz signals that have been studied in recent years in the pursuit of extending the dating range of quartz.

1.4.1 Extending the quartz dating range

The applicability of blue stimulated OSL signal is commonly limited by the saturation of the luminescence signal at ~200 Gy, resulting in a quartz dating limit between 100 and 150 ka for typical environmental dose rates (Wintle and Murray, 2006). Consequently, in an attempt to extend the range of quartz dating beyond this limitation, other luminescence signals from quartz have been proposed, e.g. the slow OSL component (Singarayer et al., 2000), isothermal thermoluminescence (ITL; Jain et al., 2005), thermally transferred OSL (TT-OSL; Wang et al., 2006a,b) and violet stimulated luminescence (VSL; Jain, 2009).

The most commonly used luminescence signal for dating is related to the fast component OSL signal (originated from the 325 °C TL trap). However, several studies have attempted to use the slow OSL component, which is attributed to a deeper trap than the fast OSL trap and was found to saturate at much higher dose than the fast OSL component in the same sample (e.g. S3: Singarayer and Bailey, 2003; S4: Jain et al., 2003). However, the applicability of this method is compromised by sensitivity change, thermal transfer, and poor bleaching of the signal (Ankjærgaard et al., 2013).

The thermoluminescence (TL) signal of quartz saturates more slowly than the OSL, thus allowing the dating of older samples. However, this technique has some drawbacks such as releasing trap charges associated with both light-sensitive and light-insensitive components, poor separation of signal from different traps, and unwanted signal due to black body radiation caused by high temperature heating. In order to solve these issues, a modified approach, which is called ITL, was proposed by Jain et al. (2005) where the TL signal is recorded while the sample is held at a constant temperature. The quartz ITL signal measured at 310 °C has about an order of magnitude higher dose saturation level compared to the fast component OSL signal. However, the application of the SAR protocol to the quartz ITL signal is hampered by sensitivity changes which result in D_e overestimation (Buylaert et al., 2006; Huot et al., 2006). Vandenberghe et al. (2009) were able to address this problem by reducing both preheat and ITL stimulation temperatures.

The TT-OSL signal is a light sensitive signal observed following the initial depletion of the main OSL signal and the application of a preheat treatment to induce a transfer of charge from other less light sensitive traps into the main quartz OSL trap (Duller and Wintle, 2012). It was observed that the TT-OSL signal is several orders of magnitude smaller than the initial OSL signal, but it can grow

to very high doses of ~>20000 Gy (Wang et al., 2006a). This shows the potential of this signal to extend the age range back to 1 Ma (Duller and Wintle, 2012). However, this signal has some major drawbacks: i) the resetting of the signal by sunlight is slow (e.g. Tsukamoto et al., 2008; Porat et al., 2009), which can result in residual signals, leading to age overestimation, and ii) the thermal stability of the signal is low (e.g. Adamiec et al., 2010; Faershtein et al., 2018), which can significantly limit the applicable age range.

VSL is based on the use of a violet stimulation (405 nm) to measure the luminescence from deeper traps than those accessible by blue light (Jain, 2009). The initial study by Jain (2009) has shown that the VSL signal after initial blue light stimulation (i.e. post-blue VSL) can grow with dose up to 1000 Gy (compared with ~100 Gy for the initial OSL signal from the same grains). Later studies on characteristics of the VSL signal have demonstrated that this signal is closely associated with the 375 °C TL peak in quartz (Ankjærgaard et al., 2013; Hernandez and Mercier, 2015), originating from a deep trap at about 1.9 eV with a thermal lifetime of ~10^{11} years at 10 °C and no athermal loss (Ankjærgaard et al., 2013), suggesting VSL as a promising candidate for extending luminescence dating to the Ma timescale. However, the application of SAR protocol for VSL is not straightforward due to trapping sensitivity changes during measurement cycles that cannot be corrected for (Ankjærgaard et al., 2015; Colarossi et al., 2018). In general, the maximum limit of VSL dating using the SAR protocol has been suggested to be ~200 Gy (Ankjærgaard et al., 2013; Porat et al., 2018) as D_e estimates above this value showed age underestimation of up to 80% (e.g. Ankjærgaard et al., 2015; Colarossi et al., 2018). However, multiple aliquot methods seem to be a promising approach in VSL dating. Ankjærgaard (2019) reported a good agreement between VSL ages and independent chronology up to ~500 ka and ~900 ka, using the multiple-aliquot additive-dose (MAAD) and multiple-aliquot regenerative-dose (MAR) protocol, respectively.

1.5 Outline of the thesis

The overall aim of this research project is to extend the dating range of quartz by a detailed study of VSL and ITL signals. The thesis consists of six chapters including the Introduction (Chapter 1) and Conclusions (Chapter 6). The main part (Chapters 2-5) is written as four standalone scientific articles, which have been published in peer-reviewed scientific journals. A brief overview of each chapter is listed below.

Chapter 2

This chapter is published in *Quaternary Geochronology* as:

Rahimzadeh, N., Tsukamoto, S., Thiel, C., Frechen, M., 2023. Progress and pitfalls of the SAR protocol for the quartz violet stimulated luminescence (VSL) signal: A case study from Sardinia. Quaternary Geochronology 75, 101433.

In this chapter, the applicability of the SAR protocol for the VSL signal is evaluated. The main aim of this chapter is to propose an improved SAR VSL protocol since previous studies showed that the application of the SAR procedure is not straightforward and needs more refinement. We therefore first establish an optimised SAR protocol by systematically investigating the behaviour of the VSL signal under different measurement conditions. The validity of an optimised SAR VSL protocol is then evaluated on four coarse-grained quartz samples from Sardinia, for which OSL and post-IR IRSL ages are available. Although all procedural tests of the SAR protocol (i.e. recycling ratio, recuperation, dose recovery) are successfully passed, the significant VSL age underestimation (~50%), which might be due to trapping sensitivity change, is observed for one sample.

Chapter 3

This chapter is published in *Quaternary Geochronology* as:

Rahimzadeh, N., Tsukamoto, S., Zhang, J., Long, H., 2021. Natural and laboratory dose response curves of quartz violet stimulated luminescence (VSL): Exploring the multiple aliquot regenerative dose (MAR) protocol. Quaternary Geochronology 65, 101194.

Since the quartz VSL dating using the SAR protocol has not been successfully carried out to date samples with large natural dose (Chapter 2), this chapter investigates the reliability of MAR protocol for the VSL signal, using fine-grained quartz samples from the Luochuan Potou section of the Chinese Loess Plateau with

independent age control up to ~1400 ka. The application of the MAR protocol resulted in significant age underestimation beyond ~100 ka. We show that this underestimation is not due to the poor thermal stability of the signal nor the type of light source used during the bleaching pretreatment of the MAR protocol, but rather due to the divergence of the natural DRC from the laboratory generated DRC at ~250 Gy. Unlike the natural DRC, the VSL signal continues to increase at high laboratory doses in the laboratory generated DRC; suggesting the linear growth component of the laboratory generated MAR DRC could be a laboratory artefact and does not exist in nature. It contradicts the study by Ankjærgaard (2019), who showed that the MAR DRC using coarse-grained quartz from the same region (Luochuan) can reproduce the shape of the natural DRC. These observations highlight the need for a detailed comparison of the differences in VSL signal characteristics from coarse- and fine-grain size fractions.

Chapter 4

This chapter is published in *Quaternary Geochronology* as:

Rahimzadeh, N., Tsukamoto, S., Zhang, J., 2022. A comparative study of sand- and silt-sized quartz fractions for MAR-VSL dating using loess-palaeosol deposits in southern Germany. Quaternary Geochronology 70, 101276.

To further confirm the observation, made in Chapter 3, that different grain size fractions of quartz has different VSL characteristics, a direct comparison study between different grain size fractions from the same sets of sample is carried out in this chapter. This chapter assesses the VSL dose response pattern of coarse- (63-100 μm) and fine-grained (4-11 μm) quartz from the loess-palaeosol sequence in southern Germany. The comparison of VSL MAR DRCs using regeneration doses up to ~1000 Gy for both grain size fractions indicates that they are almost similar in shape. The constructed laboratory DRCs to very high doses (up to ~6000 Gy) show continuous signal growth at high doses, particularly in the case of fine-grained quartz, thereby confirming our previous observation in Chapter 3.

Chapter 5

This chapter is published in *Radiation Measurements* as:

Rahimzadeh, N., Zhang, J., Tsukamoto, S., Long, H., 2023. Characteristics of the quartz isothermal thermoluminescence (ITL) signal from the 375 °C peak and its potential for extending the age limit of quartz dating. Radiation Measurements 161, 106899.

Whilst Chapters 2, 3, and 4 focused on the VSL signal, this chapter focuses on the ITL signal from quartz. The original work on the quartz ITL signal measured at 330 °C (ITL_{330}; Murray and Wintle, 2000) has shown that this method can measure deep traps in quartz, i.e. 375 °CTL peak, therefore has the potential to extend the dating limit of quartz. In this chapter, we first provide new information on the characteristics of the ITL_{330} signal. We then investigate the reliability of the multiple aliquot methods, i.e. MAR and MAAD, by comparing obtained ITL_{330} ages against independent chronology for nine fine-grained quartz samples from the Luochuan section with ages up to ~700 ka. Finally, we take the opportunity to compare this signal to the VSL signal, as both signals originate from the same TL peak in quartz.

References

Adamiec, G., Aitken, M.J., 1998. Dose-rate conversion factors: update. Ancient TL 16, 37-50.

Adamiec, G., Duller, G.A.T., Roberts, H.M., Wintle, A.G., 2010. Improving the TT-OSL SAR protocol through source trap characterisation. Radiation Measurement 45, 768-777.

Aitken, M.J., 1998. An introduction to Optical Dating. Oxford University Press, Oxford, UK.

Ankjærgaard, C., 2019. Exploring multiple-aliquot methods for quartz violet stimulated luminescence dating. Quaternary Geochronology 51, 99-109.

Ankjærgaard, C., Guralnik, B., Porat, N., Heimann, A., Jain, M., Wallinga, J., 2015. Violet stimulated luminescence: geo-or thermochronometer? Radiation Measurement 81, 78-84.

Ankjærgaard, C., Jain, M., Wallinga, J., 2013. Towards dating Quaternary sediments using the quartz Violet Stimulated Luminescence (VSL) signal. Quaternary Geochronology 18, 99-109.

Buylaert, J.-P., Murray, A.S., Huot, S., Vriend, M.G.A., Vandenberghe, D., De Corte, F., Van den haute, P., 2006. A comparison of quartz OSL and isothermal TL measurements on Chinese loess. Radiation Protection Dosimetry 119, 474-478.

Colarossi, D., Chapot, M.S., Duller, G.A., Roberts, H.M., 2018. Testing single aliquot regenerative dose (SAR) protocols for violet stimulated luminescence. Radiation Measurement 120, 104-109.

Colarossi, D., Duller, G.A.T., Roberts, H.M., Tooth, S., Lyons, R., 2015. Comparison of paired quartz and feldspar post-IR IRSL dose distributions in poorly bleached fluvial sediments from South Africa. Quaternary Geochronology 30, 233-238.

Duller, G.A.T., 1991. Equivalent dose determination using single aliquots. Nuclear Trucks and Radiation Measurements 18, 371-378.

Duller, G.A.T., 2008. Single-grain optical dating of Quaternary sediments: why aliquot size matters in luminescence dating. Boreas 37, 589-612.

Duller, G.A.T., Wintle, A.G., 2012. A review of the thermally transferred optically stimulated luminescence signal from quartz for dating sediments. Quaternary Geochronology 7, 6-20.

Faershtein, G., Guralnik, B., Lambert, R., Matmon, A., Porat, N., 2018. Investigating the thermal stability of TT-OSL main source trap. Radiation Measurement 119, 102-111.

Guérin, G., Mercier, N., Adamiec, G., 2011. Dose-rate conversion factors: update. Ancient TL 29, 5-8.

Heller, F., Liu, T.S., 1982. Magnetostratigraphical dating of loess deposits in China. Nature 300, 431-433.

Hernandez, M., Mercier, N., 2015. Characteristics of the post-blue VSL signal from sedimentary quartz. Radiation Measurement 78, 1-8.

Huntley, D.J., Lamothe, M., 2001. Ubiquity of anomalous fading in K-feldspars and the measurement and correction for it in optical dating. Canadian Journal of Earth Science 38, 1093-1106.

Huot, S., Buylaert, J.-P., Murray, A.S., 2006. Isothermal thermoluminescence signals from quartz. Radiation Measurement 41, 1285-1293.

Jacobs, Z., 2008. Luminescence chronologies for coastal and marine sediments. Boreas 37, 508-535.

Jain, M., 2009. Extending the dose range: probing deep traps in quartz with 3.06 eV photons. Radiation Measurement 44, 445-452.

Jain, M., Ankjærgaard, C., 2011. Towards a non-fading signal in feldspar: Insight into charge transport and tunnelling from time-resolved optically stimulated luminescence. Radiation Measurements 46, 292-309.

Jain, M., Bøtter-Jensen, L., Murray, A.S., Denby, P.M., Tsukamoto, S., Gibling, M.R., 2005. Revisiting TL: dose measurement beyond the OSL range using SAR. Ancient TL 23, 9-24.

Jain, M., Murray, A.S., Bøtter-Jensen, L., 2003. Characterisation of blue-light stimulated luminescence components in different quartz samples: implications for dose measurement. Radiation Measurement 37, 441-449.

Kars, R.H., Wallinga, J., Cohen, K.M., 2008. A new approach towards anomalous fading correction for feldspar IRSL dating — Tests on samples in field saturation. Radiation Measurement 43, 786-790.

Kawamura, K., Parrenin, F., Lisiecki, L., Uemura, R., Vimeux, F., Severinghaus, J.P., Hutterli, M.A., Nakazawa, T., Aoki, S., Jouzel, J., Raymo, M.E., Matsumoto, K., Nakata, H., Motoyama, H., Fujita, S., Goto-Azuma, K., Fujii, Y., Watanabe, O., 2007. Northern

Hemisphere forcing of climatic cycles in Antarctica over the past 360,000 years. Nature 448, 912-917.

Lamothe, M., Auclair, M., Hamzaoui, C., Huot, S., 2003. Towards a prediction of long-term anomalous fading of feldspar IRSL. Radiation Measurement 37, 493-498.

Lamothe, M., Forget Brisson, L., and Hardy, F., 2020. Circumvention of anomalous fading in feldspar luminescence dating using Post-Isothermal IRSL. Quaternary Geochronology 57, 101062.

Li, B., Li, S.-H., 2011. Luminescence dating of K-feldspar from sediments: A protocol without anomalous fading correction. Quaternary Geochronology 6, 468-479.

Liritzis, I., Stamoulis, K., Papachristodoulou, C., Ioannides, K., 2013. A re-evaluation of radiation dose-rate conversion factors Mediterranean Archaeology and Archaeometry 13, 1-15.

Lisiecki, L.E., Raymo, M.E., 2005. A Pliocene-Pleistocene stack of 57 globally distributed benthic δ18O records. Paleoceanography 20, 1-17.

Lüthgens, C., Böse, M., Krbetschek, M., 2010. On the age of young morainic morphology in the area ascribed to the maximum extent of the Weichselian glaciation in north-eastern Germany. Quaternary International 222, 72-79.

Mejdahl, V., Bøtter-Jensen, L., 1994. Luminescence dating of archaeological materials using a new technique based on single aliquot measurements. Quaternary Science Reviews 13, 551-554.

Murray, A.S., Arnold, L.J., Buylaert, J.-P., Guérin, G., Qin, J., Singhvi, A.K., Smedley, R., Thomsen, K.J., 2021. Optically stimulated luminescence dating using quartz. Nature Reviews Methods Primers 1, 71.

Murray, A.S., Roberts, R.G., 1997. Determining the burial time of single grains of quartz using optically stimulated luminescence. Earth and Planetary Science Letters 152, 163-180.

Murray, A.S., Thomsen, K.J., Masuda, N., Buylaert, J.P., Jain, M., 2012. Identifying wellbleached quartz using the different bleaching rates of quartz and feldspar luminescence signals. Radiation Measurement 47, 688-695.

Murray, A.S., Wintle, A.G., 2000. Luminescence dating of quartz using an improved single aliquot regenerative-dose protocol. Radiation Measurements 33, 57-73.

Porat, N., Duller, G.A.T., Roberts, H.M., Wintle, A.G., 2009. A simplified SAR protocol for TT-OSL. Radiation Measurement 44, 538-542.

Porat, N., Jain, M., Ronen, A., Horwitz, L.K., 2018. A contribution to late middle Paleolithic chronology of the levant: new luminescence ages for the Atlit railway bridge site, Coastal plain. Israel. Quaternary International 464, 32-42.

Prasad, A.K., Poolton, N.R.J., Kook, M., Jain, M., 2017. Optical dating in a new light: A direct, non-destructive probe of trapped electrons. Scientific Reports 7, 1-15.

Prescott, J.R., Stephan, L.G., 1982. The contribution of cosmic radiation to the environmental dose for thermoluminescene dating - Latitude, altitude and depth dependences. PACT 6, 17-25.

Reimann, T., Naumann, M., Tsukamoto, S., Frechen, M., 2010. Luminescence dating of coastal sediments from the Baltic Sea coastal barrier-spit Darss-Zingst, NE Germany. Geomorphology 122, 264-273.

Rhodes, E.J., 2011. Optically stimulated luminescence dating of sediments over the past 200,000 years. Annual Review of Earth and Planetary Science 39, 461-488.

Rittenour, T.M., 2008. Luminescence dating of fluvial deposits: applications to geomorphic, palaeoseismic and archaeological research. Boreas 37, 613-635.

Roberts, H.M., 2008. The development and application of luminescence dating to loess deposits: a perspective on the past, present and future. Boreas 37, 483-507.

Singarayer, J.S., Bailey, R.M., 2003. Further investigations of the quartz optically stimulated luminescence components using linear modulation. Radiation Measurement 37, 451-458.

Singarayer, J.S., Bailey, R.M., Rhodes, E.J., 2000. Potential of the slow component of quartz OSL for age determination of sedimentary samples. Radiation Measurement 32, 873-880.

Spooner, N.A., 1994. The anomalous fading of infrared-stimulated luminescence from feldspars. Radiation Measurements 23, 625-632.

Thiel, C., Buylaert, J.-P., Murray, A., Terhorst, B., Hofer, I., Tsukamoto, S., Frechen, M., 2011. Luminescence dating of the Stratzig loess profile (Austria) – Testing the potential of an elevated temperature post-IR IRSL protocol. Quaternary International 234, 23-31.

Thomsen, K.J., Murray, A.S., Jain, M., Bøtter-Jensen, L. 2008: Laboratory fading rates of various luminescence signals from feldspar-rich sediment extracts. Radiation Measurements 43, 1474-1486.

Tsukamoto, S., Duller, G.A.T., Wintle, A.G., 2008. Characteristics of thermally transferred optically stimulated luminescence (TT-OSL) in quartz and its potential for dating sediments. Radiation Measurement 43, 1204-1218.

Tsukamoto, S., Kondo, R., Lauer, T., Jain, M., 2017. Pulsed IRSL: A stable and fast bleaching luminescence signal from feldspar for dating Quaternary sediments. Quaternary Geochronology 41, 26-36.

Vandenberghe, D.A.G., Jain, M., Murray, A.S., 2009. Equivalent dose determination using a quartz isothermal TL signal. Radiation Measurement 44, 439-444.

Wallinga, J., Bos, A.J.J., Dorenbos, P., Murray, A.S., and Schokker, J., 2007. A test case for anomalous fading correction in IRSL dating. Quaternary Geochronology 2, 216-221.

Wang, X.L., Lu, Y.C., Wintle, A.G., 2006a. Recuperated OSL dating of fine-grained quartz in Chinese loess. Quaternary Geochronology 1, 89-100.

Wang, X.L., Wintle, A.G., Lu, Y.C., 2006b. Thermally transferred luminescence in fine-grained quartz from Chinese loess: basic observations. Radiation Measurement 41, 649-658.

Wintle, A.G., Murray, A.S., 2006. A review of quartz optically stimulated luminescence characteristics and their relevance in single-aliquot regeneration dating protocols. Radiation Measurement 41, 369-391.

CHAPTER 2

Progress and pitfalls of the SAR protocol for the quartz violet stimulated luminescence (VSL) signal: A case study from Sardinia

Rahimzadeh, N., Tsukamoto, S., Thiel, C., Frechen, M.

Published on *Quaternary Geochronology*

https://doi.org/10.1016/j.quageo.2023.101433

Author contributions

Rahimzadeh, N. Conceptualization, Methodology, Data curation, Formal analysis, Visualization, Writing- original draft, Writing- review and editing,; Tsukamoto, S. Conceptualization, Methodology, Validation, Writing- review and editing, Supervision; Thiel. S. Conceptualization, Resources, Methodology, Validation, Writing- review and editing; Frechen, M. Resources.

ABSTRACT

In the quest for extending the upper age limit of optically stimulated luminescence (OSL) dating of quartz, it was shown that violet stimulated luminescence (VSL) may be a promising candidate. However, difficulties in the application of the single aliquot regenerative dose (SAR) protocol for VSL has been reported in previous studies. In this study, a set of experiments was carried out to investigate the behaviour of the VSL signal under different measurement conditions with the aim to improve the SAR VSL protocol in terms of passing the procedural tests of the SAR protocol, i.e., recycling ratio, recuperation and dose recovery. The validity of an optimised SAR protocol was then evaluated on four coarse-grained quartz samples from Sardinia, for which previously reported OSL and post-IR IRSL ages are available. Our result showed that all measured aliquots meet the recuperation, recycling ratio and dose recovery criteria, indicating that the proposed protocol is suitable for the studied samples. The obtained VSL and reference ages agree within uncertainty (2σ) for most of the samples except one sample with a largest expected equivalent dose of ~320 Gy, for which the VSL significantly (~50%) underestimates despite satisfactory dose recovery result. This underestimation is most likely due to trapping sensitivity change between the natural and all subsequent regenerated VSL signals induced by the first preheating in the SAR procedure, which is likely dose dependent. To minimise sensitivity change, the sensitivity-corrected multiple aliquot regenerative dose (SC-MAR) protocol was applied. The SC-MAR protocol yields VSL ages in agreement with reference ages for two samples (1σ); the other two samples show overestimation. We show that the observed age overestimation can be explained by incomplete resetting of the natural signal after 7 days SOL2 exposure used for the SC-MAR procedure. Bleaching experiments confirm variable bleaching behaviour among different samples. However, it is unclear whether this different bleaching behaviour arises from measuring samples with different bleaching histories, mineralogical compositions, or VSL source trap properties.

2.1 Introduction

Optically stimulated luminescence (OSL) dating is a widely accepted dating method in Quaternary research to establish an absolute chronology for terrestrial sedimentary sequences (e.g., Preusser et al., 2009). This dating method enables determination of the time elapsed since the last exposure of sediment to sunlight, i.e., the deposition age (Aitken, 1998). Quartz and feldspar are the two most widely used minerals in OSL dating exhibiting different luminescence properties. The

quartz OSL signal presents some advantages over the feldspar infrared stimulated luminescence (IRSL) signal, e.g., stable luminescence signal over time and faster bleachability under natural light conditions (Murray et al., 2012; Colarossi et al., 2015), which makes more likely the full resetting of the luminescence signal before the last burial event. However, the applicability of blue stimulated OSL is commonly limited to ~150 Gy (Chapot et al., 2012). This limitation, which is mainly caused by the saturation of the OSL signal with dose, is defined to be two times the characteristic saturation dose ($2D_0$), where D_0 is the dose level characteristic of the dose response curve (Wintle and Murray, 2006). In the quest for extending this limitation, other luminescence signals from quartz have been proposed, e.g., the slow OSL component (Singarayer et al., 2000), isothermal thermoluminescence (ITL; Jain et al., 2005), thermally transferred OSL (TT-OSL; Wang et al., 2006a,b) and violet stimulated luminescence (VSL; Jain, 2009).

The slow OSL component (S3: Singarayer and Bailey, 2003; S4: Jain et al., 2003) is attributed to a deeper trap than the fast OSL trap and is presented after preheating to 500 °C. This component has shown a higher characteristic saturation dose than the fast OSL component in the same sample. However, the applicability of the slow component dating method is limited due to thermal transfer, sensitivity change, and poor bleaching of the signal (Ankjærgaard et al., 2013; Wintle and Adamiec, 2017).

The quartz ITL signal measured at 310°C has about an order of magnitude higher dose saturation level compared to the fast component OSL signal. This signal originates from a set of traps with different optical depths and saturation characteristics, with only part of it related to the fast component OSL signal (325°C TL trap) (Jain et al., 2005; Choi et al., 2006). However, application of the SAR protocol to the quartz ITL signal at 310°C was found to result in equivalent dose (D_e) overestimation, which is the result of sensitivity change that occurs during the natural ITL signal measurement (Buylaert et al., 2006; Huot et al., 2006). A solution to avoid the initial sensitivity change has been proposed by Vandenberghe et al. (2009) by reducing both preheat and ITL stimulation temperatures. However, the proposed protocol in their study has not been widely applied.

The main steps of TT-OSL measurements involve an optical stimulation to remove the conventional OSL signal, and heat treatment to thermally transfer electrons from other less light sensitive traps into the main OSL dating trap at 325 °C (Duller and Wintle, 2012). Since the first TT-OSL studies using a multiple aliquot protocol to date fine-grained quartz (Wang et al., 2006a, b), several studies have

aimed at developing a single aliquot regenerative (SAR) dose TT-OSL protocol (e.g., Wang et al., 2007; Tsukamoto et al., 2008; Porat et al., 2009; Stevens et al., 2009; Adamiec et al., 2010; Jacobs et al., 2011). TT-OSL has major drawbacks such as slow resetting of the TT-OSL signal by sunlight (Tsukamoto et al., 2008; Kim et al., 2009; Porat et al., 2009) and the short thermal lifetime of the signal (few hundred thousand to a few million years; Li and Li, 2006; Adamiec et al., 2010; Shen et al., 2011; Thiel et al., 2012; Faershtein et al., 2018). The latter might significantly limit the applicable age range.

While the previously mentioned methods, with the exception of ITL, make use of blue stimulation, VSL is based on the use of a violet stimulation (405 nm) to measure the luminescence from deeper traps than those accessible by blue light (Jain, 2009). As initially demonstrated by Jain (2009), the quartz VSL signal after initial blue light stimulation (post-blue VSL) can grow with dose up to 1kGy (compared to ~100 Gy for the initial OSL signal from the same grains), with D_0 values in general 5-15 times larger than those of the fast component blue OSL signal. Later studies confirmed that the origin of the post-blue VSL signal is associated with the TL peak at 375 °C in quartz (Ankjærgaard et al., 2013; Hernandez and Mercier, 2015) with a thermal lifetime of $\sim 10^{11}$ years at 10 °C (Ankjærgaard et al., 2013, 2015, Rahimzadeh et al., 2021) and no athermal loss (Ankjærgaard et al., 2013), suggesting VSL as a possible candidate for extending luminescence dating to the Ma timescale.

In this study, we test different SAR VSL protocols by means of dose recovery experiments. Based on these results we establish an optimised SAR protocol by systematically exploring the behaviour of the VSL signal under different measurement conditions. This optimised SAR VSL protocol (following Colarossi et al., 2018) as well as single aliquot regeneration added (SARA) dose and multiple aliquot regenerative (MAR) dose dating protocols (Rahimzadeh et al., 2021) are then applied on four coarse-grained quartz samples from Sardinia to investigate the applicability of these methods for extending the dating limit of quartz. For these samples, a comparison of VSL and blue OSL ages is possible because the samples received low doses in a carbonate-rich environment. Furthermore, post-infrared IRSL (pIRIR) ages from feldspar are available (Thiel et al., 2010).

2.2 Material and methods

2.2.1 Samples and their previous age assignments

The four samples measured in this study originate from the coastal environment at the San Giovanni di Sinis section, western Sardinia (Fig. 2.1). The studied samples were taken from two adjacent outcrops: San Giovanni northern (sample SG_1 and SG_3) and southern (sample SG_2 and SG_4) sections.

Samples SG_1 and SG_2 were taken from carbonate-rich laminated consolidated sands, attributed to aeolian deposition and foreshore environment, respectively (Lecca and Carboni, 2007). Sample SG_3 came from carbonate-rich consolidated sands with coarse quartz pebbles, whereas sample SG_4 was taken from cemented fine sand layers containing shell detritus, both interpreted as foreshore and backshore dune deposits (Pascucci et al., 2014). Quartz OSL D_e values of SG_1 and SG_2 are 130±7 Gy and 73±3 Gy, respectively. Note that for SG_2 two different aliquot sizes (6 mm and 2.5 mm) were used for D_e determination in the original study (Thiel et al., 2010). Although the ages obtained from these two aliquot sizes were consistent, there were a few outliers showing larger D_e values. Therefore, we use the mean D_e value of 73±3 Gy obtained from the 2.5 mm aliquots for our reference. The blue OSL signals of SG_3 and SG_4 were found to be in saturation. The $pIRIR_{225}$ D_e values of these two samples were 398±6 Gy and 325±8 Gy, respectively. The dose rates for all samples had to be recalculated due to an erroneous set-up in the spreadsheet used for the calculation in Thiel et al. (2010). In the course of the recalculation, we further updated the data to use the most recent conversion factors of Liritzis et al. (2013), and beta attenuation factor of Guérin et al. (2012). The recalculated dose rates were lower than those previously published (Table 2.1), thus increasing the ages but not changing the overall interpretation.

The recalculated quartz OSL ages are 136±9 ka for SG_1 and 133±7 ka for SG_2, pointing to the transition between MIS6 and MIS5e. Using the recalculated dose rates, a fading correction following the method of Huntley and Lamothe (2001) was applied to the fading uncorrected $pIRIR_{225}$ ages, resulting in fading-corrected ages of 198±17 ka and 234±30 ka, respectively, which points to deposition shortly before and during MIS 7. In the following sections, the recalculated ages presented above are used as reference ages.

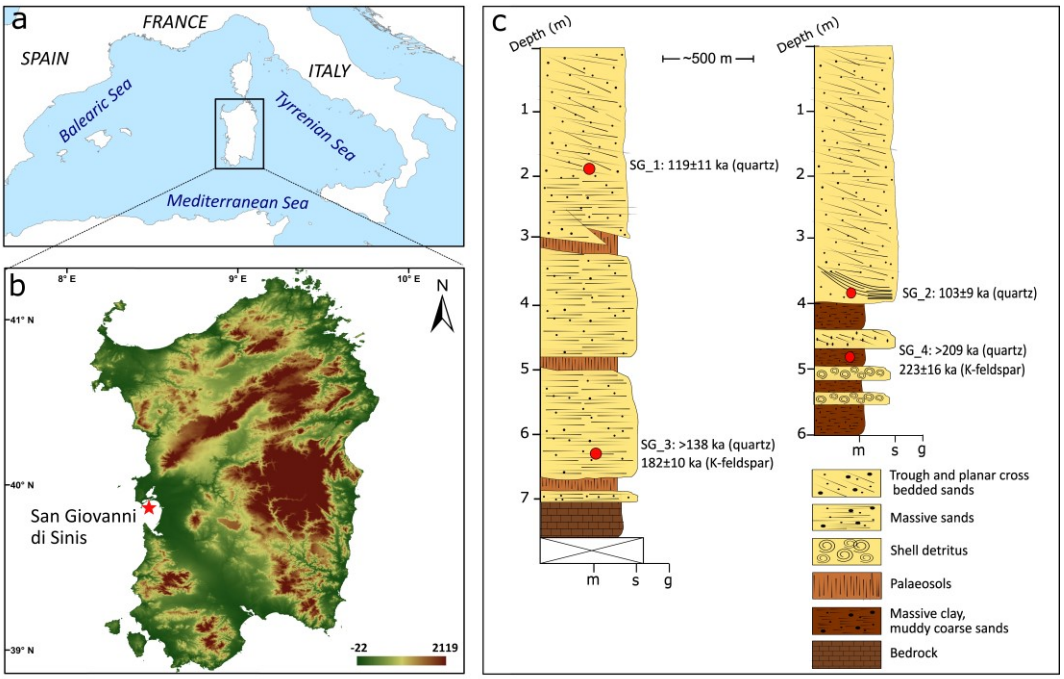

Figure 2.1: (a) location of Sardinia in the Mediterranean Sea and (b) the geographical setting of the Sardinia (based on SRTM data with 30 m resolution). The red star indicates the location of the sampling site, (c) the stratigraphic logs of the studied sections, modified from Coltorti et al. (2010). OSL ages (red circle symbol) obtained from previous study (Thiel et al., 2010).

Table 2.1: Published (Thiel et al., 2010) and recalculated dose rates and ages. The expected recalculated ages are being used for discussion. For details see text.

sample	Dose rate (Gy/ka)		Equivalent dose (Gy)		Age (ka)		Recalculated dose rate (Gy/ka)		Recalculated age (ka)	
	Quartz	Feldspar	OSL	Fading uncorr. $pIRIR_{225}$	OSL	Fading corr. $pIRIR_{225}$[c]	Quartz	Feldspar	OSL	Fading corr. $pIRIR_{225}$
SG_1	1.09±0.11	n.a.	130±7	n.a.	119±11	n.a.	0.95±0.04	n.a.	136±9	n.a
SG_2	0.71±0.08	n.a.	73±3	n.a.	103±9	n.a.	0.55±0.02	n.a.	133±7	n.a
SG_3	1.81±0.13	2.41±0.13	249±9 321±14[a]	398±6	>138[b]	182±10	1.62±0.06	2.29±0.20	>153[b]	198±17
SG_4	1.00±0.11	1.60±0.11	208±12 215±12[a]	325±8	>209[b]	223±16	0.92±0.05	1.57±0.20	>226[b]	234±30

Acronyms: (un)corr.= (un)corrected

[a] Expected quartz D_e from fading corrected $pIRIR_{225}$ age (recalculated) and quartz dose rate (recalculated)

[b] Minimum age

[c] Fading corrected following Huntley and Lamothe (2001)

2.2.2 Sample preparation and measurement equipment

Details on the chemical preparation of the samples are given in Thiel et al. (2010). The purified quartz extracts (100-200 μm) were mounted as aliquots of 2.5 mm in diameter on stainless-steel discs using silicone spray as adhesive. All luminescence measurements were performed using Risø TL/OSL DA-20 readers equipped with an automated detection and stimulation head (DASH; Lapp et al., 2015) and adapted for stimulation with both blue LEDs (470 nm) and a violet laser diode (405 nm). The VSL signals were detected through a combination of a 5 mm Hoya U340 and a Semrock brightline 340 nm (FF01-340/26) filters. Laboratory irradiation was carried out using a calibrated $^{90}Sr/^{90}Y$ beta source, with a dose rate of ~0.094 Gy s^{-1}.

2.3 Refining the SAR VSL protocol

The VSL protocol used in this study (Table 2.2) builds on the discoveries and advances that have been made since the initial VSL measurement by Jain (2009), which involves a preheat to 340°C for 10 s, followed by a blue OSL bleach (125 °C, 100 s) before measuring the VSL signal at 20°C to remove slow OSL components. Following a test dose measurement, the less stringent cut-heat (340 °C, 1 s) was chosen to avoid sensitivity changes and reduce the influence of the slow OSL components. In addition, a high temperature (500 °C, 100 s) blue bleach at the end of each cycle was used to reduce the amount of charge in the sample remaining at the end of the SAR cycle (i.e., recuperation). Since then, numerous studies have attempted to modify these steps to improve measurement results, e.g., reducing sensitivity change (Ankjærgaard et al., 2013, 2015, 2016; Hernandez and Mercier, 2015; Colarossi et al., 2018; Ankjærgaard, 2019). However, the maximum limit of VSL dating using the SAR protocol has been suggested to be ~200 Gy (Ankjærgaard et al., 2013; Porat et al., 2018) as D_e estimates above this value showed age underestimation of up to 80% (e.g., Ankjærgaard et al., 2015; Colarossi et al., 2018; Sontag-González et al., 2020). In a more recent study, Medialdea et al. (2022) investigated the suitability of the SAR VSL protocol through a series of dose recovery tests and showed that the SAR VSL protocol can recover the laboratory given doses up to 370 Gy.

Table 2.2: VSL protocol for D_e measurement from Colarossi et al. (2018) and the proposed VSL protocol used in this study. For the SAR approach, the protocol is recycled back to step 1 after step 10. For the MAR approach, a 7-day SOL2 bleaching was carried out prior to step 1 and then each aliquot was measured using steps 1-9 only once to obtain L_x/T_x.

Step	a) Colarossi et al. (2018)	b) Proposed protocol	Observed
1	Dose	Dose	
2	Preheat (280°C/ 10 s)	Preheat (280°C/ 10 s)	
3	Blue bleach (125 °C/ 40 s)	Blue bleach (125 °C/ 40 s)	
4	VSL (30 °C/ 500 s)	VSL (125 °C/ 500 s)	L_x
5	Violet bleach (200 °C/ 500 s)	Violet bleach (240 °C/ 500 s)	
6	Test dose	Test dose	
7	Preheat (280°C/ 10 s)	Preheat (280°C/ 10 s)	
8	Blue bleach (125 °C/ 40 s)	Blue bleach (125 °C/ 40 s)	
9	VSL (30 °C/ 500 s)	VSL (125 °C/ 500 s)	T_x
10	Violet bleach (200 °C/ 500 s)	Violet bleach (240 °C/ 500 s)	

To select a suitable SAR protocol, dose recovery experiments were conducted on three aliquots of sample SG_3 following different protocols (Protocols A-D in Table S2.1; Ankjærgaard et al., 2013, 2015, 2016; Colarossi et al., 2018). Prior to measurements, the aliquots were bleached instrumentally in the luminescence reader using two violet stimulations at room temperature for 1,000 s separated by a 10,000 s pause; this pause was used to allow any charge trapped in shallow traps to decay. The aliquots were then given a laboratory beta dose of ~90 Gy and measured using the SAR protocols listed in table S2.1. All these protocols failed to recover a given dose and showed large sensitivity changes (Fig. S2.1), except Protocol D by Colarossi et al. (2018), for which, however, large recuperation (~15%) was observed. Therefore, to reduce recuperation, we modified some parameters in the protocol, which are described in the following section.

2.3.1 Modifications and test performances

In the SAR protocol of Colarossi et al. (2018; Table 2.2a) the post-blue VSL signal was measured at 30 °C to reduce the instrumental background (Hernandez and Mercier, 2015). They further used an additional bleaching step (VSL at 200 °C, 500 s) after each regenerative dose and test dose measurement. In contrast, we recorded the post-blue VSL signal at 125°C to avoid re-trapping of charges in the 110 °C TL peak of quartz. Fig. 2.2 shows the TL glow curve of sample SG_3 for different violet stimulation temperatures of 30 and 125 °C. An aliquot of sample SG_3 was first sensitised through repeated cycles of irradiation and annealing. The TL response to a ~45 Gy regenerative dose was then measured after blue light stimulation (125 °C for 40 s) and violet stimulation at different temperatures (30

and 125 °C) for durations of 5, 20, 50, 100, 300, and 500 s. As shown in Fig. 2.2b, measuring VSL at 125 °C clearly removes the shallow TL peak at 110 °C.

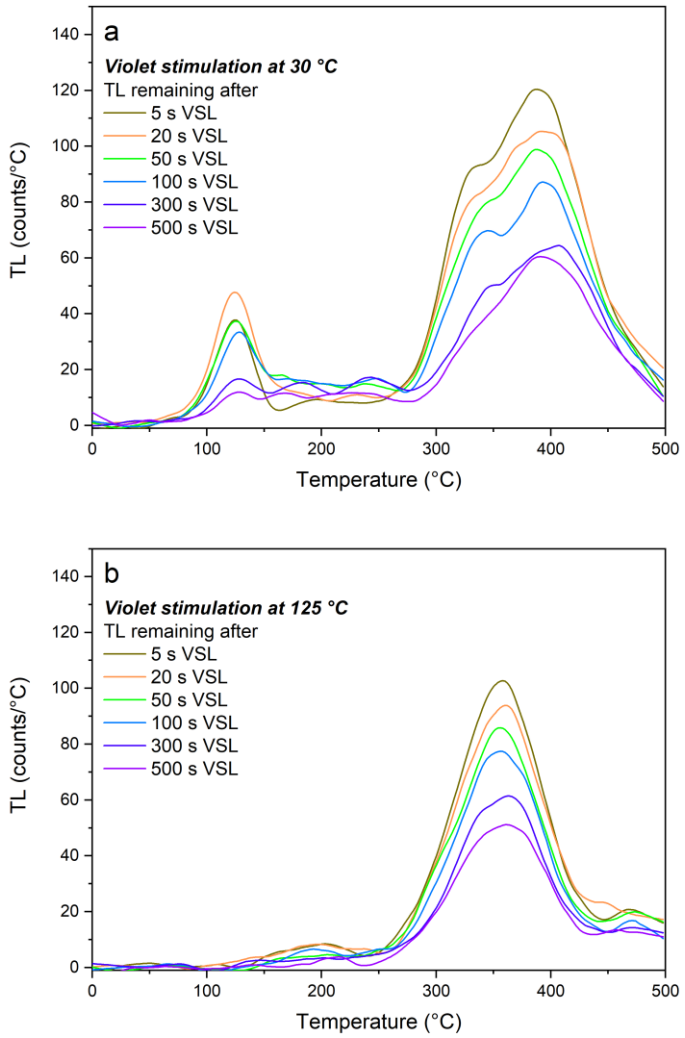

Figure 2.2: TL glow curves recorded after an irradiation dose of 45 Gy followed by a preheat (at 280 °C, 10 s), blue light stimulation (at 125 °C, 40 s) and violet stimulation at 30 °C (a) and 125 °C (b) for various durations (see legend) for sample SG_3.

Furthermore, the influence of preheat temperature on the recuperation was investigated on natural aliquots of sample SG_3. The preheat temperatures were set to 160-320 °C with an interval of 40 °C with a fixed violet bleach at 200 °C for 500 s. After administering a test dose of 36 Gy, the cut-heat temperature was set to equal the preheat temperature. The mean D_e of three aliquots was calculated for each preheat temperature, except for temperatures between 160 and 240 °C, where one of the three aliquots were rejected because the natural signal was above the signal saturation level of the dose response curve (Fig. 2.3a). Large inter-aliquot scattering and large sensitivity change during the SAR cycles were

observed for the temperatures <280 °C (Fig. 2.3a). In contrast, there is a systematic trend of increasing recuperation value with preheat temperature (Fig. 2.3b).

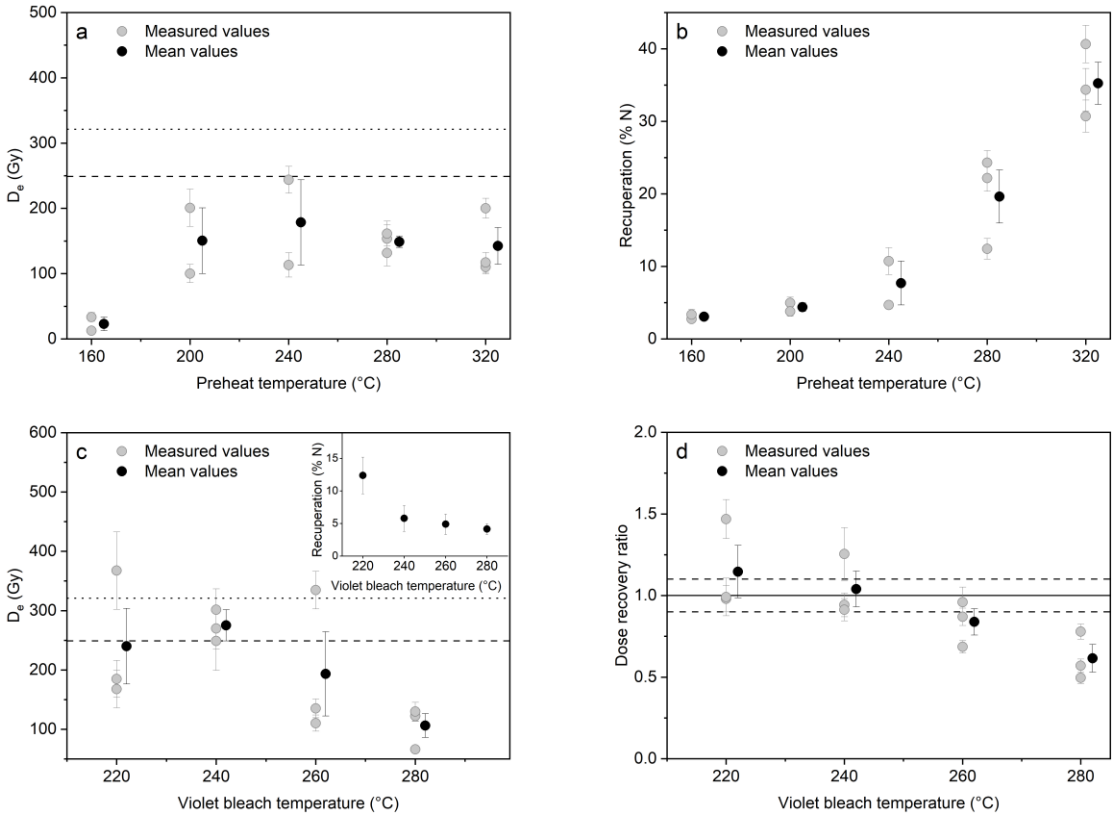

Figure 2.3: (a,b) Preheat plateau test on sample SG_3 using varying preheat temperatures showing the measured natural D_e (a) and recuperation values (b), (c,d) Natural D_e measurements and dose recovery results using various violet bleach temperatures on the same sample. Grey data points represent the individual aliquot values, and data points in black are mean ± standard error with 5 °C offset. The minimum D_e from blue OSL and expected quartz D_e from $pIRIR_{225}$ are denoted by the dashed line and dotted line, respectively (a and c). The inset in (c) shows the recuperation values for different violet bleach temperatures.

In a second step, different violet bleach temperature experiments ranging from 220 °C to 280 °C with an interval of 20 °C were carried out on the same sample to evaluate the effect of the violet bleach temperature (Table 2.2, steps 5 and 10) on recuperation (Fig. 2.3c, d). The preheat temperature was fixed at 280 °C for this experiment due to i) the potential for re-trapping of the VSL signal into the 220 °C and 260 °C quartz TL traps (Ankjærgaard et al., 2013), ii) the possible effect of high preheat temperature (i.e., >300 °C) on the trapping efficiency (Ankjærgaard et al., 2016), and iii) to avoid the reduction of the dim post-blue VSL signal (Colarossi et al., 2018). Three aliquots were measured per violet bleach temperature. There is an apparent trend of decreasing recuperation with increased violet bleach temperature, ranging from 12.4±2.8 % (220 °C) to 4.2±0.8 % (280 °C) (Fig. 2.3c inset). Fig. 2.3c shows that the obtained D_e from the 240 °C violet bleach was

consistent within uncertainty with the minimum D_e from blue OSL and also close to the expected quartz D_e (calculated from fading corrected $pIRIR_{225}$ age and quartz dose rate; cf. Table 2.1). The same tendency was observed from a violet bleach temperature at 220 °C, although a higher recuperation was obtained. Further support for the validity of 240 °C violet bleach temperature can be indicated by the satisfactory measured to given dose value.

The dose recovery test using the same range of violet bleach temperatures as above was carried out on sample SG_3. Three aliquots per temperature were bleached in the luminescence reader as described in section 2.3. The aliquots were then given a laboratory beta dose of ~90 Gy and subsequently measured in a similar manner described above. In addition, three bleached aliquots received no laboratory dose and were used to determine the residual dose remaining after bleaching. A residual dose of ~8 Gy was obtained. Mean measured to given dose ratios (without subtraction of the residual) show a monotonic decrease with violet bleach temperature (from 1.15±0.16 at 220 °C to 0.62±0.08 at 280 °C; Fig. 2.3d). We obtained satisfactory dose recovery results (1.04±0.18) using a violet bleach at 240 °C. Consequently, violet stimulation at 125 °C (Table 2.2b, steps 4 and 9) and violet bleach at 240 °C (Table 2.2b, steps 5 and 10) were selected for D_e determination. The proposed protocol is outlined in Table 2.2b.

2.3.2 Equivalent dose determination and protocol performance

Dose response curves were measured using the protocol in Table 2.2b, using six aliquots per sample. The test dose used for all samples was ~40 Gy. The curves were fitted with a double saturating exponential function. A representative SAR VSL dose response curve for sample SG_3 with characteristic doses of $D_{0,1}$ ~70 Gy and $D_{0,2}$ ~2860 Gy is shown in Fig. 2.4a. D_es were determined using the initial VSL signals integrated over 2.5 s and subtraction of an early background from the following 15 s of the decay curve. An early background subtraction was used to minimise the contribution from re-trapping in the later part of the decay curves (Ankjærgaard et al., 2013, 2016). Equivalent doses were accepted if the signal was >3 σ above the background, the recuperation signal was <5% of the natural signal, and the recycle ratio was within 10% of unity; all aliquots passed these criteria (Fig. 2.5a, b). The mean VSL D_e values measured from six aliquots range between 62±3 Gy (SG_2) to 196±33 Gy (SG_4) (Table 2.3).

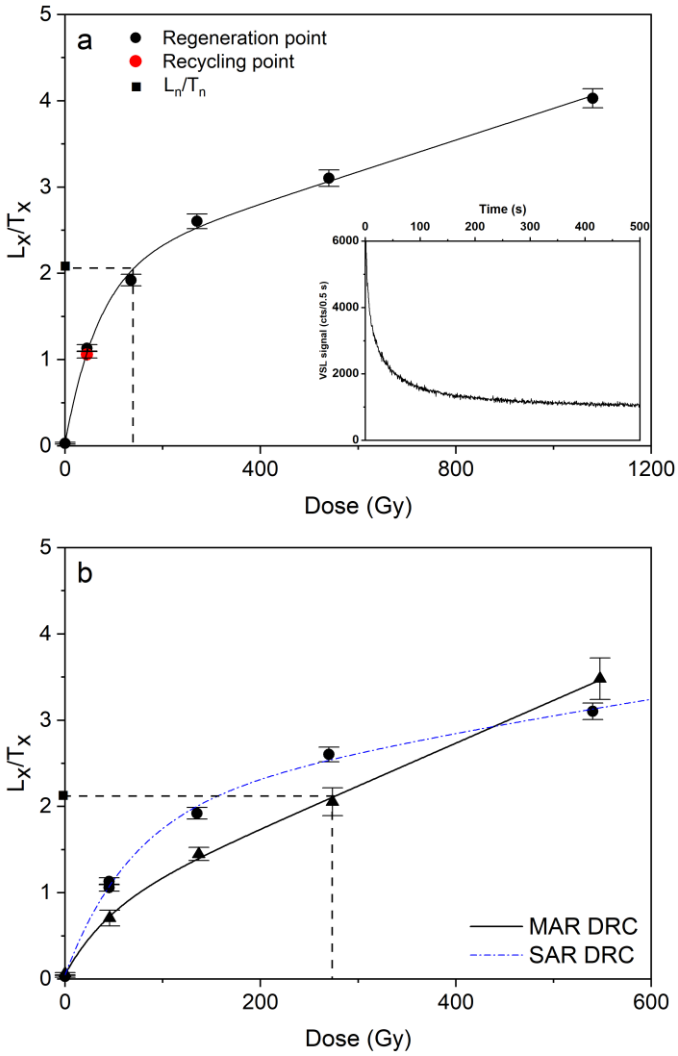

Figure 2.4: Dose response curves produced using both SAR (a) and sensitivity-corrected MAR (b) protocol for sample SG_3. The inset shows the natural VSL decay curve of the SAR experiment. The SAR dose response curve from (a) in dashed blue line replotted with the MAR dose response curve in (b).

The reliability of the proposed VSL protocol was then checked by means of a dose recovery test for all samples. Three aliquots per sample were bleached in the luminescence reader using two violet light stimulations for 1,000 s separated by a 10,000 s pause. The bleached aliquots were then given a beta dose of ~135 Gy and the dose measured using the protocol in Table 2.2b with the same test dose used for D_e determination. For all samples, the measured to given dose ratios fall in the suggested range for quartz OSL of 0.9-1.1 (Wintle and Murray, 2006) (Fig. 2.5c), implying the reliability of the proposed VSL protocol.

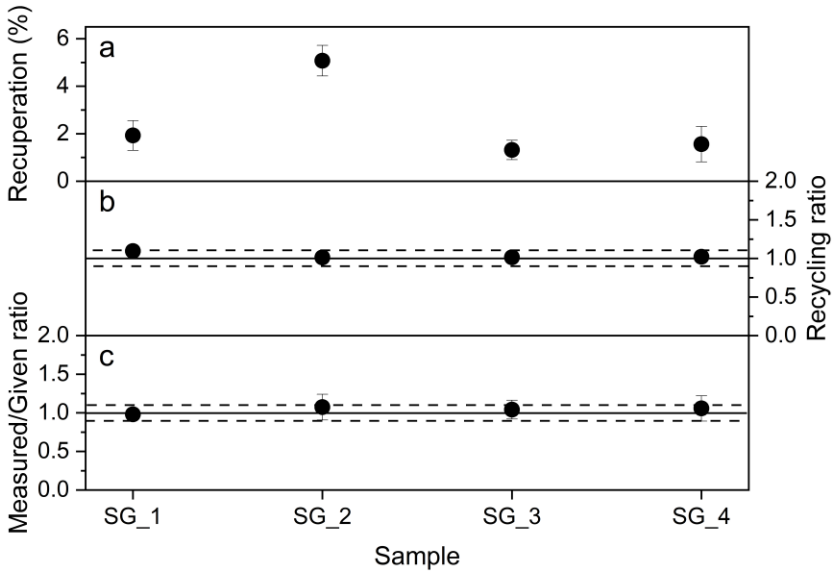

Figure 2.5: Summary of recuperation values (a) recycling ratios (b) and measured to given dose ratios (c) for all studied samples using the SAR protocol.

2.4 Comparison of SAR VSL ages

The SAR VSL ages of SG_1 and SG_2 agree with the reference age within 2σ and 1σ uncertainty, respectively. For the older two samples, SG_3 is significantly younger than the reference age whereas the SAR VSL age of SG_4 is consistent with the reference age (Table 2.3, Fig. 2.6). The underestimation of SG_3 is especially noteworthy as it showed good performance in the dose recovery experiment. However, it should be noted that the 135 Gy given dose is much smaller than the expected equivalent dose of ~320 Gy (Table 2.1), and thus the successful dose recovery does not guarantee the ability of the SAR protocol for a much higher natural dose.

VSL age underestimation using SAR protocols for samples with large natural dose have been reported previously (Ankjærgaard et al., 2013, 2015, 2016; Morthekai et al., 2015; Colarossi et al., 2018; Sontag-González et al., 2020). Ankjærgaard et al. (2013) demonstrated agreement between estimated VSL and obtained OSL D_es up to 200 Gy. Ankjærgaard et al. (2015) reported age underestimation of samples in the age range of 0.7-1.6 Ma and explained that either by the thermal history of the studied site, which may have caused thermal resetting of the VSL signal, or by using an insufficient measurement protocol, which cannot correctly translate the natural signal into the equivalent laboratory dose. Ankjærgaard et al. (2016) concluded that application of the SAR procedure for VSL dating is quite problematic due to sensitivity change occurring between the measurement of the natural signal and all subsequent regenerated signals,

which are not corrected for by measuring the response to a test dose, and thus may cause dose underestimation. Using the modified multiple-aliquot additive-dose (MAAD) and multiple-aliquot regenerative-dose (MAR) procedures, Ankjærgaard (2019) reported good agreement between estimated VSL ages and independent chronology up to ~500 ka and ~900 ka, respectively.

Table 2.3: Measured VSL D_e and resulting VSL age using different procedures.

sample	SAR protocol		MAR protocol		SARA protocol		Reference age (ka)
	D_e±se (Gy)	Age (ka)	D_e±se (Gy)	Age (ka)	D_e±se (Gy)	age (ka)	
SG_1	91±14	95±16	126±27	133±29			136±9
SG_2	62±3	114±7	119±10	217±20			133±7
SG_3	135±9	83±6	288±24	178±16	125±64	77±40	198±17
SG_4	196±33	214±38	302±50	329±58			234±30

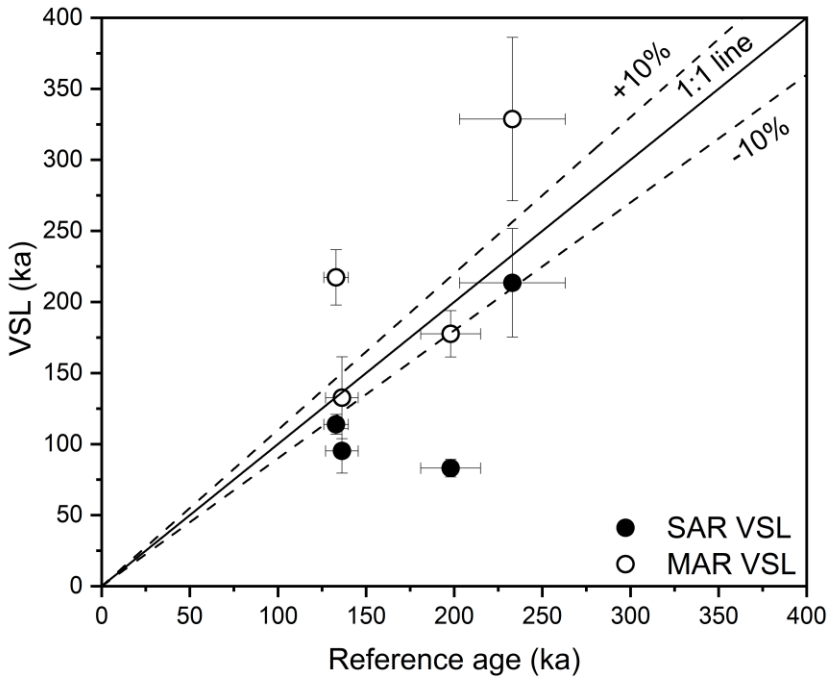

Figure 2.6: Estimated VSL ages using a SAR and a sensitivity-corrected MAR protocol as a function of the recalculated reference ages (OSL and $pIRIR_{225}$) from Thiel et al. (2010). The solid line is 1:1 line, and the dashed lines represent ±10%.

2.5 Application of a SARA procedure

To further investigate if a trapping efficiency change induced by preheating is responsible for this equivalent dose underestimation, we performed single aliquot regeneration added (SARA; Mejdahl and Bøtter-Jensen, 1994) dose measurements. Trapping sensitivity changes induced by the first preheat can be overcome if laboratory irradiations are given prior to heating of the sample, as is the case for the SARA protocol. Here we combined a SAR protocol (Table 2.2b) with the SARA experiment, i.e., SAR-SARA (Wallinga et al., 2000; Kars et al., 2014; Tsukamoto et al., 2017). In this procedure, groups of aliquots, which retain their natural dose, are given a range of added doses before measuring their D_es using the SAR protocol (Table S2.2). The estimated D_e values are plotted against its added laboratory dose, giving a linear relationship between the added dose and D_e, and the intercept on the x-axis indicates the SARA D_e, assuming that any trapping sensitivity change is the same for all aliquots regardless of added laboratory dose (Fig. S2.2). Any sensitivity change is reflected in the slope of the linear regression; a slope within 10% of unity means that the sensitivity change in the SAR protocol is corrected properly, whereas deviation from unity represents an uncorrected sensitivity change and suggests that a known added dose is not successfully recovered in the measured dose. In any case, the obtained D_e is independent of sensitivity change (Buylaert et al., 2006; Kars et al., 2014).

In our experiment, 15 aliquots of sample SG_3 that still contain their natural signals were split into five batches of three aliquots each, and exposed to different radiation doses (N, N+90, N+180, N+270 and N+405 Gy). Each of the aliquots was then measured using the SAR VSL protocol (Table 2.2b). One aliquot with a 270 Gy added dose was excluded from the analysis, because of an unusually large D_e value (539±65 Gy). D_e values were plotted as a function of additive dose and fitted with a straight line (Fig. 2.7, solid black line). When the linear fitting is conducted, it is assumed that the sensitivity change in the aliquots is uniform and independent of additive dose. We note, however, that R^2 value for the fitted straight line is 0.78, indicating that the sensitivity change in the aliquots is not entirely uniform and therefore linear fitting may not be appropriate. The pattern of sensitivity change among different additive doses can be examined by calculating the measured to given dose ratio for each additive dose step. The D_e value obtained from the first step of the SARA protocol, which did not receive any radiation dose, is considered to be the natural D_e (e.g., N; Table S2.2). The difference between the natural D_e and natural+added dose D_e (e.g., N+ß; Table S2.2) was then divided by the added dose

to calculate the measured to given dose ratio, resulting in mean ratios from 1.2±0.3 to 0.6±0.1 and showing a decreasing trend with larger added dose (Fig. 2.7 inset). This has also been shown experimentally by Rahimzadeh et al. (2021) who observed that the successful recovery of a laboratory dose is dose dependent. Therefore, the SARA dataset was fitted by a single saturation exponential function (Fig. 2.7, dashed red line), yielding a D_e value of 125±64 Gy. This is consistent with the SAR D_e value, indicating that the SARA approach also fails to improve burial dose estimation. Indeed, a key assumption of the SARA protocol is that the sensitivity change is independent of additive dose and there is a linear relationship between the added dose and estimated D_e. However, the SARA dataset confirms that this assumption cannot be met for our sample here (and probably cannot be met in the majority of SARA VSL measurements).

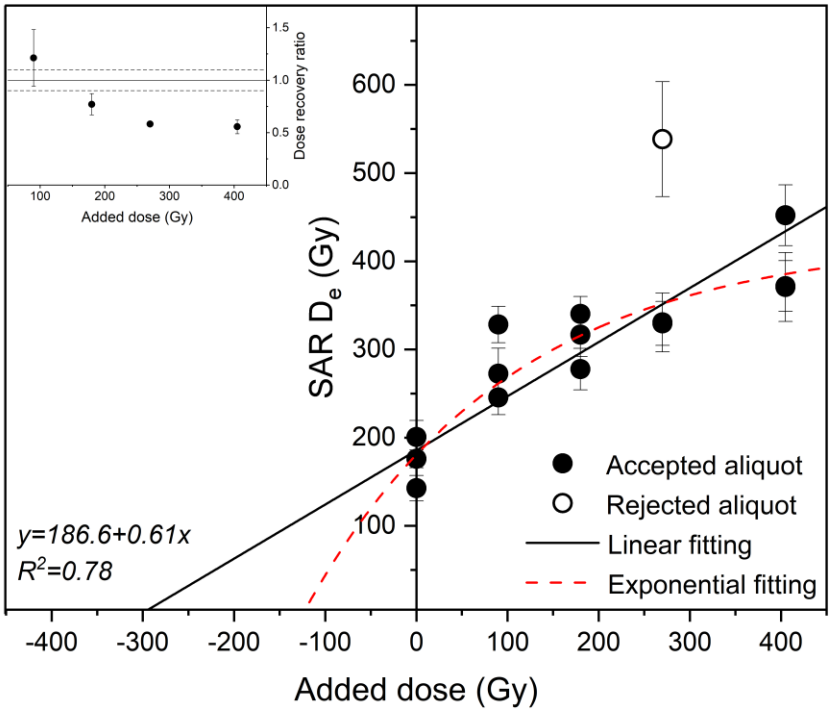

Figure 2.7: SAR-SARA result obtained on sample SG_3 with an expected dose of 321±14 Gy. The solid black and dashed red lines are the linear and single saturating exponential fit, respectively, of the SAR equivalent doses. The inset shows the calculated measured to given dose ratio for each additive dose step of the SAR-SARA experiment.

2.6 Application of a MAR procedure

Sensitivity change induced by repeated treatments (i.e., laboratory irradiation, preheating and stimulation) of the SAR protocol on the same subsample can be monitored and corrected by measuring the response to a fixed test dose. To test whether cumulative sensitivity change in the SAR protocol, which was not accounted for by test dose sensitivity monitoring, is the reason for SAR VSL

underestimation, the sensitivity-corrected MAR protocol (SC-MAR, Lu et al., 2007) was carried out. Unlike the SAR protocol, in this method the luminescence signal is measured only twice for each aliquot; once for a natural/regeneration dose, and again for a test dose to measure the aliquot's sensitivity. Dose response curves are generated by sensitivity corrected regenerative dose signals (L_x/T_x) from multiple aliquots.

For the application of the SC-MAR protocol, a total of 20 aliquots for each sample were first bleached in the solar simulator (Hönle SOL2) for 7 days (Ankjærgaard, 2019). The bleached aliquots were then divided into five groups of four aliquots each. For constructing the MAR dose response curve (Fig. 2.4b), each group was exposed to different regenerative doses ranging from 0 to 540 Gy and measured using the protocol in Table 2.2b with the same test dose (~40 Gy) as used in the SAR measurements. To estimate the equivalent doses, the average of six L_n/T_n values from the SAR measurements were interpolated onto the MAR dose response curves. It has to be noted that all these natural signals from the SAR protocol were measured prior to preheating which might cause sensitivity change. The obtained MAR VSL D_es are presented in Table 2.3; the values lie between 119±10 Gy (SG_2) and 302±50 Gy (SG_4) with corresponding ages ranging from 217±20 ka to 329±58 ka. The MAR VSL ages and the reference ages agree within 1σ uncertainty for two of the four samples (SG_1 and SG_3); one sample (SG_4) agrees at 2σ uncertainty and one sample (SG_2) is just beyond 2σ (Table 2.3; Fig. 2.6, open circles). The potential effect of incomplete bleaching after 7 days SOL2 exposure was tested to investigate whether this could be the reason for the observed age overestimation of two samples (SG_2 and SG_4).

2.7 Degree of signal bleaching

For constructing the MAR dose response curve, the dosimetric signal should be reset prior to adding doses. Therefore, it is important to ensure that the VSL signal is completely removed. When the L_x/T_x values of 0 Gy regenerative dose were compared with the initial signal intensity (L_n/T_n) (i.e., signal loss), it was found that they reached a level of ~10% of the initial signal intensity after 7 days of bleaching for sample SG_2 and SG_4. However, the sensitivity-corrected 0 Gy regenerative signal was ~1% and ~3% of the natural signal for samples SG_1 and SG_3, respectively (Fig. S2.3). Interestingly, the two samples (SG_2 and SG_4) showing a lower signal loss were taken from the same outcrop. Consequently, it is of interest to investigate the SOL2 bleaching stability of the VSL signal from two different sections.

We therefore conducted a bleaching test on samples SG_1 and SG_2. Four aliquots per each bleaching duration were bleached in the SOL2 for varying amounts of time ranging between 0 and 4 days (without bleach, 10 min, 2 hr, 8 hr, 1 day, 2 days, 4 days and 7 days). Note that the sensitivity-corrected natural signal of the SAR measurement and the sensitivity-corrected 0 Gy regenerative dose of the MAR measurement were used for 0 s and 7 days bleaching time, respectively. This bleaching experiment shows that two representative samples from two different sections are not bleached at similar rates (Fig. 2.8; blue circles). After 10 min of bleaching, the VSL signal of sample SG_1 was reduced to 18% of the initial signal (Fig. 2.8a), whilst the VSL signal of sample SG_2 was only reduced to 43% (Fig. 2.8b). Furthermore, Figure 2.8 shows that sample SG_2 is incompletely bleached even after 7 days of SOL2 exposure; the VSL signal is still at 10% of its original level, while the VSL signal of sample SG_1 depletes to a negligible level (~1%). Assuming that the VSL D_e should be similar to the OSL D_e, the residual dose after 7 days bleaching was determined by multiplying the signal loss (% of initial L_n/T_n intensity for 7 days) by the OSL D_e, yielding a residual dose of ~1.4 Gy and ~7.2 Gy for sample SG_1 and SG_2, respectively. This result is in line with Ankjærgaard (2019), who suggested caution in using the MAR method for samples with residuals of more than 5% and recommended a longer bleaching duration or an incomplete bleaching correction for those samples.

In addition to investigating the SOL2 bleaching of the VSL signal, it is also of interest to examine the bleachability of the VSL signal with violet stimulation. Three groups with four aliquots in each were bleached with the violet laser between 600 s and 28800 s (Fig. 2.8, red squares). The depletion of the VSL signal due to the SOL2 exposure and laser stimulation was consistent for both samples, except for a bleaching duration of 8 hrs (28800 s) for sample SG_2, for which the remaining dose of the VSL signal after violet stimulation is significantly lower than that of the solar simulator (Fig. 2.8b). This suggests that there is no marked difference between the two bleaching treatments for the investigated durations here. Furthermore, data sets from both bleaching experiments using violet and SOL2 stimulation exhibited a similar patterns in bleaching decay rate; i.e., a higher bleaching decay rate of sample SG_1 (Fig. 2.8).

Moreover, from Fig. 2.8 two features become apparent: i) the larger inter-aliquot scatter can be observed for sample SG_2, particularly for long bleaching durations, and ii) the opposite relationship between the SOL2 simulator and the violet laser for the two samples, i.e., solar simulator appears to be slightly more

effective to bleach sample SG_1, while the violet laser is more effective on sample SG_2. These observations support the interpretation that the bleaching behaviour of the VSL signal is sample dependent.

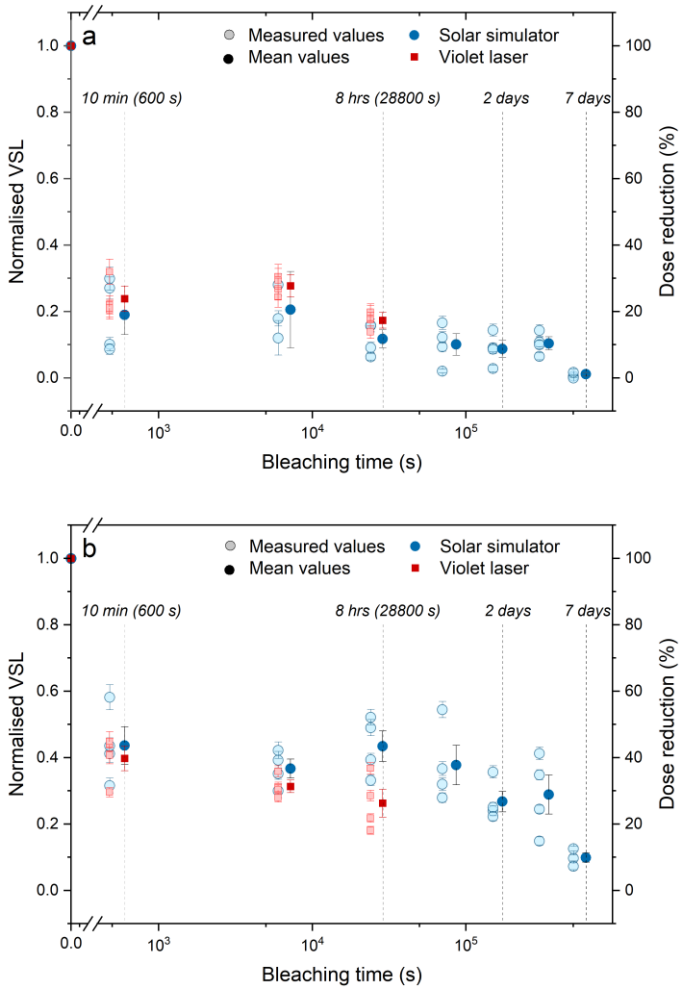

Figure 2.8: Natural VSL signal remaining of sample SG_1 (a) and SG_2 (b) after bleaching with a Hönle SOL2 solar simulator (blue circle) and the violet laser (red square) as a function of bleaching time. Data points in light colour represent the individual aliquot values, and the mean values and standard errors from four aliquots are shown in dark colour. Data are normalised to the initial point with zero bleaching.

Different bleaching behaviour among different samples can be explained in several ways. One possible explanation could be related to the retention of some residual charges at the time of burial, which can subsequently be attributed to the sediment transport process and depositional environment. An alternative explanation is the provenance of the quartz. Two samples SG_2 and SG_4, which show MAR age overestimation, were collected from the southern outcrop. According to Lecca and Carboni (2007), sample SG_2 is interpreted as foreshore deposits resulting from sea level highstand during MIS 5. In addition, the presence of the shell detritus in sample SG_4 points to foreshore environment; according to

Pascucci et al. (2014) backshore dune deposition is also possible. SG_1 from the northern outcrop is aeolian in origin and thus may have different mineralogy compared to the two foreshore deposits at the southern outcrop. The sand unit from which SG_3 was sampled exhibits quartz pebbles, which may indicate a sediment input from land and thus a slightly different mineralogy.

Another explanation for the different bleaching behaviour follows Ankjærgaard (2019), who has shown a two-step decay of the VSL bleaching depletion profile. She concluded that there are at least two separate traps with different bleaching stabilities in the VSL signal; the 375 °C TL trap and a photo- or thermally transferred signal from a deeper trap which is much harder to optically bleach than the 375 °C trap. Therefore, it remains unclear whether different observed VSL residuals here reflect effects arising from measuring samples with different bleaching histories, mineralogical compositions or VSL source trap properties. A full explanation of the mechanism behind the different bleaching stabilities amongst samples demands more detailed investigation in terms of bleaching behaviour and mineralogical composition, which, however, goes beyond the scope of this study.

2.8 Conclusions

In this study, four coarse-grained quartz samples from the coastal environment at the San Giovanni di Sinis succession, western Sardinia, were used for VSL dating. The main aim of this study was to propose an improved SAR VSL protocol, since previous works reported the application of the SAR procedure was problematic. Based on a series of experiments on parameters such as violet stimulation temperature, preheat temperature and violet bleach temperature, the measurement results were evaluated. Laboratory tests (recycling ratio, recuperation and dose recovery) showed satisfactory performance of the proposed VSL protocol for samples under investigation here.

For the SAR VSL method, significant age underestimation was observed in one out of the four samples, even though it has met the standard dose recovery criteria. Following the possibility that the SAR procedure cannot adequately correct for sensitivity change occurring between the measurement of the natural signal and the subsequent test dose signal, we conducted SARA measurements on this sample (SG_3). However, the basic assumption of the SARA approach, that sensitivity change is independent of the additive dose, was not met in this study and thus application of the SARA protocol also failed to improve the dose estimation.

Ankjærgaard et al. (2016) suggested that the origin of underestimation is a trapping sensitivity change between the natural and all regenerated signals due to the preheat used in the protocol, which should be detected by a dose recovery experiment. Since the dose recovery ratio was within the acceptable 10% of unity, it seems likely that the ability to successfully recover a laboratory dose is dose dependent, which is further supported by estimating the measured to given dose ratio for each additive dose step in the SARA experiment. Regardless of whether this is the main problem, or more than one problem exists, further investigations are required for refinement of the SAR VSL protocol.

The MAR VSL ages are consistent with reference ages in two out of the four samples (SG_1 and SG_3); the other two samples (SG_2 and SG_4) show overestimation. For the MAR protocol, it is necessary to remove the natural luminescence signal prior to irradiation. Therefore, it can be assumed that the incomplete bleaching of the VSL signal could be a cause for this apparent age overestimation. Here, the MAR datasets appear to support this assumption; the VSL signal of sample SG_2 and SG_4 depletes to 10% of the initial signal intensity (L_n/T_n) after 7 days of SOL2 bleaching, while the remaining VSL signal of the other two samples (SG_1 and SG_3) were lower than 3%.

In summary, attempts to use the SAR-type protocol for VSL have not been straightforward so far and need more refinement, therefore the multiple aliquot methods, i.e., MAR and MAAD, seem to be a promising approach in VSL dating. While the MAAD method may be hampered by the availability of a modern sample that should be analogue to the environmental conditions of the older one, the MAR approach appears to be the most applicable method. However, based on the MAR dataset from this study, there seems to be an indication that the magnitude of the residual VSL signal is different amongst samples. Therefore, further investigation is needed to understand the mechanism(s) involved in different bleaching behaviour of the VSL signal.

Acknowledgments

The authors are grateful for the detailed comments and suggestions of two anonymous reviewers that helped to improve the manuscript.

References

Adamiec, G., Duller, G.A.T., Roberts, H.M., Wintle, A.G., 2010. Improving the TT-OSL SAR protocol through source trap characterisation. Radiat. Meas. 45, 768–777.

Aitken, M.J., 1998. An Introduction to Optical Dating: the Dating of Quaternary Sediments by the Use of Photon-Stimulated Luminescence. Oxford University Press.

Ankjærgaard, C., Jain, M., Wallinga, J., 2013. Towards dating Quaternary sediments using the quartz Violet Stimulated Luminescence (VSL) signal. Quat. Geochronol. 18, 99–109.

Ankjærgaard, C., Guralnik, B., Porat, N., Heimann, A., Jain, M., Wallinga, J., 2015. Violet stimulated luminescence: geo-or thermochronometer? Radiat. Meas. 81, 78-84.

Ankjærgaard, C., Guralnik, B., Buylaert, J.-P., Reimann, T., Yi, S.W., Wallinga, J., 2016. Violet stimulated luminescence dating of quartz from Luochuan (Chinese loess plateau): agreement with independent chronology up to ~600 ka. Quat. Geochronol. 34, 33-46.

Ankjærgaard, C., 2019. Exploring multiple-aliquot methods for quartz violet stimulated luminescence dating. Quat. Geochronol. 51, 99-109.

Buylaert, J.-P., Murray, A.S., Huot, S., Vriend, M.G.A., Vandenberghe, D., De Corte, F., Van den haute, P., 2006. A comparison of quartz OSL and isothermal TL measurements on Chinese loess. Radiat. Prot. Dosim. 119, 474–478.

Chapot, M.S., Roberts, H.M., Duller, G.A.T., Lai, Z.P., 2012. A comparison of natural- and laboratory-generated dose response curves for quartz optically stimulated luminescence signals from Chinese Loess. Radiat. Meas. 47, 1045-1052.

Choi, J.H., Murray, A.S., Cheong, C.S., Hong, H.W., 2006. Estimation of equivalent dose using quartz isothermal TL and the SAR procedure. Quat. Geochronol. 1, 101–108.

Colarossi, D., Duller, G.A.T., Roberts, H.M., Tooth, S., Lyons, R., 2015. Comparison of paired quartz and feldspar post-IR IRSL dose distributions in poorly bleached fluvial sediments from South Africa. Quat. Geochronol. 30, 233–238.

Colarossi, D., Chapot, M.S., Duller, G.A., Roberts, H.M., 2018. Testing single aliquot regenerative dose (SAR) protocols for violet stimulated luminescence. Radiat. Meas. 120, 104-109.

Coltorti, M., Melis, E., Patta, D., 2010. Geomorphology, stratigraphy and facies analysis of some Late Pleistocene and Holocene key deposits along the coast of Sardinia (Italy). Quat. Int. 222, 19-35.

Duller, G.A.T., Wintle, A.G., 2012. A review of the thermally transferred optically stimulated luminescence signal from quartz for dating sediments. Quat. Geochronol. 7, 6–20.

Faershtein, G., Guralnik, B., Lambert, R., Matmon, A., Porat, N., 2018. Investigating the thermal stability of TT-OSL main source trap. Radiat. Meas. 119, 102–111.

Guérin, G., Mercier, N., Nathan, R., Adamiec, C., Lefrais, Y., 2012. On the use of the infinite matrix assumption and associated concepts: a critical review. Radiat. Meas. 47, 778-785.

Hernandez, M., Mercier, N., 2015. Characteristics of the post-blue VSL signal from sedimentary quartz. Radiat. Meas. 78, 1-8.

Huntley, D.J., Lamothe, M., 2001. Ubiquity of anomalous fading in K-feldspars and the measurement and correction for it in optical dating. Can. J. Earth Sci. 38, 1093-1106.

Huot, S., Buylaert, J.-P., Murray, A.S., 2006. Isothermal thermoluminescence signals from quartz. Radiat. Meas. 41, 1285–1293.

Jacobs, Z., Roberts, R.G., Lachlan, T.J., Karkanas, P., Marean, C.W., Roberts, D.L., 2011. Development of the SAR TT-OSL procedure for dating Middle Pleistocene dune and shallow marine deposits along the southern Cape coast of South Africa. Quat. Geochronol. 6, 491–513.

Jain, M., Murray, A.S., Bøtter-Jensen, L., 2003. Characterisation of blue-light stimulated luminescence components in different quartz samples: implications for dose measurement. Radiat. Meas. 37, 441–449.

Jain, M., Bøtter-Jensen, L., Murray, A.S., Denby, P.M., Tsukamoto, S., Gibling, M.R., 2005. Revisiting TL: dose measurement beyond the OSL range using SAR. Ancient TL 23, 9–24.

Jain, M., 2009. Extending the dose range: Probing deep traps in quartz with 3.06 eV photons. Radiat. Meas. 44, 445–452.

Kars, R.H., Wallinga, J., Cohen, K.M., 2008. A new approach towards anomalous fading correction for feldspar IRSL dating- tests on samples in field saturation. Radiat. Meas. 43, 786–790.

Kim, J.C., Duller, G.A.T., Roberts, H.M., Wintle, A.G., Lee, Y.I., Yi, S.B., 2009. Dose dependence of thermally transferred optically stimulated luminescence signals in quartz. Radiat. Meas. 44, 132–143.

Lapp, T., Kook, M., Murray, A.S., Thomsen, K.J., Buylaert, J.-P., Jain, M., 2015. A new luminescence detection and stimulation head for the Risø TL/OSL reader. Radiat. Meas. 81, 178-184.

Lecca, L., Carboni, S., 2007. The Tyrrhenian section of San Giovanni di Sinis (Sardinia): stratigraphic record of an irregular single high stand. Riv. Ital. 13, 509–523.

Li, B., Li, S.H., 2006. Studies of thermal stability of charges associated with thermal transfer of OSL from quartz. J. Phys. D. Appl. Phys. 39, 2941–2949.

Liritzis, I., Stamoulis, K., Papachristodoulou, C., Ioannides, K., 2013. A re-evaluation of radiation dose-rate conversion factors. Mediterr. Archaeol. Archaeom. 13, 1-15.

Lu, Y.C., Wang, X.L., Wintle, A.G., 2007. A new OSL chronology for dust accumulation in the last 130,000 yr for the Chinese Loess Plateau. Quat. Res. 67, 152-160.

Medialdea, A., Brill, D., King, G.E., Zander, A., Lopez-Ramirez, M.R., Bartz, M., Brückner, H., 2022. Violet stimulated luminescence as an alternative for dating complex colluvial sediments in the Atacama Desert. Quat. Geochronol. 71, 101337.

Mejdahl, V., Bøtter-Jensen, L., 1994. Luminescence dating of archaeological materials using a new technique based on single aliquot measurements. Quat. Sci. Rev. 13, 551-554.

Morthekai, P., Chauhan, P.R., Jain, M., Shukla, A.D., Rajapara, H.M., Krishnan, K., Sant, D.A., Patnaik, R., Reddy, D.V., Singhvi, A.K., 2015. Thermally re-distributed IRSL (RD-IRSL): A new possibility of dating sediments near B/M boundary. Quat. Geochronol. 30, 154-160.

Murray, A.S., Thomsen, K.J., Masuda, N., Buylaert, J.P., Jain, M., 2012. Identifying well-bleached quartz using the different bleaching rates of quartz and feldspar luminescence signals. Radiat. Meas. 47, 688–695.

Pascucci, V., Sechi, D., Andreucci, S., 2014. Middle Pleistocene to Holocene coastal evolution of NW Sardinia (Mediterranean Sea, Italy). Quat. Int. 328-329, 3-20.

Porat, N., Duller, G.A.T., Roberts, H.M., Wintle, A.G., 2009. A simplified SAR protocol for TT-OSL. Radiat. Meas. 44, 538–542.

Porat, N., Jain, M., Ronen, A., Horwitz, L.K., 2018. A contribution to late middle Paleolithic chronology of the levant: new luminescence ages for the Atlit railway bridge site, Coastal plain, Israel. Quat. Int. 464, 32-42.

Preusser, F., L. Chithambo, M., Götte, T., Martini, M., Ramseyer, K., J. Sendezera, E., J. Susino, G., G. Wintle, A., 2009. Quartz as a natural luminescence dosimeter. Earth-Sci. Rev. 97, 184–214.

Rahimzadeh, N., Tsukamoto, S., Zhang, J., Long, H., 2021. Natural and laboratory dose response curves of quartz violet stimulated luminescence (VSL): Exploring the multiple aliquot regenerative-dose (MAR) protocol. Quat. Geochronol. 65, 101194.

Shen, Z.X., Mauz, B., Lang, A., 2011. Source-trap characterization of thermally transferred OSL in quartz. J. Phys. D. Appl. Phys. 44, 295405.

Singarayer, J.S., Bailey, R.M., Rhodes, E.J., 2000. Potential of the slow component of quartz OSL for age determination of sedimentary samples. Radiat. Meas. 32, 873–880.

Singarayer, J.S., Bailey, R.M., 2003. Further investigations of the quartz optically stimulated luminescence components using linear modulation. Radiat. Meas. 37, 451–458.

Sontag-González, M., Frouin, M., Li, B., Schwenninger, J.-L., 2020. Assessing the dating potential of violet stimulated luminescence protocols. Geochronometria.

Stevens, T., Buylaert, J.-P., Murray, A.S., 2009. Towards development of a broadly-applicable SAR TT-OSL dating protocol for quartz. Radiat. Meas. 44, 639–645.

Thiel, C., Coltorti, M., Tsukamoto, S., Frechen, M., 2010. Geochronology for some key sites along the coast of Sardinia (Italy). Quat. Int. 222, 36–47.

Thiel, C., Buylaert, J.-P., Murray, A.S., Elmejdoub, N., Jedoui, Y., 2012. A comparison of TT-OSL and post-IR IRSL dating of coastal deposits on Cap Bon peninsula, north-eastern Tunisia. Quat. Geochronol. 10, 209–217.

Tsukamoto, S., Duller, G.A.T., Wintle, A.G., 2008. Characteristics of thermally transferred optically stimulated luminescence (TT-OSL) in quartz and its potential for dating sediments. Radiat. Meas. 43, 1204–1218.

Tsukamoto, S., Porat, N., Ankjærgaard, C., 2017. Dose recovery and residual dose of quartz ESR signals using modern sediments: implication for single aliquot ESR dating. Radiat. Meas. 106, 472-476.

Vandenberghe, D.A.G., Jain, M., Murray, A.S., 2009. Equivalent dose determination using a quartz isothermal TL signal. Radiat. Meas. 44, 439-444.

Wallinga, J., Murray, A., Duller, G., 2000. Underestimation of equivalent dose in single-aliquot optical dating of feldspars caused by preheating. Radiat. Meas. 32, 691-695.

Wang, X.L., Lu, Y.C., Wintle, A.G., 2006a. Recuperated OSL dating of fine-grained quartz in Chinese loess. Quat. Geochron. 1, 89–100.

Wang, X.L., Wintle, A.G., Lu, Y.C., 2006b. Thermally transferred luminescence in fine-grained quartz from Chinese loess: Basic observations. Radiat. Meas. 41, 649–658.

Wang, X.L., Wintle, A.G., Lu, Y.C., 2007. Testing a single-aliquot protocol for recuperated OSL dating. Radiat. Meas. 42, 380–391.

Wintle, A.G., 2008. Luminescence dating: where it has been and where it is going. Boreas 37, 471–482.

Wintle, A.G., Murray, A.S., 2006. A review of quartz optically stimulated luminescence characteristics and their relevance in single-aliquot regeneration dating protocols. Radiat. Meas. 41, 369–391.

Wintle, A.G., Adamiec, G., 2017. Optically stimulated luminescence signals from quartz: A review. Radiat. Meas. 98, 10–33.

Supplementary Material- Progress and pitfalls of the SAR protocol for the quartz violet stimulated luminescence (VSL) signal: A case study from Sardinia

Rahimzadeh, N., Tsukamoto, S., Thiel, C., Frechen, M.

Published on *Quaternary Geochronology*

https://doi.org/10.1016/j.quageo.2023.101433

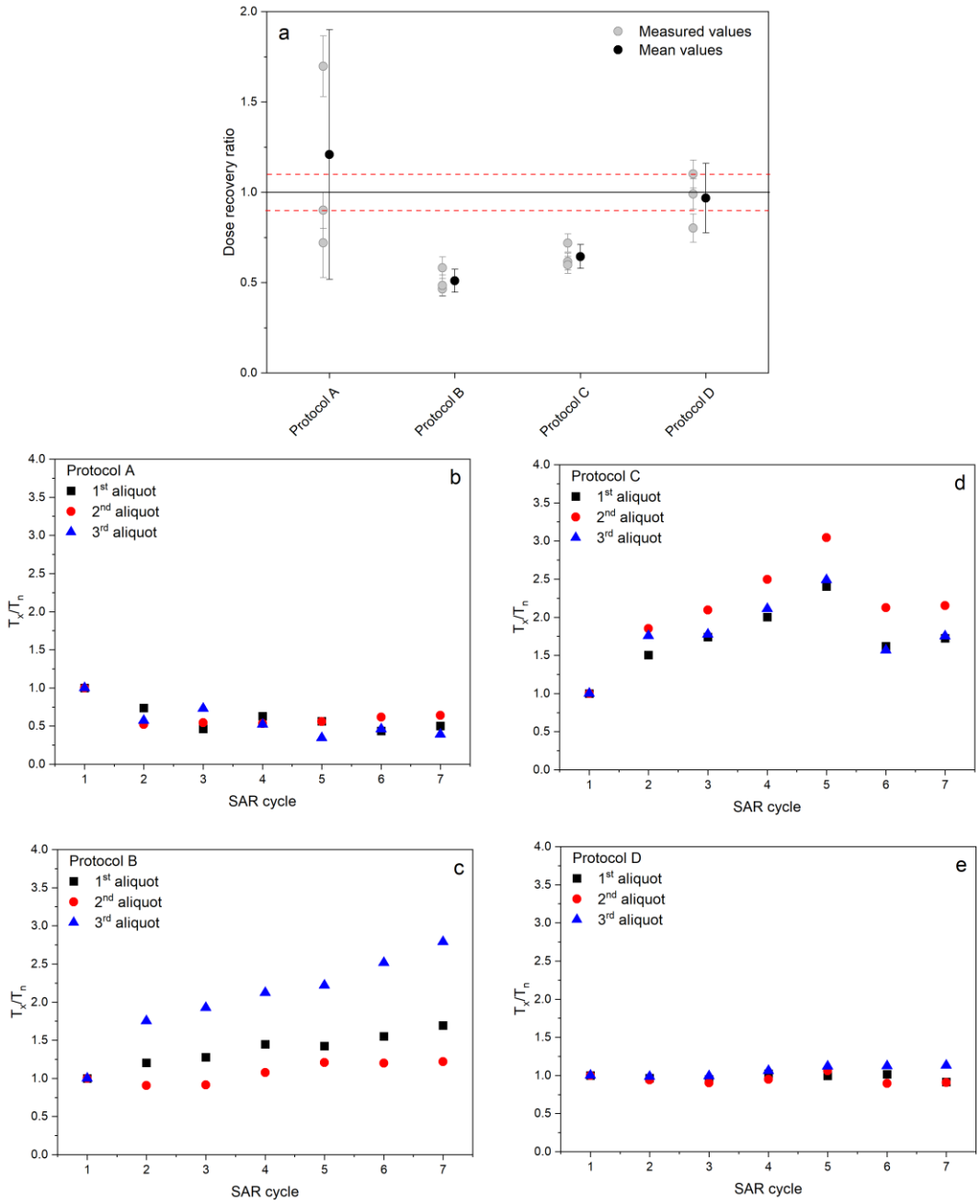

Figure S2.1: a) mean measured to given dose ratios using different SAR protocols listed in Table S2.1. Three aliquots of sample SG_3 were bleached by violet light (two VSL for 1,000 s seperated by a 10,000 s pause) prior to irradiation with a known beta dose (90 Gy). Data points in grey represent the individual aliquot values, and the mean values and standard errors are shown in black. Sensitivity change during SAR cycles (i.e., T_x/T_n) for protocol A (b), protocol B (c), protocol C (d) and protocol D (e).

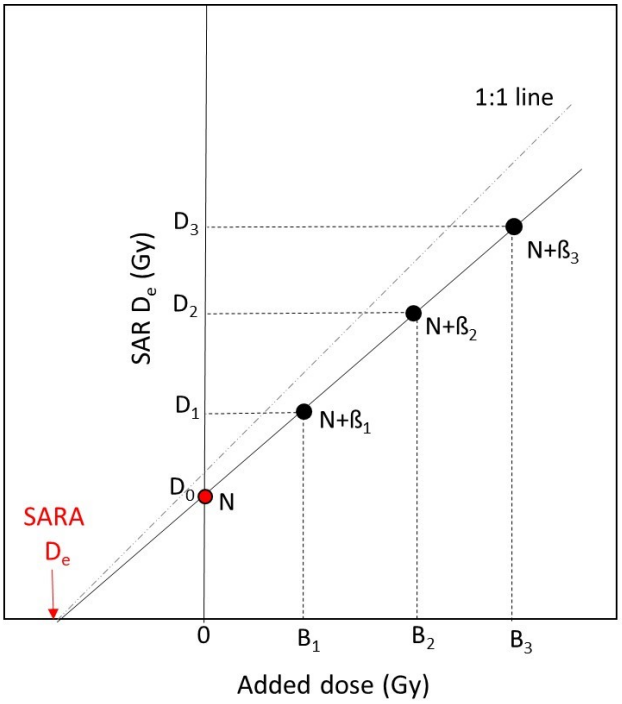

Figure S2.2: Schematic visualisation of a SAR-SARA experiment. The dots represent the SAR equivalent doses. The solid line is the linear fit of the SAR equivalent doses, and the SARA equivalent dose is obtained from extrapolating the linear fit. The grey dashed line represents the 1:1 line between the SAR equivalent dose and added dose.

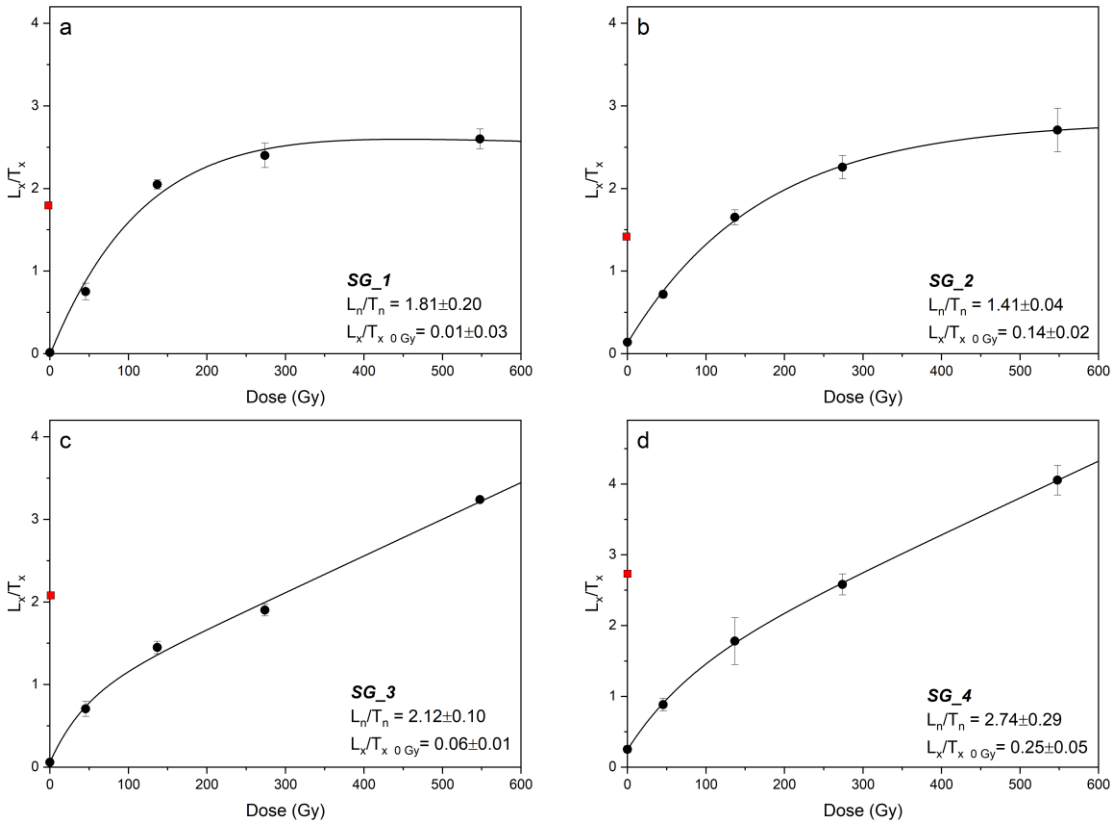

Figure S2.3: MAR dose response curves measured for all samples. The red squares denote the L_n/T_n values. After 7 days of SOL2 exposure, the sensitivity-corrected 0 Gy regenerative signal is ~10% of the initial signal intensity (L_n/T_n) for samples SG_2 (b) and SG_4 (d). However, for samples SG_1 (a) and SG_3 (c), it reduced to ~1% and ~3%, respectively.

Table S2.1: The four different SAR protocols tested using sample SG_3.

Step	Protocol A Ankjærgaard et al. (2013)	Protocol B Ankjærgaard et al. (2015)	Protocol C Ankjærgaard et al. (2016)	Protocol D Colarossi et al. (2018)	Observed
1	Dose	Dose	Dose	Dose	
2		Preheat (280°C/ 10 s)	Preheat (300°C/ 100 s)	Preheat (280°C/ 10 s)	
3	Blue bleach (280 °C/ 100 s)	Blue bleach (125 °C/ 40 s)	Blue bleach (125 °C/ 100 s)	Blue bleach (125 °C/ 40 s)	
4	VSL (125°C/ 100 s)	VSL (30 °C/ 500 s)	VSL (30 °C/ 500 s)	VSL (30 °C/ 500 s)	L_x
5				Violet bleach (200 °C/ 500 s)	
6	Test dose	Test dose	Test dose	Test dose	
7		Preheat (280°C/ 10 s)	Preheat (300°C/ 100 s)	Preheat (280°C/ 10 s)	
8	Blue bleach (270 °C/ 100 s)	Blue bleach (125 °C/ 40 s)	Blue bleach (125 °C/ 100 s)	Blue bleach (125 °C/ 40 s)	
9	VSL (125°C/ 100 s)	VSL (30 °C/ 500 s)	VSL (30 °C/ 500 s)	VSL (30 °C/ 500 s)	T_x
10	Violet bleach (280°C/ 200 s)	Violet bleach (380°C/ 200 s)	TL bleach (500°C/ 20 s)	Violet bleach (200 °C/ 500 s)	

Table S2.2: Overview of the steps in the SAR-SARA experiment on sample SG_3. The SAR protocol listed in Table 2.2b was used to estimate the single aliquot D_e.

Disc number	Treatment	SAR D_e
1,3,5	None	N
7,9,11	Beta dose	N+ ß$_1$ 90 Gy
13,15,17	Beta dose	N+ ß$_2$ 180 Gy
19,21,23	Beta dose	N+ ß$_3$ 270 Gy
25,27,29	Beta dose	N+ ß$_4$ 405 Gy

CHAPTER 3

Natural and laboratory dose response curves of quartz violet stimulated luminescence (VSL): Exploring the multiple aliquot regenerative dose (MAR) protocol

Rahimzadeh, N., Tsukamoto, S., Zhang, J., Long, H.

Published on *Quaternary Geochronology*

https://doi.org/10.1016/j.quageo.2021.101194

Author contributions

Rahimzadeh, N. Conceptualization, Methodology, Data curation, Formal analysis, Visualization, Writing- original draft, Writing- review and editing,; Tsukamoto, S. Conceptualization, Methodology, Validation, Writing- review and editing, Supervision; Zhang. J. Conceptualization, Methodology, Validation, Writing- review and editing; Long, H. Resources, Partly funding acquisition, Writing- review and editing.

ABSTRACT

Previous studies observed that the single aliquot regenerative dose (SAR) protocol is problematic for the quartz violet stimulated luminescence (VSL) signal. We therefore evaluate the reliability of multiple aliquot approaches, i.e. single aliquot regeneration and added dose (SARA) and sensitivity-corrected multiple aliquot regenerative dose (SC-MAR) protocols, for the first time using fine-grained quartz samples from a Chinese loess-palaeosol sequence in Luochuan with reference ages ranging from ~25 ka to ~1400 ka. Applying the SARA protocol on one sample with an expected natural dose of ~700 Gy, yielded a SARA D_e that was consistent with independent D_e. Although this result is very encouraging, the applicability of this method is limited to samples for which the natural dose is far from signal saturation. Using the MAR protocol, all estimated VSL ages significantly underestimate the expected ages, except the two youngest samples. We show that the observed age discrepancy is not due to the thermal instability of the signal nor to the bleaching treatment in the MAR protocol, but is related to the different shapes of the natural- and laboratory-generated dose response curves (DRCs). Unlike the natural DRC, the VSL signal continues to increase at high laboratory doses in the laboratory generated DRC; suggesting that there is additional linear growth in the laboratory DRC, which does not exist in nature. The deviation between the natural- and laboratory-generated DRCs points out that the maximum dating limit of fine-grained quartz VSL on the Luochuan section under selected measurement conditions using the MAR protocol is ~250 Gy. However, it is remarkable that the natural VSL DRC saturates at about 900 Gy, which would potentially allow dating at the Luochuan section using VSL up to ca. 300 ka.

3.1 Introduction

Quartz optically stimulated luminescence (OSL) dating is widely used to establish the chronology of Quaternary deposits (e.g. Wintle and Adamiec, 2017), but its applicability is commonly limited to ~150 Gy (Chapot et al., 2012). The violet stimulated luminescence signal (VSL) from quartz, which probes traps deeper than those accessible by blue light, has been observed to grow with doses up to about 1000 Gy (Jain, 2009), ~10 times higher than the OSL from the same grains. Further studies confirmed that the VSL signal originates from a trap associated with the TL peak at ~380 °C in quartz (Ankjærgaard et al., 2013; Hernandez and Mercier, 2015), and is thermally stable with a lifetime of $\sim 10^{11}$ years at 10 °C (Ankjærgaard et al., 2013, 2015) with no athermal loss (Ankjærgaard et al., 2013);

thus giving the potential to extend the age range of quartz luminescence dating to cover the full Quaternary period.

The single aliquot regenerative dose (SAR) method (Murray and Wintle, 2000) for the VSL signal showed limited success. Few studies observed agreement between the estimated SAR VSL and OSL equivalent doses (D_es) up to ~200 Gy (Ankjærgaard et al., 2013; Porat et al., 2018). However, several studies indicated an underestimation of ~50% or more for samples with larger natural doses (Ankjærgaard et al., 2015, 2016; Morthekai et al., 2015; Colarossi et al., 2018; Sontag-González et al., 2020). Ankjærgaard et al. (2016) concluded that the SAR protocol for VSL dating is compromised by trapping sensitivity changes induced by heating. Indeed, the SAR procedure is designed to monitor and correct the potential sensitivity changes that occur during multiple regeneration cycles by measuring the response to a test dose. However, any sensitivity change that occurs before the first test dose measurement is not detected (Murray and Wintle, 2000). As a result, other approaches, i.e. single aliquot regeneration and added dose (SARA; Mejdahl and Bøtter-Jensen, 1994), multiple aliquot additive dose (MAAD; Aitken, 1998) and multiple aliquot regenerative dose (MAR; Aitken, 1998) protocols have been carried out in an attempt to overcome this obstacle (Ankjærgaard et al., 2016; Colarossi et al., 2018; Ankjærgaard, 2019). Ankjærgaard (2019) demonstrated good agreement between obtained VSL ages and independent chronology up to ~500 ka and 900 ka using the MAAD and MAR protocols, respectively.

In this study, we investigate 13 fine-grained quartz samples from Luochuan, China, with depositional ages between ~25 and ~1400 ka (Ding et al., 2002) with the aim of testing the applicability of multiple aliquot approaches, i.e. SARA and MAR, to overcome the cumulative sensitivity change of the SAR protocol for VSL. The standardised growth curve (SGC) procedure developed by Li et al. (2015) is carried out in order to measure old samples with high D_e values for a limited measurement time. The impacts of the thermal lifetime of the signal and light source of bleaching on the MAR dose response curve (DRC) are investigated. Finally, we take the opportunity to construct the natural DRC to determine the maximum limit of VSL at this site, and compare it to the laboratory-generated DRC in order to test their similarity.

3.2 Material and methods

3.2.1 Sample description and preparation

For this study, a total of 13 luminescence samples were collected from the Luochuan Potou section of the Chinese Loess Plateau (Fig. 3.1); ranging from unit L1 (11–73 ka) to L15 (1240–1263 ka) (Ding et al., 2002). Of these, four samples (LUM 3704, 3707, 3710, 3712) were also used in Li et al. (2018), Tsukamoto et al. (2018) and Richter et al. (2020) for the investigation of the K-feldspar IRSL and quartz electron spin resonance (ESR) signals utilising sand-sized grains.

All sample preparation was carried out under subdued red light conditions. Chemical treatments with hydrochloric acid (HCl; 10%) for 4 h, followed by overnight soaking in sodium oxalate ($Na_2C_2O_4$; 0.1 N) and hydrogen peroxide (H_2O_2, 30%) were conducted to remove carbonate, mineral aggregates and organic matter, respectively. The fine-grained fraction (4–11 µm) of the samples was separated by repeated settling and washing using a centrifuge (cf. Frechen et al., 1996). The extracted 4–11 µm fraction was further etched using hydrofluorosilicic acid (H_2SiF_6) for 5 days to extract the quartz fraction. For luminescence measurement, the quartz extracts were settled from suspension in deionized water onto aluminum discs (2 mg per disc).

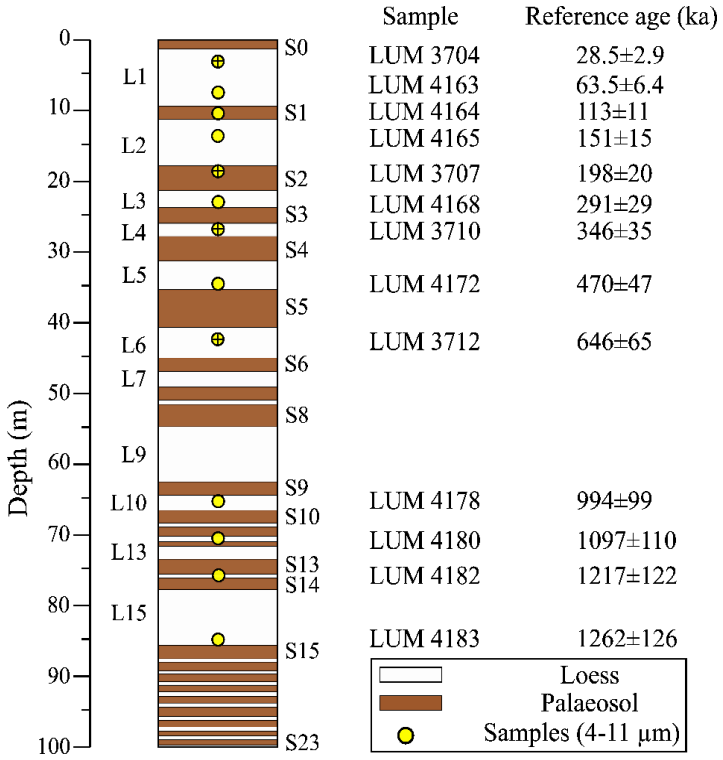

Figure 3. 1: Graphic sedimentary log of the Luochuan section, the sampling position and reference ages (Ding et al., 2002). Samples marked as crossed circle were also investigated by Li et al. (2018), Tsukamoto et al. (2018) and Richter et al. (2020).

3.2.2 Luminescence instrumentation and measurement protocol

All luminescence measurements were performed using a TL/OSL Risø DA-20 reader, equipped with an automated stimulation head (DASH) (Lapp et al., 2015), which is adapted for stimulation with both blue LEDs (470 nm; 80 mW cm^{-2}) and a violet laser diode (405 nm; 100 mW cm^{-2}). The latter includes a combination of a laser line bandpass filter, which transmits 402±15 nm, and an ITOS GG395 glass filter (3 mm) to cut off its short wavelength tail. The aliquots were stimulated with 80% of the maximum power of the violet laser diode, and the resulting VSL signals were detected through a combination of 5-mm Hoya U340 and a Semrock brightline 340 nm (FF01-340/26) filters. Laboratory irradiation was carried out using a $^{90}Sr/^{90}Y$ beta source, with a dose rate of 0.069 Gy s^{-1} for fine grains.

The VSL protocol used in this study (Table 3.1) is based on Colarossi et al. (2018), which includes an additional bleaching step (VSL at 200 °C, 500 s) after each regenerative and test dose measurement to reduce recuperation and minimise sensitivity changes (Hernandez and Mercier, 2015), but with two main differences: (i) violet stimulation at 125 °C (rather than 30 ◦ C) to avoid re-trapping of charges in the 110 °C TL peak of quartz, and (ii) VSL bleach at 240 °C (instead of 200 °C) after each VSL measurement, as this showed the lowest recuperation value. All DRCs were fitted with a double saturating exponential function (Fig. 3.2), and equivalent doses were determined using the initial VSL signal integrated over the first 2.5 s (first 5 channels) and subtracting an early background from the following 15 s (6–36 channels) to minimise the contribution from re-trapping in the later part of the decay curves (Ankjærgaard et al., 2013, 2016).

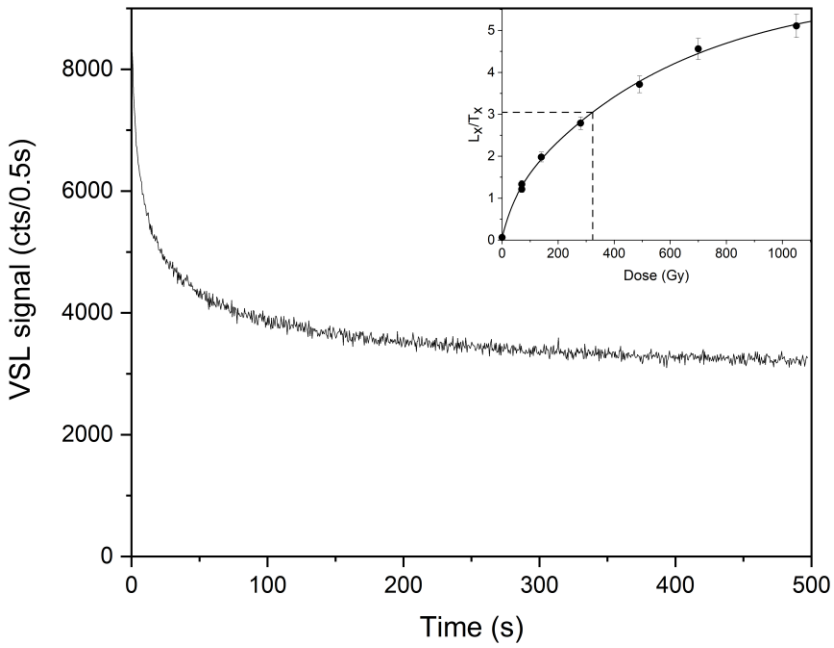

Figure 3.2: Example of natural VSL decay curve and dose response curve (inset) for one aliquot of sample LUM 3707 from the SAR-SARA experiment.

Table 3.1: VSL dating protocol used in this study. For the MAR approach, a 7-day SOL2 bleaching was carried out prior to step 1. For the natural measurement, the given dose in step 1 is 0 Gy. For the SAR approach, the protocol is returned to step 1 after step 10.

Step	VSL protocol	Observed
1	Given dose (x Gy)	
2	Preheat (280 °C, 10 s)	
3	Blue bleach (125 °C, 40 s)	
4	VSL (125 °C, 500 s)	L_x
5	Violet bleach (240 °C, 500 s)	
6	Test dose	
7	Preheat (280°C, 10 s)	
8	Blue bleach (125 °C, 40 s)	
9	VSL (125 °C, 500 s)	T_x
10	Violet bleach (240 °C, 500 s)	

3.2.3 Environmental dose rates and natural expected doses

The radionuclide concentrations of U, Th and K for all studied samples were determined using high-resolution gamma spectrometry; the results are summarized in Table 3.2. The environmental dose rates were subsequently calculated using the conversion factors of Liritzis et al. (2013), beta attenuation factor of Guérin et al. (2012), and assuming a water content of 15±5% and 20±5% for loess and palaeosol samples, respectively (Lu et al., 2007). A small cosmic dose rate of <0.2 Gy ka^{-1} was calculated based on Prescott and Hutton (1994) and incorporated into the total dose rate. The a-value was taken as 0.04±0.02 for fine-grained quartz (Rees-Jones and Tite, 1997). Note that for those samples (LUM 3704, 3707, 3710, 3712), which were investigated in the Li et al. (2018), Tsukamoto et al. (2018) and Richter et al. (2020), the mean radionuclides concentrations from both gamma spectrometry and neutron activation analysis (NAA) methods were used in their study, which were in agreement.

The expected ages arise from a linear interpolation of two boundary ages (i.e. loess-palaeosol transition) from the Chiloparts record (Ding et al., 2002), with an assumed 10% uncertainty. The expected natural doses were then obtained by multiplying the reference age of each sample by its measured dose rate (Table 3.2).

3.3 SARA VSL measurements

The conventional method of obtaining D_e using a SAR protocol has been proven problematic for the VSL signal, due to trapping sensitivity change between the natural and all subsequent regenerated VSL signals induced by the first preheating (Ankjærgaard et al., 2016). The effect of preheating on the trapping efficiency can be circumvented, if laboratory irradiations are given prior to heating of the sample. To test the validity of this, the SARA approach, which is a combination of single and multiple aliquot methods (Mejdahl and Bøtter-Jensen, 1994), was conducted. In this study, SAR protocol in combination with the SARA experiment, i.e. SAR-SARA, was used (Wallinga et al., 2000; Kars et al., 2014; Tsukamoto et al., 2017). In the SAR-SARA procedure, prior to the natural luminescence measurement, a range of known doses are added to a group of aliquots that retained their natural signal, except one group which does not receive any additional dose. The equivalent dose for each group is measured using the SAR protocol. The measured D_es are plotted as a function of added dose, giving a linear relationship between the added dose and SAR D_e (Fig. 3.3), and the intercept on the horizontal axis represents the SAR-SARA D_e. Any sensitivity change is reflected in the slope of the linear regression; if

the sensitivity change in the SAR protocol is corrected properly, the slope of the linear regression should be unity. The slope of a SAR-SARA regression line is therefore equivalent to the dose recovery ratio (Kars et al., 2014; Tsukamoto et al., 2017). In the case of failure of the sensitivity correction, the slope deviates from unity and the measured D_e does not reflect the natural plus added dose. However, in all cases, the estimated SARA D_e is independent of sensitivity change (Buylaert et al., 2006; Kars et al., 2014).

In this study, SAR-SARA measurements were carried out on sample LUM 3707 with an expected natural dose of ~700 Gy. 21 aliquots were divided into 7 batches with 3 aliquots in each. Except for the first batch, in which the natural D_e was estimated with the SAR protocol (Table 3.1), for other batches a range of beta doses (70 Gy, 140 Gy, 210 Gy, 280 Gy, 350 Gy and 490 Gy) were added to the natural aliquots prior to any treatment. Two aliquots with the 210 Gy and 350 Gy added dose were excluded from the analysis based on the recycling ratio, which was outside ±10% from unity. The mean recycling ratio and recuperation was 0.99±0.03 (n=19) and 1.8±0.5% (n=21), respectively. The results are shown in Fig. 3.3, giving a SAR-SARA D_e of 581±130 Gy, which is consistent with the expected D_e of ~700 Gy. Note the slope of 0.54 0.09 (Fig. 3.3), which shows a large sensitivity change not corrected by the SAR protocol. This result is, however, contradicting the observation of Colarossi et al. (2018), who showed a significant dose underestimation for a sample with a large natural dose (~463 Gy) using the SARA protocol. Although the SARA procedure produced a relatively good agreement between VSL D_e and independent D_e, this method might not be ideal for dating older sediments. With the SARA protocol, the increase of luminescence signal by adding doses on top of the natural dose is necessary. Therefore, this method is only suitable for samples for which the natural dose is far from signal saturation, and might not be the best choice for dating old sediments. Moreover, this method is time consuming.

Table 3.2: Summary of dosimetry data, expected natural equivalent doses and dating results using the MAR protocol. The reference ages were calculated following Ding et al. (2002) with a presumed 10 % uncertainty.

LUM No.	Unit	Depth (m)	U (ppm)	Th (ppm)	K (%)	Dose rate (Gy/ka)	Expected age (ka)	Expected dose (Gy)	MAR VSL dose (Gy)	MAR VSL age (ka)
3704	L1	3.5	2.8±0.1	11.5±0.2	1.9±0.1	3.56±0.18	28.5±2.9	102±11	111±11	31.1±3.5
4163	L1	7.9	2.6±0.2	11.4±0.6	1.9±0.1	3.33±0.18	63.5±6.4	212±24	171±14	51.3±5.1
4164	S1	10.9	2.9±0.2	13.2±0.7	2.1±0.1	3.65±0.18	113±11	411±46	247±17	67.7±5.7
4165	L2	13.9	2.5±0.2	11.2±0.6	1.9±0.1	3.37±0.18	151±15	507±57	342±29	102±10
3707	S2	18.3	2.8±0.1	13.8±0.2	2.1±0.1	3.63±0.18	198±20	719±80	382±27	105±9
4168	L3	23.1	2.2±0.1	11.1±0.6	1.8±0.1	3.15±0.17	291±29	919±104	331±29	105±11
3710	L4	26.6	2.5±0.1	11.7±0.2	1.9±0.1	3.36±0.17	346±35	1161±131	454±36	135±13
4172	L5	34.9	2.4±0.1	11.5±0.7	1.9±0.1	3.30±0.17	470±47	1553±176	636±50	193±18
3712	L6	42.6	2.5±0.1	11.2±0.2	1.8±0.1	3.20±0.17	646±65	2069±233	583±48	182±18
4178	L10	65.2	2.8±0.2	13.3±0.8	2.2±0.1	3.80±0.20	994±99	3774±426	1196±93	315±30
4180	L12	71.1	2.7±0.2	11.9±0.7	1.9±0.1	3.38±0.18	1097±110	3711±421	1914±101	566±43
4182	L14	76.3	2.5±0.2	11.3±0.6	1.8±0.1	3.19±0.17	1217±122	3886±441	1776±112	556±46
4183	L15	85.6	2.2±0.1	12.1±0.7	2.0±0.1	3.36±0.18	1262±126	4239±480	1719±88	512±38

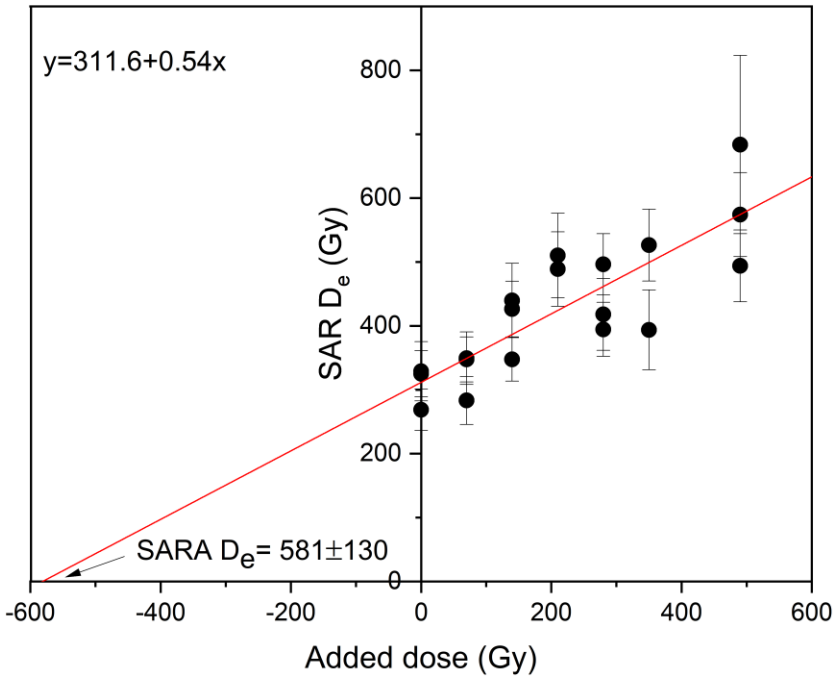

Figure 3.3: Result of SARA procedure for sample LUM 3707 with an expected natural dose of ~700 Gy. The red line is the linear fit of the SAR equivalent doses.

3.4 MAR VSL measurements

Despite the encouraging result of the SARA approach in the previous section, this method is not appropriate for samples for which the natural dose is close to saturation. It is therefore of interest to test the MAR protocol (Aitken, 1998). Unlike the SAR protocol, which involves a series of regeneration cycles on the same aliquot, the MAR protocol measures a luminescence signal of each aliquot only twice; once for a natural/regeneration dose, and again for a test dose to measure the aliquot's sensitivity (Chapot et al., 2012). In this study, a sensitivity-corrected MAR protocol (SC-MAR; Lu et al., 2007) was used, where the sensitivity corrected natural signal (L_n/T_n) was interpolated onto the DRC constructed by the sensitivity corrected regenerative dose signal (L_x/T_x) from multiple aliquots. The SGC approach was used, in order to reduce the amount of instrument time required for obtaining large chronological data. Four samples (LUM 3704, 3707, 3710, 4168) were used to construct the MAR SGC. A total of 80 aliquots (16 from LUM 3704, 24 from LUM 3707, 20 from LUM 3710 and 20 from LUM 4168) were bleached in the solar simulator (Hönle SOL2) for 7 days (Ankjærgaard, 2019). Three aliquots of sample LUM 3707 (with an expected dose of ~700 Gy) were used to determine the residual dose remaining after bleaching using the SAR protocol, and yielded a negligible residual dose of ~10 Gy (~1.5% of expected D_e); indicating the efficiency of the bleaching treatment in resetting the VSL signal (assuming that the residual dose is proportional to the accumulated dose). The remainder of the bleached

aliquots were then split into several batches with 4 aliquots in each, exposed to different regenerative doses ranging from 0 to ~5000 Gy and measured using the protocol in Table 3.1 with a fixed test dose of 200 Gy.

Fig. 3.4a shows the MAR SGC for individual aliquots from various samples. To reduce the variation of aliquots between different samples, the least-square normalisation (LS-normalisation) procedure was applied with the "numOSL" R package (Li et al., 2016; Peng and Li, 2017) to the data in Fig. 3.4a. This resulted in the normalised data and best fitted curve shown in Fig. 3.4b. This method involves an iterative scaling and fitting procedure that takes all of the L_x/T_x ratios into account when constructing the SGC (Li et al., 2016). To estimate the D_e values, a group of aliquots (12 aliquots for each sample) were used to measure the natural signals (L_n) and signals of fixed test dose of 200 Gy (T_n). Another group of fresh aliquots (6 aliquots per sample) were bleached for 7 days in the solar simulator and then given a regenerative dose (D_r) close to the expected D_e and a subsequent test dose of 200 Gy. The average sensitivity-corrected natural signal (L_n/T_n) was then normalised by the average sensitivity-corrected regenerative-dose signal (L_r/T_r) with the following equation:

$$f(D_e) = \left(\frac{L_n/T_n}{L_r/T_r}\right) * f(D_r) \tag{3.1}$$

where the $f(D_r)$ is the corresponding functional value of D_r on the SGC. The re-normalised natural signal ($f(D_e)$) was projected on the LS-normalised MAR SGC to obtain D_e. The SGC construction and D_e determinations were performed using the R package "numOSL" (Peng and Li, 2017).

The MAR VSL D_e values range between 111±11 Gy and 1914±101 Gy, with corresponding ages ranging from 31.1±3.5 ka to 566±43 ka (Table 3.2). When the VSL ages are compared with the independent ages (Fig. 3.5), all estimated VSL ages significantly underestimate the independent age control, except sample LUM 3704 and 4163. It contradicts the recent study by Ankjærgaard (2019), who conducted MAR dating by constructing DRCs using two coarse grain quartz samples from the Luochuan section, with expected natural doses of 250 and 2550 Gy (hereafter DRCs termed MAR_{250} and MAR_{2550}) and produced coarse-grained quartz VSL ages in agreement with independent ages up to ~350 and ~900 ka for MAR_{250} and MAR_{2550}, respectively.

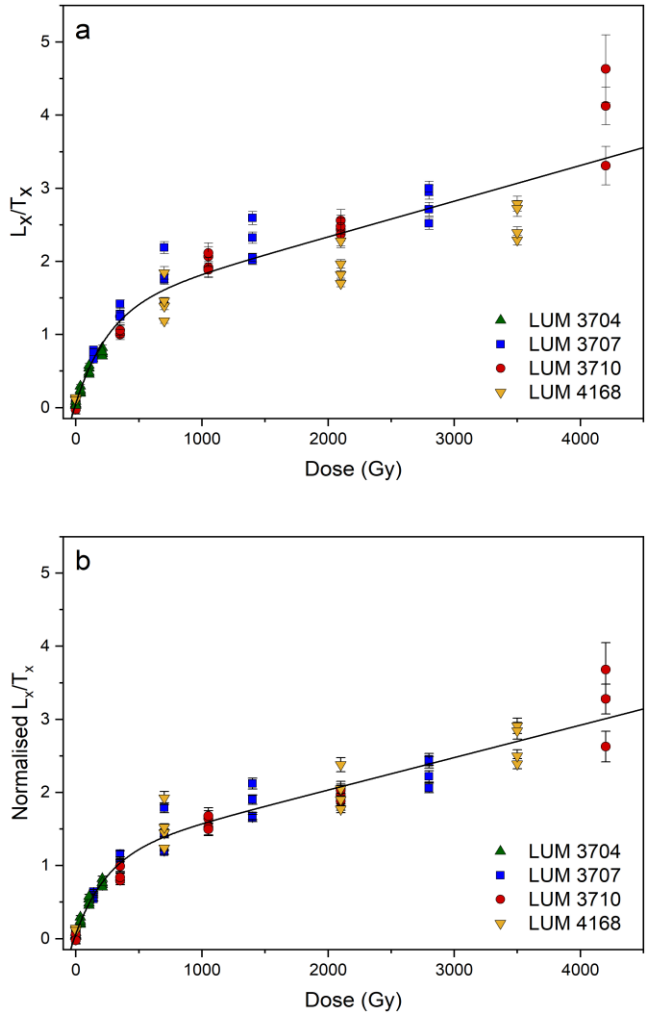

Figure 3.4: (a) MAR L_x/T_x ratios for the four samples (LUM 3704, 3707, 3710, and 4168), plotted as a function of laboratory dose; (b) same data as in panel (a) after LS-normalisation.

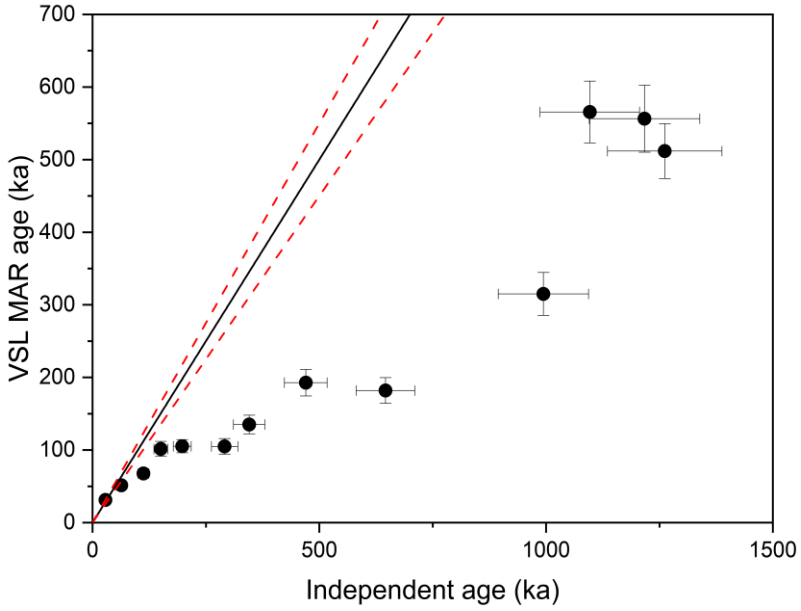

Figure 3. 5: VSL MAR ages as a function of the expected ages provided by the independent chronology. The solid line is 1:1 line, and the dashed red lines represent ±10%.

3.4.1 Effects of thermal stability

One potential explanation for age underestimation in luminescence dating is the poor thermal stability of the signal. The thermal lifetime of the VSL signal for sand-sized quartz from the Netherlands and Israel has been investigated by Ankjærgaard et al. (2013, 2015), yielding the thermal lifetime of ~10^{11} years at 10 °C. However, various lifetimes of the quartz OSL signal have been reported; the coarse silt-sized (45–63 μm) quartz from the Luochuan loess section has a lifetime of about 0.3 Ma at 20 °C (Lai and Fan, 2014), much shorter than the previously reported lifetime of ~850 Ma at 20 °C for sand-sized quartz from Australia (Wintle and Murray, 1998). In a single-grain study on sand sized quartz (180–212 μm) from North China, Rui et al. (2019) showed that there was a significant inter-grain variation on the lifetimes of OSL signals of quartz grains within one sample, and age underestimation was caused by the low thermal stability of the OSL signal. Therefore, similar variations in the thermal stability of the VSL signal may equally exist.

An isothermal annealing experiment was carried out in order to calculate the thermal lifetime of the VSL signal for fine-grained quartz from Luochuan. An aliquot of sample LUM 3707 was irradiated with 140 Gy, preheated to 280 °C for 10 s, bleached by blue light at 125 °C for 40 s, and held at different temperatures between 240 and 320 °C (with a 20 °C increment) for various holding times (up to 20,000 s at 240 °C) before the violet stimulation at 125 °C. The VSL response to a test dose of 70 Gy was used for sensitivity correction. Since the thermal decay of the VSL signal does not follow first order kinetics, the effective thermal lifetime (τ_{eff}) was derived using the following equation from Ankjærgaard et al. (2013); stretched hyperbolic function, which has been later used in fitting feldspar luminescence signals (termed general order kinetic; Guralnik et al., 2015a,b):

$$I(t) = (1 + ct/\tau_{eff})^{-1/c}, \qquad c > 0 \tag{3.2}$$

where $I(t)$ is the intensity of the VSL signal at time t, and c is a dimensionless parameter accounting for deviation from first-order kinetics. The isothermal decay curves are shown in Fig. 3.6; the inset shows the kinetic parameters (E and s) of the VSL signal. The fitted kinetic order (c+1) is ~1.5 (Fig. 3.6), and even if the data were forced to fit with the first-order kinetics model, the parameters still gave similar values of trap depths and thermal stabilities.

The thermal lifetime of the VSL signal at a mean annual air temperature (10 °C, Hu et al., 2015; Chapot et al., 2016) was calculated as ~ 4.6×10^{12} years, consistent with lifetime estimates for the VSL signal of sand-sized quartz (i.e. 10^{11} years, Ankjærgaard et al., 2013, 2015), and is thus well beyond the age of interest for dating. This suggests that the thermal instability of the signal is not responsible for the observed age underestimation.

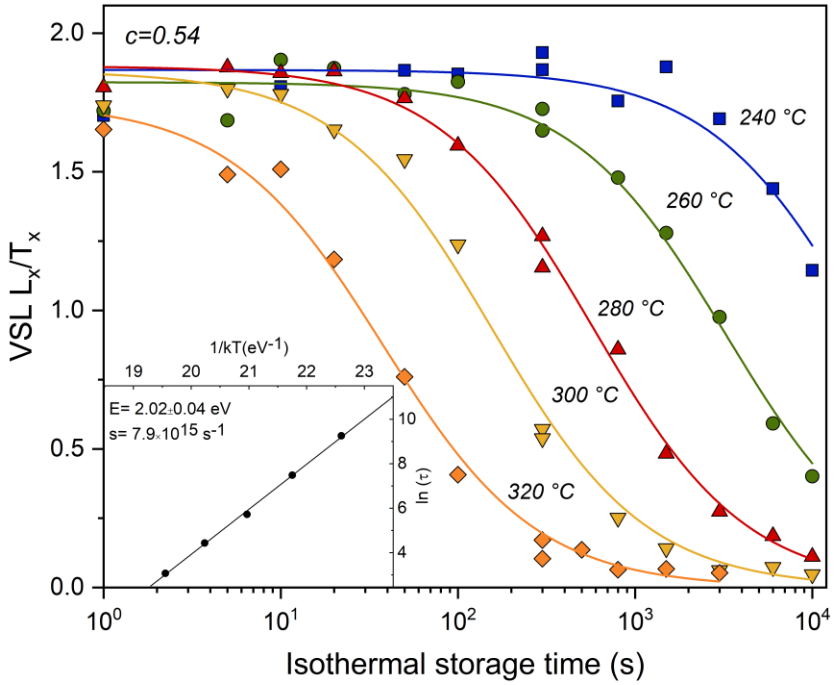

Figure 3.4: Isothermal heating experiments for sample LUM 3707 at temperatures between 240 and 320 °C. The data was fitted using a stretched hyperbolic equation (Ankjærgaard et al., 2013; their equation (2)), the inset shows the kinetic parameters (E and s) of the VSL signal. The curve fitting was carried out with the Origin 2020 software using an iterative Levenberg-Marquardt algorithm.

3.4.2 Effects of the bleaching source

Choi et al. (2009) studied the dependence of the dose recovery ratio of the quartz OSL signal on the types of bleaching sources (i.e. blue LEDs, solar simulator and natural light). They concluded that a sensitivity change is induced by long-time solar simulator bleaching, which resulted in the underestimation of the measured to given dose ratio. Therefore, dose recovery tests were performed on sample LUM 3707 using the SAR protocol with different bleaching sources, i.e. SOL2 and violet light, to see whether there are differences in dose recovery results. The aliquots were bleached with SOL2 (7 days) or violet light (two rounds of violet light stimulation at room temperature for 1000 s separated by a 10,000 s pause) and irradiated with a beta dose of 140 Gy, 280 Gy, 560 Gy and 840 Gy. Three aliquots were measured for each given dose using the SAR protocol (Table 3.1) with a fixed

test dose of 10% of the given dose for each bleaching treatment. Three bleached aliquots received no laboratory dose and were used to determine the residual dose remaining after bleaching. The residual dose was 9.8±2.0 Gy and 18.2±2.2 Gy for SOL2 and violet light bleaching, respectively, and was subtracted from the individual D_e values measured for all given doses. Mean dose recovery ratios range from 0.64±0.04 to 0.95±0.10 for SOL2 bleaching (Fig. 3.7a) and show an apparent trend of increasing dose recovery ratio with larger given dose. Similar underestimation was reported by Choi et al. (2009) for quartz OSL signal. In contrast, in the case of violet light bleaching, the given doses were successfully recovered for all the given doses, except the lowest given dose (140 Gy), for which the dose recovery ratio is more than 10% from unity (1.14 ± 0.01) (Fig. 3.7b).

To confirm whether the bleaching procedure in this study is the reason for age underestimation, the MAR DRC for LUM 3707 was also produced when using violet light as a bleaching source (Fig. 3.7c). The estimated D_e (284±12 Gy) is smaller than the value obtained using SOL2 bleaching, and it still significantly underestimates the expected D_e, i.e. ~700 Gy; suggesting that sensitivity change caused by bleaching by the SOL2 is not responsible for the age underestimation.

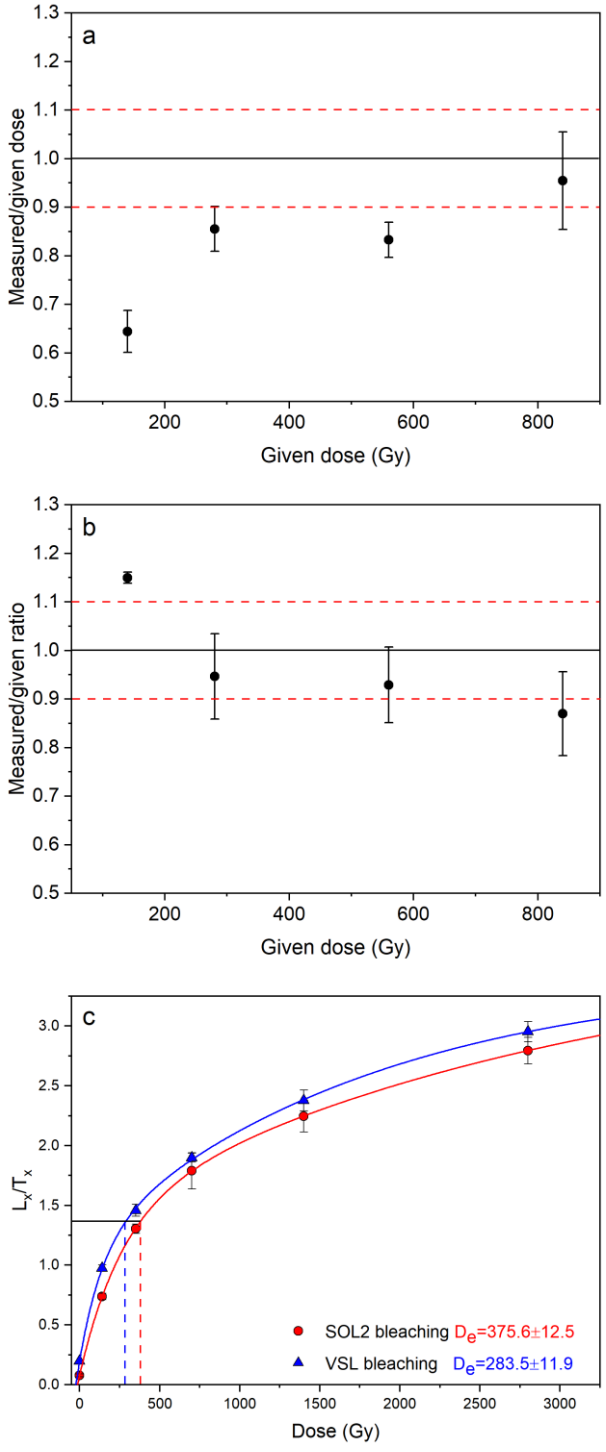

Figure 3.5: Mean measured to given dose ratios using the SAR protocol for sample LUM 3707 for given doses ranging between ~140 Gy and ~840 Gy with a fixed test dose of 10% of given dose and with residual dose subtraction. The aliquots were bleached by (a) SOL2 (7 days) and (b) violet light (two VSL for 1000 s separated by a 10,000 s pause); (c) MAR DRCs for sample LUM 3707 using SOL2 (filled circle) and VSL (filled triangle) bleaching treatment. Note that the data from section 4 was used for the construction of the MAR DRC using SOL2 bleaching.

3.4.3 Comparison of natural and laboratory DRCs

The comparison of natural and laboratory generated DRCs has so far been attempted in this study site for different luminescence and ESR signals (e.g. OSL: Chapot et al., 2012; thermally transferred OSL (TT-OSL): Chapot et al., 2016; feldspar post-infrared (IR) infrared stimulated luminescence at 225 °C ($pIRIR_{225}$) and pulsed IR at 50 °C (Pulsed IR_{50}): Li et al., 2018; ESR: Tsukamoto et al., 2018; VSL: Ankjærgaard et al., 2016; Ankjærgaard, 2019), and it showed that the onset of deviation between natural and laboratory DRCs at a certain dose caused large age underestimation beyond that dose. To investigate whether this dissimilarity in shapes of natural and laboratory DRCs could be the cause of the age underestimation in this study, the natural DRC was built.

Following the approach of Chapot et al. (2012), the natural DRC was constructed by plotting the L_n/T_n signals against the expected accumulated dose, and then was fitted with a double saturating exponential function (Fig. 3.8, solid line) yielding D_0 values of ~220 and ~860 Gy. The upper dating limit is defined by the characteristic saturation dose ($2D_0$), as suggested by Wintle and Murray (2006) for single saturating exponential growth. However, using the $2D_0$ criterion is not appropriate for dose response curves fitted with a double saturating exponential function. The maximum limit can also be derived by calculating the dose corresponding to the signal intensity that is 15% below the signal intensity at saturation (Wintle and Murray, 2006). For the natural VSL DRC, this value is ~900 Gy; much smaller than the value reported for coarse-grained quartz in Ankjærgaard (2019) (~2700 Gy), though she used the $2D_{0,2}$ saturation criteria. It should be noted that, if the natural DRC is fitted with a single saturating exponential function, the corresponding $2D_0$ value is ~950 Gy, which is close to that obtained from 85% of the saturated signal intensity. With the average dose rate of 3 Gy/ka from the Luochuan section, the upper dating limit of the VSL signal at this site was estimated to be ca. 300 ka under selected protocol and measurement conditions. The constant vertical offset of 0.19±0.14 in the natural DRC (Fig. 3.8, solid line), suggests a difficult-to-bleach component of the VSL signal, similar to that calculated in Ankjærgaard (2019) (i.e. 0.20±0.03). From the fitted natural curve, a ~45 Gy residual dose was calculated, which is slightly larger than that estimated in a previous study (i.e. ~30 Gy; Ankjærgaard, 2019).

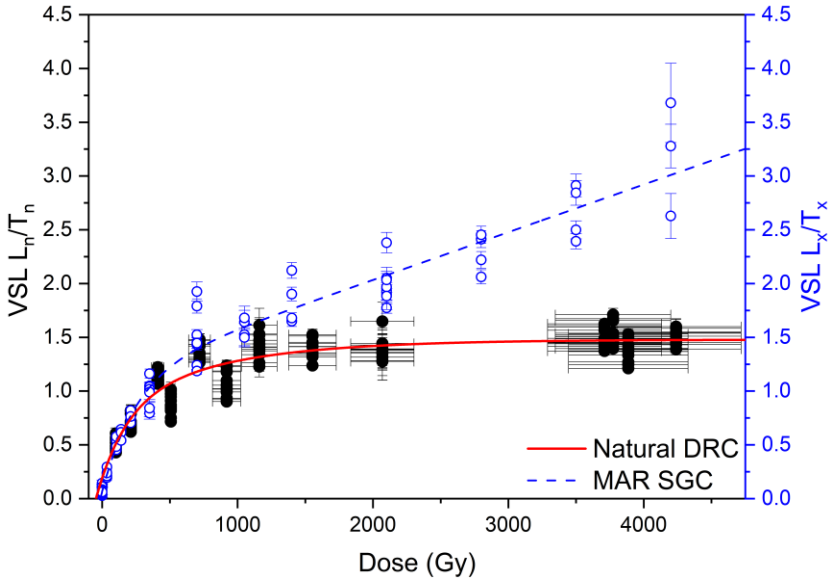

Figure 3. 6: The MAR SGC from Fig. 3.4b in dashed blue re-plotted with a natural VSL DRC. The data was fitted with the double saturating exponential function. The natural DRC has characteristic dose of $D_{0,1}$–220 Gy and $D_{0,2}$–860 Gy, and the offset of 0.2±0.1. The MAR SGC has value of $D_{0,1}$–250 Gy and $D_{0,2}$–139,000 Gy. The large difference between $D_{0,2}$ of natural DRC and MAR SGC results in age underestimation.

The MAR DRC from Fig. 3.4b is replotted with the natural DRC (Fig. 3.8, dashed line). It shows that the natural and MAR DRCs start to diverge in shape after ~250 Gy. MAR DRC has a $D_{0,1}$ of ~250 Gy and $D_{0,2}$ of ~139,000 Gy; the large difference between $D_{0,2}$ of natural and MAR DRCs results in age underestimation. Unlike the natural DRC, the laboratory generated MAR DRC continues to grow above the saturated L_n/T_n value observed in nature (a value of ~1.3; 15% below the signal intensity at saturation), suggesting the linear growth of the laboratory DRC could be a laboratory artefact (Lai, 2009; Chapot et al., 2012). An additional growth component of the quartz OSL at high doses has also been previously reported (Roberts and Duller, 2004; Murray et al., 2008; Lai, 2009; Lowick and Preusser, 2010; Lowick et al., 2010; Chapot et al., 2012). Possible origins of the linear component in the high dose response region could be an additional trap or luminescence recombination center (Lai et al., 2008), defect creation caused by large laboratory irradiation dose (Chawla et al., 1998), or the saturation of a competing nonradiative recombination center (Woda et al., 2002; Lowick et al., 2010).

3.5 Discussion and conclusions

In this study, 13 fine-grained quartz samples with ages up to 1.2 Ma from the Luochuan section were used for VSL dating. The SARA approach was carried out on one sample with an expected natural dose of ~700 Gy. The SARA estimated D_e was consistent with independent D_e. Although this method might not be the preferred protocol for dating old sediments, further investigations are needed, as the SARA protocol appears to be a promising approach in extending the dating range of quartz.

The application of the MAR protocol for D_e estimation resulted in significant age underestimation beyond ~100 ka. We have shown that age underestimation cannot be attributed to either low thermal stability of the signal or bleaching treatment prior to the MAR protocol, but is related to the shape dissimilarity between the natural and regenerated DRCs; they start to diverge in shape after ~250 Gy. In the laboratory-generated MAR DRC, the normalised VSL signals continue to grow at high laboratory doses, whereas the natural DRC reaches a saturation level (Fig. 3.8), suggesting that the additional linear growth of the laboratory DRC might be a laboratory artefact and does not occur in nature. A recent study by Ankjærgaard (2019) showed that the MAR DRCs using two coarse grain quartz samples with an expected natural dose of 250 Gy (MAR_{250}) and 2550 Gy (MAR_{2550}) from the same region (Luochuan section) can reproduce the shape of the natural DRC, with 45% (MAR_{250}) and 81% (MAR_{2550}) of all samples yielding MAR ages in agreement with independent age control. However, it has to be noted that the coarse quartz fraction was used in her study. Different saturation characteristics, and subsequently different growth patterns of DRC for different grain size fractions of quartz, and consequential age discrepancies have been reported by several comparative studies on quartz OSL signal (e.g. Timar-Gabor et al., 2011; 2015a; Timar-Gabor and Wintle, 2013; Constantin et al., 2015; Anechitei-Deacu et al., 2018); demonstrating a lower D_e estimation and higher characteristic saturation dose for the fine grain fraction. Additionally, Timar-Gabor et al. (2015b) showed that the difference between natural and laboratory OSL DRCs was more pronounced in the case of fine grains. These quartz OSL based studies suggested that the additional component in the high dose region of laboratory DRC cannot be considered reliable and should be used cautiously; especially in the case of fine grain fractions. However, since no direct comparison between fine grain and coarse grain fractions from the same sample has been carried out for VSL signal, further investigation is required to confirm these observations, to test the

reliability of VSL dating using quartz of different grain sizes, and to understand the mechanism underlying this grain-size dependency of saturation characteristics.

Acknowledgments

We thank Petra Posimowski and Sabine Mogwitz for sample preparation and gamma spectrometry measurements. Gwynlyn Buchanan is thanked for language corrections. Jingran Zhang, Zhong He and Linhai Yang are thanked for their assistance in the field. We also thank both anonymous reviewers for their constructive comments and suggestions. This work was partially supported by the National Natural Science Foundation of China (No. 41977381).

References

Aitken, M.J., 1998. An Introduction to Optical Dating: the Dating of Quaternary Sediments by the Use of Photon-Stimulated Luminescence. Oxford University Press.

Anechitei-Deacu, V., Timar-Gabor, A., Constantin, D., Trandafir-Antohi, O., Del Valle, L., Fornós, J.J., Gómez-Pujol, L.L., Wintle, A.G., 2018. Assessing the maximum limit of SAR-OSL dating using quartz of different grain sizes. Geochronometria 45, 146-159.

Ankjærgaard, C., Jain, M., Wallinga, J., 2013. Towards dating quaternary sediments using the quartz violet stimulated luminescence (VSL) signal. Quat. Geochronol. 18, 99-109.

Ankjærgaard, C., Guralnik, B., Porat, N., Heimann, A., Jain, M., Wallinga, J., 2015. Violet stimulated luminescence: geo-or thermochronometer? Radiat. Meas. 81, 78-84.

Ankjærgaard, C., Guralnik, B., Buylaert, J.-P., Reimann, T., Yi, S.W., Wallinga, J., 2016. Violet stimulated luminescence dating of quartz from Luochuan (Chinese loess plateau): agreement with independent chronology up to ~600 ka. Quat. Geochronol. 34, 33-46.

Ankjærgaard, C., 2019. Exploring multiple-aliquot methods for quartz violet stimulated luminescence dating. Quat. Geochronol. 51, 99-109.

Buylaert, J.-P., Murray, A.S., Huot, S., Vriend, M.G.A., Vandenberghe, D., De Corte, F., Van den haute, P., 2006. A comparison of quartz OSL and isothermal TL measurements on Chinese loess. Radiat. Prot. Dosimetry 119, 474-478.

Chapot, M.S., Roberts, H.M., Duller, G.A.T., Lai, Z.P., 2012. A comparison of natural- and laboratory-generated dose response curves for quartz optically stimulated luminescence signals from Chinese Loess. Radiat. Meas. 47, 1045-1052.

Chapot, M.S., Roberts, H.M., Duller, G.A., Lai, Z., 2016. Natural and laboratory TT-OSL dose response curves: testing the lifetime of the TT-OSL signal in nature. Radiat. Meas. 85, 41-50.

Chawla, S., Gundu Rao, T.K., Singhvi, A.K., 1998. Quartz thermoluminescence: dose and dose-rate effects and their implications. Radiat. Meas. 29, 53-63.

Choi, J.H., Murray, A.S., Cheong, C.S., Hong, S.C., 2009. The dependence of dose recovery experiments on the bleaching of natural quartz OSL using different light sources. Radiat. Meas. 44, 600-605.

Colarossi, D., Chapot, M.S., Duller, G.A., Roberts, H.M., 2019. Testing single aliquot regenerative dose (SAR) protocols for violet stimulated luminescence. Radiat. Meas. 120, 104-109.

Constantin, D., Camenita, A., Panaiotu, C., Necula, C., Codrea, V., Timar-Gabor, A., 2015. Fine and coarse-quartz SAR-OSL dating of Last Glacial loess in Southern Romania. Quat. Int. 357, 33-43.

Ding, Z.L., Derbyshire, E., Yang, S.L., Yu, Z.W., Xiong, S.F., Liu, T.S., 2002. Stacked 2.6-Ma grain size record from the Chinese loess based on five sections and correlation with the deep-sea δ18O record. Paleoceanography 17, 5-1-5-21.

Frechen, M., Schweitzer, U., Zander, A., 1996. Improvements in sample preparation for the fine grain technique. Ancient TL 14, 15-17.

Guérin, G., Mercier, N., Nathan, R., Adamiec, C., Lefrais, Y., 2012. On the use of the infinite matrix assumption and associated concepts: a critical review. Radiat. Meas. 47, 778-785.

Hernandez, M., Mercier, N., 2015. Characteristics of the post-blue VSL signal from sedimentary quartz. Radiat. Meas. 78, 1-8.

Guralnik, B., Li, B., Jain, M., Chen, R., Paris, R.B., Murray, A.S., Li, S.H., Pagonis, V., Valla, P.G., Herman, F., 2015a. Radiation-induced growth and isothermal decay of infrared-stimulated luminescence from feldspar. Radiat. Meas. 81, 224-231.

Guralnik, B., Jain, M., Herman, F., Ankjærgaard, C., Murray, A.S., Valla, P.G., Preusser, F., King, G.E., Chen, R., Lowick, S.E., Kook, M., Rhodes, E.J., 2015b. OSL-

thermochronometry of feldspar from the KTB borehole, Germany. Earth Planet. Sci. Lett. 423, 232-243.

Hu, P., Liu, Q., Heslop, D., Roberts, A.P., Jin, C., 2015. Soil moisture balance and magnetic enhancement in loessepaleosol sequences from the Tibetan Plateau and Chinese Loess Plateau. Earth Planet. Sci. Lett. 409, 120-132.

Jain, M., 2009. Extending the dose range: probing deep traps in quartz with 3.06 eV photons. Radiat. Meas. 44, 445-452.

Kars, R.H., Reimann, T., Wallinga, J., 2014. Are feldspar SAR protocols appropriate for post-IR IRSL dating? Quat. Geochronol. 22, 126-136.

Lai, Z.P., Brückner, H., Fülling, A., Zöller, L., 2008. Effects of thermal treatment on the growth curve shape for OSL of quartz extracted from Chinese loess. Radiat. Meas. 43, 763-766.

Lai, Z., 2009. Chronology and the upper dating limit for loess samples from Luochuan section in the Chinese Loess Plateau using quartz OSL SAR protocol. J. Asian Earth Sci. 37, 176-185.

Lai, Z.-P., Fan, A.C., 2014. Examining quartz OSL age underestimation for loess samples from Luochuan in the Chinese Loess Plateau. Geochronometria 41, 57-64.

Lapp, T., Kook, M., Murray, A.S., Thomsen, K.J., Buylaert, J.-P., Jain, M., 2015. A new luminescence detection and stimulation head for the Risø TL/OSL reader. Radiat. Meas. 81, 178-184.

Li, B., Roberts, R.G., Jacobs, Z., Li, S.H., 2015. Potential of establishing a 'global standardized growth curve' (gSGC) for optical dating of quartz from sediments. Quat. Geochronol. 27, 94-104.

Li, B., Jacobs, Z., Roberts, R.G., 2016. Investigation of the applicability of standardized growth curves for OSL dating of quartz from Haua Fteah cave, Libya. Quat. Geochronol. 35, 1-15.

Li, Y., Tsukamoto, S., Long, H., Zhang, J., Yang, L., He, Z., Frechen, M., 2018. Testing the reliability of fading correction methods for feldspar IRSL dating: A comparison between natural and simulated-natural dose response curves. Radiat. Meas. 120, 228-233.

Liritzis, I., Stamoulis, K., Papachristodoulou, C., Ioannides, K., 2013. A re-evaluation of radiation dose-rate conversion factors. Mediterr. Archaeol. Archaeom. 13, 1-15.

Lowick, S.E., Preusser, F., 2010. Investigating age underestimation in the high dose region of optically stimulated luminescence using fine grain quartz. Quat. Geochronol. 6, 33-41.

Lowick, S.E., Preusser, F., Wintle, A.G., 2010. Investigating quartz optically stimulated luminescence dose-response curves at high doses. Radiat. Meas. 45, 975-984.

Lu, Y.C., Wang, X.L., Wintle, A.G., 2007. A new OSL chronology for dust accumulation in the last 130,000 yr for the Chinese Loess Plateau. Quat. Res. 67, 152-160.

Mejdahl, V., Bøtter-Jensen, L., 1994. Luminescence dating of archaeological materials using a new technique based on single aliquot measurements. Quat. Sci. Rev. 13, 551-554.

Morthekai, P., Chauhan, P.R., Jain, M., Shukla, A.D., Rajapara, H.M., Krishnan, K., Sant, D.A., Patnaik, R., Reddy, D.V., Singhvi, A.K., 2015. Thermally re-distributed IRSL (RD-IRSL): A new possibility of dating sediments near B/M boundary. Quat. Geochronol. 30, 154-160.

Murray, A.S., Wintle, A.G., 2000. Luminescence dating of quartz using an improved single-aliquot regenerative-dose protocol. Radiat. Meas. 32, 57-73.

Murray, A., Buylaert, J.-P., Henriksen, M., Svendsen, J.-I., Mangerud, J., 2008. Testing the reliability of quartz OSL ages beyond the Eemian. Radiat. Meas. 43, 776-780.

Peng, J. and Li, B., 2017. Single-aliquot Regenerative-Dose (SAR) and Standardised Growth Curve (SGC) Equivalent Dose Determination in a Batch Model Using the R Package 'numOSL'. Ancient TL 35, 32–53.

Porat, N., Jain, M., Ronen, A., Horwitz, L.K., 2018. A contribution to late middle Paleolithic chronology of the levant: new luminescence ages for the Atlit railway bridge site, Coastal plain, Israel. Quat. Int. 464, 32-42.

Prescott, J.R., Hutton, J.T., 1994. Cosmic ray contributions to dose rates for luminescence and ESR dating large depths and long-term time variations. Radiat. Meas. 23, 497-500.

Rees-Jones, J., Tite, M.S., 1997. Optical dating results for British archaeological sediments. Archaeometry 36, 177-187.

Richter, M., Tsukamoto, S., Long, H., 2020. ESR dating of Chinese loess using the quartz Ti center: A comparison with independent age control. Quat. Int. 556, 159-164.

Roberts, H.M., Duller, G.A.T., 2004. Standardised growth curves for optical dating of sediment using multiple-grain aliquots. Radiat. Meas. 38, 241-252.

Rui, X., Li, B., Guo, Y.J., Zhang, J.F., Yuan, B.Y., Xie, F., 2019. Variability in the thermal stability of OSL signal of single-grain quartz from the Nihewan Basin, North China. Quat. Geochronol. 49, 25-30.

Sontag-González, M., Frouin, M., Li, B., Schwenninger, J.-L., 2020. Assessing the dating potential of violet stimulated luminescence protocols. Geochronometria.

Timar-Gabor, A., Vandenberghe, D.A., Vasiliniuc, S., Panaiotu, C.E., Panaiotu, C.G., Dimofte, D., Cosma, C., 2011. Optical dating of Romanian loess: a comparison between sand-sized and silt-sized quartz. Quat. Int. 240, 62-70.

Timar-Gabor, A., Wintle, A.G., 2013. On natural and laboratory generated dose response curves for quartz of different grain sizes from Romanian loess. Quat. Geochronol. 18, 34-40.

Timar-Gabor, A., Constantin, D., Marković, S.B., Jain, M., 2015a. Extending the area of investigation of fine versus coarse quartz optical ages from the Lower Danube to the Carpathian Basin. Quat. Int. 388, 168-176.

Timar-Gabor, A., Constantin, D., Buylaert, J.-P., Jain, M., Murray, A.S., Wintle, A.G., 2015b. Fundamental investigations of natural and laboratory generated SAR dose response curves for quartz OSL in the high dose range. Radiat. Meas. 81, 150-156.

Tsukamoto, S., Porat, N., Ankjærgaard, C., 2017. Dose recovery and residual dose of quartz ESR signals using modern sediments: implication for single aliquot ESR dating. Radiat. Meas. 106, 472-476.

Tsukamoto, S., Long, H., Richter, M., Li, Y., King, G.E., He, Z., Yang, L., Zhang, J., Lambert, R., 2018. Quartz natural and laboratory ESR dose response curves: A first attempt from Chinese loess. Radiat. Meas. 120, 137-142.

Wallinga, J., Murray, A., Duller, G., 2000. Underestimation of equivalent dose in single-aliquot optical dating of feldspars caused by preheating. Radiat. Meas. 32, 691-695.

Wintle, A.G., Murray, A.S., 1998. Towards the development of a preheat procedure for OSL dating of quartz. Radiat. Meas. 29, 81-94.

Wintle, A.G., Murray, A.S., 2006. A review of quartz optically stimulated luminescence characteristics and their relevance in single-aliquot regeneration dating protocols. Radiat. Meas. 41, 369-391.

Wintle, A.G., Adamiec, G., 2017. Optically stimulated luminescence signals from quartz: a review. Radiat. Meas. 98, 10-33.

Woda, C., Schilles, T., Rieser, U., Mangini, A., Wagner, G.A., 2002. Point defects and the blue emission in fired quartz at high doses: a comparative luminescence and EPR study. Radiat. Prot. Dosimetry 100, 261-264.

CHAPTER 4

A comparative study of sand- and silt-sized quartz fractions for MAR-VSL dating using loess-palaeosol deposits in southern Germany

Rahimzadeh, N., Tsukamoto, S., Zhang, J.

Published on *Quaternary Geochronology*

https://doi.org/10.1016/j.quageo.2022.101276

Author contributions

Rahimzadeh, N. Conceptualization, Methodology, Data curation, Formal analysis, Visualization, Writing- original draft, Writing- review and editing,; Tsukamoto, S. Conceptualization, Methodology, Validation, Writing- review and editing, Supervision; Zhang. J. Conceptualization, Methodology, Validation, Writing- review and editing.

ABSTRACT

Multiple-aliquot regenerative-dose violet stimulated luminescence (MAR-VSL) dating studies of the Chinese loess-palaeosol sequence in Luochuan using sand- and silt-sized quartz have previously produced inconsistent results; the VSL ages were in agreement with their independent ages up to ~900 ka for sand-sized quartz, whereas the silt-sized VSL ages underestimated the independent chronology beyond ~100 ka. Here we therefore evaluate the VSL dose response pattern of sand- (63–100 μm) and silt-sized (4–11 μm) quartz grains from the loess-palaeosol sequence in southern Germany in high resolution but with a limited age range up to ~160 ka. All the samples studied benefit from good age control provided by reliable quartz optically stimulated luminescence (OSL) ages and fading corrected feldspar post-infrared infrared stimulated luminescence at 225 °C ($pIRIR_{225}$) ages, which can be used for assessing the validity of the estimated VSL ages. The comparison of the MAR standardised dose response curve (DRC) using regeneration doses up to ~1000 Gy for both grain size fractions demonstrates that they are almost similar in shape with comparable characteristic saturation doses. The comparison of the natural and laboratory generated DRCs of each grain size reveals that they broadly overlap in the low dose range for both fractions, while in the high dose range the deviation between natural and laboratory DRCs is higher for the silt-sized quartz fraction. It is also shown that the magnitude of the characteristic saturation dose is dependent upon the size of the maximum given dose, especially for the silt-sized quartz. The constructed laboratory standardised DRCs to very high doses (up to ~6000 Gy) showed continuous signal growth at high doses, particularly in the case of silt-sized quartz grains, thereby confirming our previous observation. The sand-sized quartz has a much less pronounced linear growth component and can therefore be considered more suitable for dating samples with equivalent doses falling on the high dose region of the DRC.

4.1 Introduction

The violet stimulated luminescence signal (VSL), which examines traps deeper than those accessible by blue light, is believed to have the potential to extend the possible age range of quartz to the full Quaternary period. In the original study by Jain (2009), it was observed that the VSL signal, after initial blue light stimulation (hereafter post-blue VSL), can grow with doses up to ~1000 Gy, compared to ~100 Gy for the optically stimulated luminescence (OSL) signal from the same grains. Further investigations demonstrated that the VSL signal is thermally/athermally

stable (Ankjærgaard et al., 2013, 2015; Rahimzadeh et al., 2021a), thus it appears to be a promising candidate in extending the upper age range of quartz.

However, studies using the single aliquot regenerative dose (SAR; Murray and Wintle, 2000) method for the VSL signal have shown that the maximum limit of VSL dating using the SAR protocol is ~200 Gy (Ankjærgaard et al., 2013; Porat et al., 2018), and equivalent dose (D_e) estimations above this value showed an underestimation of up to ~80% (Morthekai et al., 2015; Ankjærgaard et al., 2016; Colarossi et al., 2018; Sontag-González et al., 2020). A possible reason for this underestimation is a trapping sensitivity change between natural and all regenerated signals induced by the first preheating, which cannot be detected in the SAR protocol (Ankjærgaard et al., 2016). In order to overcome this drawback, other approaches, i.e. multiple-aliquot additive-dose (MAAD) and multiple-aliquot regenerative-dose (MAR) protocols for the VSL signal have been tested (Ankjærgaard et al., 2016; Ankjærgaard, 2019). Ankjærgaard (2019) reported a good agreement between VSL ages and independent chronology up to ~500 ka and ~900 ka on the Luochuan section, the Chinese Loess Plateau, using the MAAD and MAR protocol, respectively. However, her study is focused on the sand-sized quartz fraction. A recent study by Rahimzadeh et al. (2021a) evaluated the reliability of the MAR protocol for the first time on silt-sized quartz fraction and showed that the MAR standardised growth curve (SGC) using the silt-sized quartz fraction from the same region (Luochuan section) can only reproduce the natural dose response curve (DRC) shape up to ~250 Gy, resulting in large age underestimation beyond ~100 ka. They concluded that the large difference between the second characteristic saturation dose (D_0) of natural and MAR DRCs, when they were fitted with a double saturating exponential function, caused this age underestimation and suggested that the linear growth component of the laboratory generated MAR DRC could be a laboratory artefact.

Several comparative studies on the quartz blue OSL signal for different grain size fractions revealed different growth patterns of DRCs, which also leads to age discrepancies (e.g. Timar-Gabor et al., 2011, 2015; Constantin et al., 2012, 2015; Anechitei-Deacu et al., 2018). These quartz OSL-based studies demonstrated a lower D_e estimation and higher D_0 for the silt-sized fraction. Hitherto, there has not been any direct comparison between different grain size fractions from the same sets of samples for the VSL signal. Therefore, the aim of this study is to assess the VSL dose response pattern using quartz with sand- (63–100 μm) and silt-sized (4–11 μm) grains. Nine quartz samples of both fractions from a loess-palaeosol

sequence in southern Germany for the last 160 ka were used for MAR VSL dating. All samples benefit from good age control provided by reliable quartz OSL ages and fading corrected feldspar post-infrared infrared stimulated luminescence at 225 °C ($pIRIR_{225}$) ages (Rahimzadeh et al., 2021b). The SGC procedure developed by Li et al. (2015) is carried out in order to reduce the amount of instrument time required for constructing the DRC at high doses. In addition, the natural DRCs for both fractions were constructed by measuring natural signals of quartz samples and they were compared to the laboratory generated DRCs in order to test their similarity.

4.2 Materials and methods

4.2.1 Sample description and preparation

The nine samples investigated in this study were taken from the Kitzingen loess-palaeosol sequence in Lower Franconia, southern Germany (Fig. 4.1a and b). The samples studied were taken from three different profiles (Fig. 4.1c; KTE, KTM, and KTW). Two samples (LUM 3266 and 3267) are from KTE, which is the youngest loess deposit in the eastern part of the outcrop. Three samples (LUM 3268–3270) are from KTM, which is located further west, and four samples (LUM 3271–3274) are from KTW, which is in the E-exposed outcrop wall. A complete description of the sampling location, geological and stratigraphical context are given in Rahimzadeh et al. (2021b).

Rahimzadeh et al. (2021b) reported sand-sized quartz OSL ages for young samples up to around 50 ka, and fading corrected $pIRIR_{225}$ ages for all samples for different grain size fractions (i.e. sand sized K-feldspar grains: 63–100 μm; silt-sized polymineral grains: 4–11 μm). The $pIRIR_{225}$ ages <40 ka, which correspond to the linear part of DRC, were corrected following the method of Huntley and Lamothe (2001). For older samples with $pIRIR_{225}$ ages in the non-linear part of the DRC, the fading correction model of Kars et al. (2008) was applied. Based on the chronological framework established by Rahimzadeh et al. (2021b), all estimated ages are in agreement with (pedo)stratigraphic designations, ranging from the Holocene to the late Pleistocene; a summary of the previous luminescence dating results is given in Table S4.1. To facilitate the comparison of results, the reference ages in this study refer only to sand-sized quartz OSL ages for the younger (<50 ka) samples and sand-sized K-feldspar $pIRIR_{225}$ ages for the older (>50 ka) samples, but it is acknowledged that all estimated ages in Rahimzadeh et al. (2021b) are mostly in agreement and thus seem equally reliable (Fig. 4.1c, Table

S4.1). Details on the chemical preparation of the samples are given in Rahimzadeh et al. (2021b). Note that for the silt-sized quartz samples, the extracted polymineral 4–11 µm fraction in Rahimzadeh et al. (2021b) was further etched using 30% hydrofluorosilicic acid (H_2SiF_6) for 5 days. The sand-sized quartz extracts were mounted as aliquots of 2.5 mm in diameter on stainless steel discs using silicone spray as ad- hesive. The silt-sized quartz extracts were settled from deionised water onto aluminium discs (2 mg per disc).

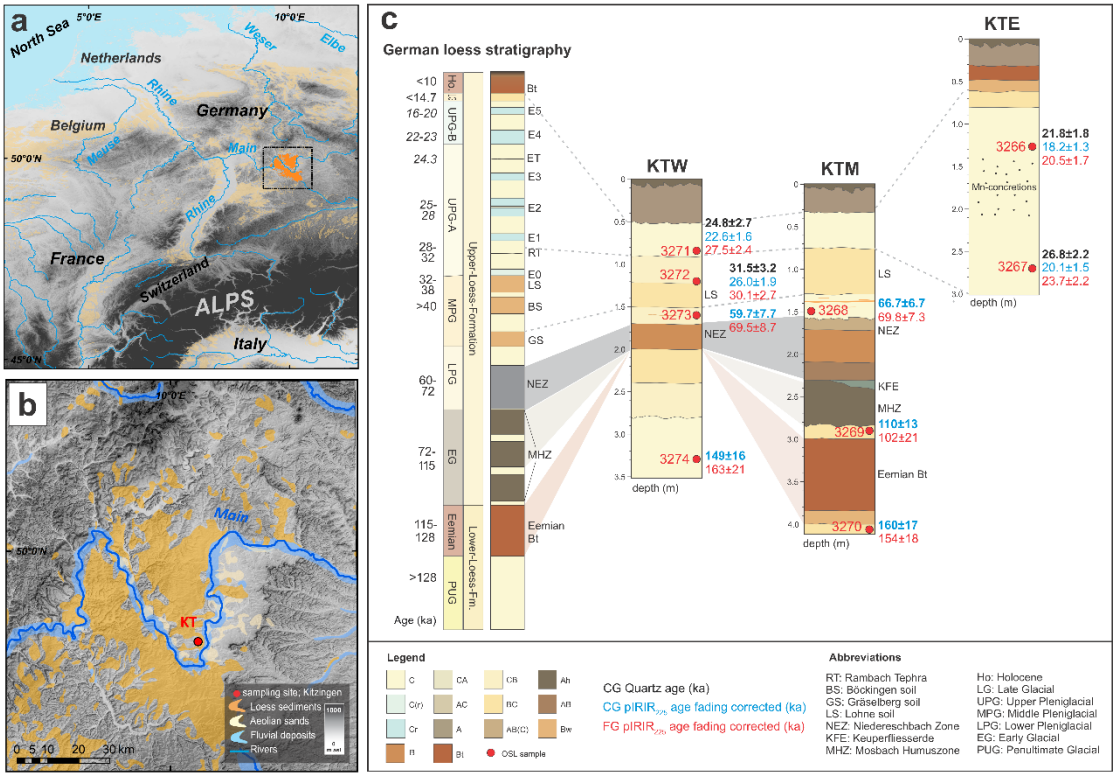

Figure 4.1: (a) Map of loess distribution in Central Europe modified after Lehmkuhl et al. (2020), (b) location of the investigated loess-palaeosol sequence (KT: Kitzingen; red circle) in the Lower Franconian loess region, southern Germany, and (c) simplified stratigraphies of the investigated profiles with a summary of quartz OSL (black), K-feldspar pIRIR$_{225}$ (blue) and polymineral pIRIR$_{225}$ (red) ages and their correlation to German loess stratigraphy (modified after Rahimzadeh et al. (2021b)). The ages shown in bold are used as reference ages in this study.

4.2.2 Instrumentation, measurement protocol and dosimetry

All luminescence investigations were carried out using a TL/OSL Risø DA-20 reader, equipped with an automated detection and stimulation head (DASH) (Lapp et al., 2015). The VSL signals were detected through a combination of a 5 mm thick Hoya U340 and a Semrock brightline 340 nm filter. Laboratory irradiation was performed using a calibrated $^{90}Sr/^{90}Y$ beta source that provides a dose rate of ~0.069 Gy s^{-1} and ~0.091 Gy s^{-1} for silt- and sand-sized quartz grains, respectively. All the measured signals were analysed using the initial VSL signal integrated over

the first 2.5 s and subtracting an early background from the following 15 s of the decay curves.

Table 4.1: VSL protocol used in this study. For the natural measurement, the given dose in step 1 is 0 Gy.

Step	VSL protocol	Observed
1	Given dose (x Gy)	
2	Preheat (280 °C, 10 s)	
3	Blue bleach (125 °C, 40 s)	
4	VSL (125 °C, 500 s)	L_x
5	Violet bleach (240 °C, 500 s)	
6	Test dose	
7	Preheat (280°C, 10 s)	
8	Blue bleach (125 °C, 40 s)	
9	VSL (125 °C, 500 s)	T_x

The MAR VSL protocol used in this study is identical to that in Rahimzadeh et al. (2021a) (Table 4.1). The SGC approach developed by Li et al. (2015) was conducted in order to obtain large amount of chronological data for a limited measurement time. Four samples (LUM 3266, 3269, 3270, and 3273) were used to construct the MAR SGC. A fixed test dose of 100 Gy was used for both grain size fractions. Aliquots were first bleached using a solar simulator (Hönle SOL2) for 7 days. From the x-intercept of the MAR SGCs (Fig. 4.2a), negligible residual doses of ~3 Gy and ~4 Gy were calculated for silt- and sand-sized quartz grains respectively, demonstrating the efficacy of this bleaching treatment in resetting the VSL signal. The bleached aliquots were divided into several groups (i.e. 5 groups for LUM 3266 and 3273, and 7 groups for LUM 3269 and 3270) with 4 aliquots in each, exposed to different regenerative doses ranging from 0 Gy to ~6000 Gy. Note that the SGCs extending up to ~1000 Gy were used for the D_e estimation, as the maximum expected D_e for the studied samples is ~500 Gy (Table 4.2). The SGCs of both grain size fractions were built from all L_x/T_x ratios fitted with a single saturating exponential function (Fig. S4.1 a and c). The least-square normalisation (LS-normalisation) method implemented in the R package 'numOSL' (Peng and Li, 2017) was conducted on the data in Fig. S4.1 a and c, to reduce the inter-aliquot variation between the different samples (Fig. S4.1 b and d). In order to obtain the D_e values, a group of 6 aliquots for each sample were used to measure the sensitivity-corrected natural signal (L_n/T_n). Another group of fresh aliquots was bleached in the solar simulator for 7 days and then given a regenerative dose (D_r) that was close to the expected D_e, and the signals were

measured (L_r/T_r). The average L_n/T_n was then normalised by the average L_r/T_r. The re-normalised natural signal was interpolated onto the LS-normalised MAR SGC to estimate D_e.

The radionuclide concentrations reported by Rahimzadeh et al. (2021b) were used to calculate the dose rates of silt- and sand-sized quartz fractions. The environmental dose rates were calculated using the conversion factor of Gúerin et al. (2011), beta attenuation factor of Mejdahl (1979). An a-value of 0.04±0.02 (Rees-Jones and Tite, 1997) was applied for silt-sized quartz grains. A water content of 15±5% was assumed for all samples, except LUM 3269, 3270, and 3274 which were collected from the well-developed palaeosol and loess below and for which a water content of 20±5% was applied. A cosmic dose rate was calculated based on Prescott and Hutton (1994) and Prescott and Stephan (1982). The dose rate information is summarised in Table 4.2.

Table 4.2: Summary of calculated dose rates, expected natural equivalent doses, and dating results using the MAR protocol. The expected equivalent dose was calculated by multiplying the environmental dose rate by the reference age from Rahimzadeh et al. (2021b). For details see text.

LUM No.	Expected age (ka)	Grains size (μm)	Dose rate (Gy/ka)	Expected dose (Gy)	MAR VSL dose (Gy)	MAR VSL age (ka)
3266	21.8±1.8	4-11	3.38±0.22	73.7±7.7	65.6±9.6	19.4±3.1
		63-100	2.96±0.21	64.5±6.9	116±7	39.1±3.5
3267	26.8±2.2	4-11	3.37±0.22	90.3±9.4	98.9±9.9	29.4±3.5
		63-100	2.94±0.20	78.7±8.4	109±8	37.2±3.7
3268	66.7±6.7	4-11	3.37±0.21	224±26	266±22	79.0±8.1
		63-100	2.97±0.20	198±24	258±9	86.8±6.6
3269	110±13	4-11	3.57±0.22	393±53	279±11	78.2±5.7
		63-100	3.12±0.20	344±47	292±16	93.5±8.0
3270	160±17	4-11	3.22±0.19	517±62	320±40	99.5±13.8
		63-100	2.85±0.20	458±57	361±26	127±13
3271	24.8±2.7	4-11	3.06±0.21	75.8±9.6	82.3±13	26.9±4.6
		63-100	2.68±0.19	66.5±8.6	119±9	44.3±4.6
3272	31.5±3.2	4-11	3.05±0.21	96.2±11.8	89.4±10.9	29.3±4.1
		63-100	2.67±0.19	84.0±10.5	110±7	41.3±3.9
3273	59.7±7.7	4-11	3.44±0.22	205±30	223±8	64.9±4.8
		63-100	3.01±0.21	180±26	184±6	61.0±4.7
3274	149±16	4-11	3.05±0.19	455±55	368±49	121±18
		63-100	2.69±0.19	402±50	538±65	200±28

4.3 Results and discussion

4.3.1 Dose response curves of different grain size fractions

Previous studies regarding the quartz OSL age discrepancy between the two grain size fractions demonstrated that this discrepancy might be attributed to the different growth patterns of DRCs for the silt- and sand- sized quartz fractions (e.g. Timar-Gabor et al., 2017). Based on these studies, the deviation between DRCs of the different grain size fractions at around 100 Gy could be the cause of the age discrepancy beyond ~40 ka (based on the environmental dose rate). It is therefore of interest to compare the VSL dose response patterns of different grain sizes of quartz. For both fractions, the sensitivity corrected growth curves extending up to 1000 Gy were constructed using the MAR protocol. The comparison between VSL MAR SGCs for silt- and sand-sized quartz reveals that they are almost similar in shape, with a D_0 of 306±23 Gy and 367±32 Gy for the silt and sand quartz grains, respectively (Fig. 4.2a). However, note that these DRCs did not reach full saturation and therefore the D_0 values could be underestimated. This issue will be further discussed in section 4.3.3.

In addition to comparing the laboratory constructed DRC shapes of different grain size fractions, it is also useful to compare the natural and laboratory generated DRCs of each grain size and test their similarity. The natural DRC for each grain size fraction was constructed by plotting the sensitivity corrected natural signal against the expected D_e, which was obtained by multiplying the reference age by its measured dose rate, and then was fitted with a single saturating exponential function, yielding D_0 values of 166±35 Gy and 150±12 Gy for the silt- and sand-sized quartz, respectively (Fig. 4.2b and c, solid line). The MAR SGC of each grain size fraction (Fig. 4.2b and c, dashed line) was replotted with the corresponding natural DRC. It can be clearly seen from Fig. 4.2b that the shape of the natural DRC can be reproduced within 95% confidence by the laboratory DRC for the silt-sized quartz grains, although the laboratory DRC starts to deviate from the natural DRC at around 300 Gy. While in the case of sand-sized fraction, the natural and laboratory DRCs deviate from each other at very low doses. Similar results were observed by Timar-Gabor and Wintle (2013), who studied the OSL signal of the different quartz fractions from Romanian loess, and found that the natural and laboratory DRCs of silt-sized quartz fraction overlap each other for doses up to ~200 Gy, while for the sand-sized quartz grains they deviate from each other at doses as low as 50 Gy.

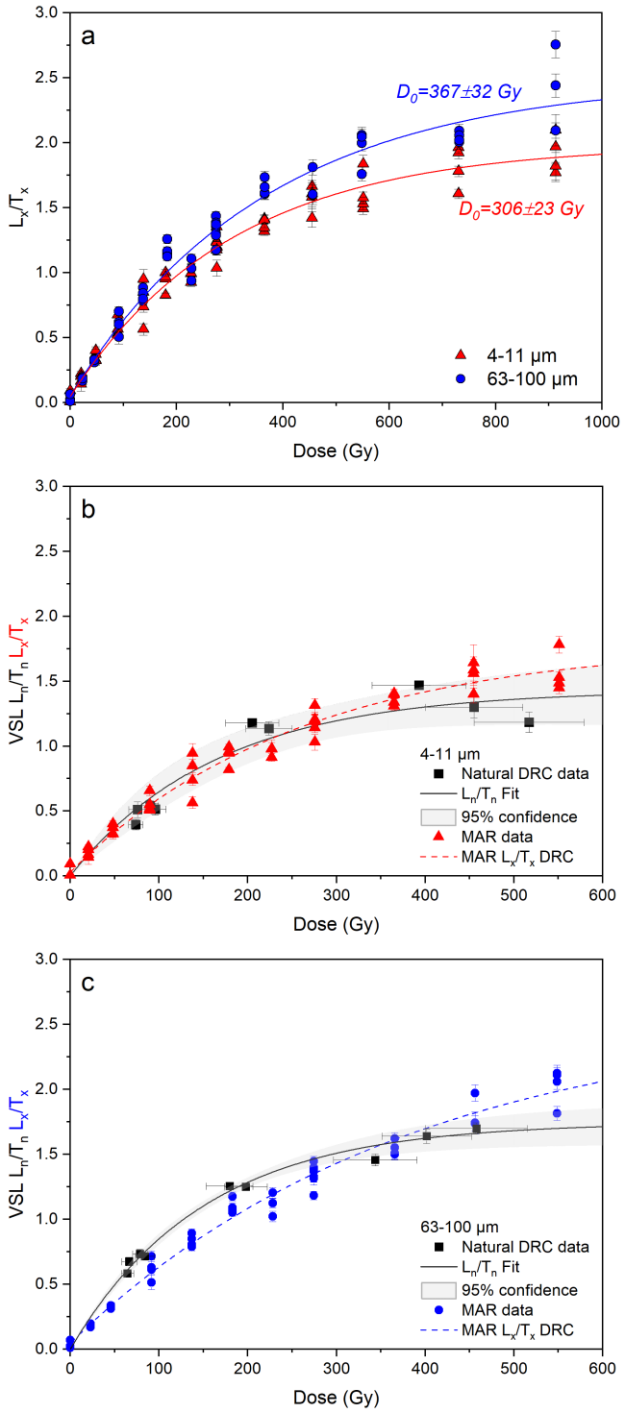

Figure 4.2: (a) Comparison of the MAR laboratory SGCs for the silt- (triangle) and sand-sized (circle) quartz grains; (b,c) comparison of the natural and laboratory generated DRCs for the silt- (b) and sand-sized (c) quartz grains. For each natural sample, the mean L_n/T_n and standard deviation from six aliquots are plotted against the expected equivalent dose. Data are fitted using a single saturating exponential function.

4.3.2 Equivalent dose estimates and ages

A summary of all the information relevant to the D_e values and obtained ages is given in Table 4.2. To estimate the D_e values, the re-normalised natural signals

were interpolated onto the LS-normalised MAR SGC (Fig. 4.2a). The estimated VSL ages for silt-sized quartz ranging from ~19 ka to ~121 ka, while for the counterpart sand-sized quartz VSL ages ranging from ~39 ka to ~200 ka were obtained (Table 4.2). Comparison of the estimated VSL ages from two different grain sizes shows that the VSL ages obtained from sand-sized quartz are consistently older than the VSL ages from the silt-sized fraction (Table 4.2, Fig. 4.3a). For five of the nine samples (LUM 3267, 3268, 3269, 3270 and 3273) the VSL ages from both grain size fractions are in agreement within uncertainties; all other samples show overestimation of sand- sized VSL ages compared to the silt-sized VSL ages (Fig. 4.3a).

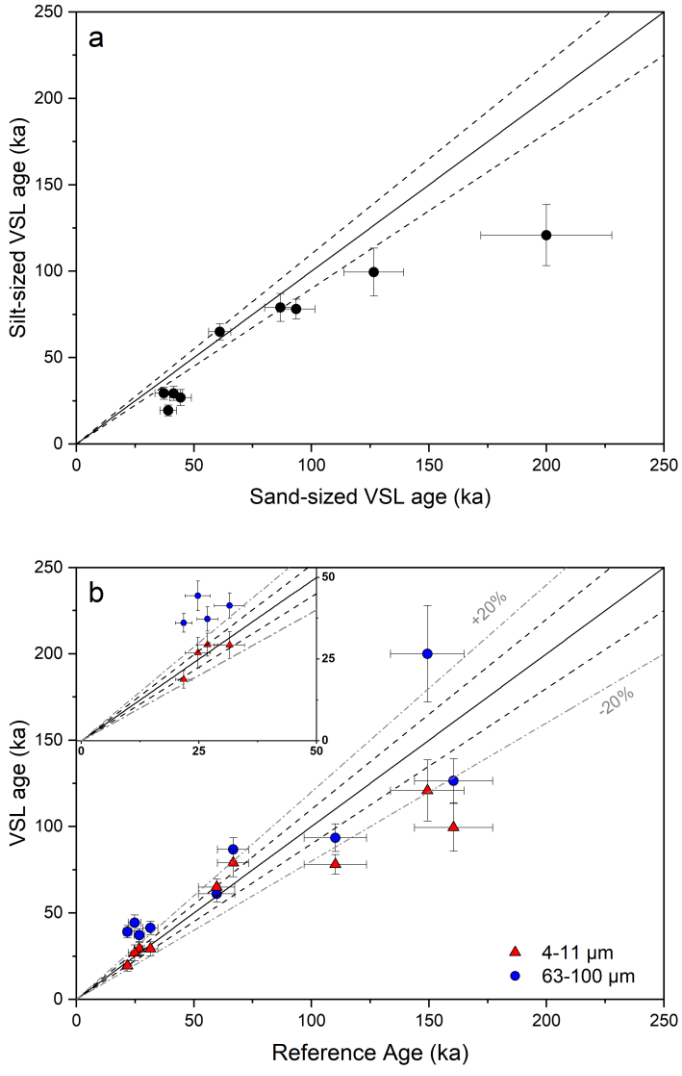

Figure 4.3: (a) Silt-sized VSL ages plotted against sand-sized VSL ages; (b) estimated VSL ages using silt- (triangle) and sand-sized (circle) quartz as a function of the reference ages from Rahimzadeh et al. (2021b). The error bar refers to 1σ. The solid line is 1:1 line, and the dashed lines represent ±10%.

The VSL ages obtained from different grain size fractions were further plotted against reference ages in Fig. 4.3b. For the four youngest samples, for which the

reference ages are younger than 50 ka, all of the silt-sized VSL ages are in good agreement with the reference ages. However, the VSL ages from the sand-sized fraction are significantly older than the reference ages, except sample LUM 3272 whose VSL age is consistent with the reference age within two standard deviations (inset to Fig. 4.3b). The comparison between estimated VSL ages and reference ages for the five oldest samples demonstrates that all VSL ages are consistent with the reference ages within two standard deviations, except one silt-sized sample (LUM 3270), whose VSL age underestimates the reference age (Fig. 4.3b).

One possible explanation for the sand-sized VSL age overestimation could be poor bleaching of the coarse material. While further investigation is needed, it is regarded unlikely to be the main reason for the observed age overestimation. These age offsets indeed require residual doses of at least tens of Gy, which seems unlikely for aeolian sediments (i.e. loess). Comparison of the natural and MAR DRCs (Fig. 4.2b and c) reveals that the observed age discrepancy is likely to be related to the deviation between the natural and laboratory DRCs for each grain size fraction rather than the deviation of laboratory DRCs between two grain size fractions. Although the laboratory SGCs from the two grain size fractions start to diverge in shape after ~100 Gy (Fig. 4.2a), it has to be noted that the environmental dose rate of the silt quartz grains is about 14% higher than the sand-sized quartz (Table 4.2). Considering this natural dose rate difference, the D_e values which were obtained for samples with L_n/T_n intensity up to ~1.5 give similar ages for both grain size fractions. Therefore, the different shapes of the laboratory DRCs could not be the cause of age discrepancy between the two grain sizes (at least for samples with L_n/T_n <~1.5). However, the comparison of the natural and laboratory DRCs for each grain size fraction shows that the low dose region of the laboratory DRC of sand-sized quartz is below the natural DRC, which first results in the age overestimation and then gives roughly corrected age at higher doses (Fig. 4.2c), while for the silt-sized quartz they overly each other within 95% confidence (Fig. 4.2b). However, it has to be noted that there is a systematic tendency for the silt-sized VSL ages towards underestimation with increasing age (Fig. 4.3a). Although the VSL ages from silt-sized quartz are consistent with reference ages, the MAR SGC starts to deviate from the natural DRC at ~300 Gy (Fig. 4.2b) and therefore would tend to underestimate the 1:1 line in Fig. 4.3b beyond ~100 ka.

4.3.3 Dose response curves to high doses

As discussed earlier in the introduction, Rahimzadeh et al. (2021a) suggested that an additional linear component in the high dose region of the laboratory DRC was the reason for the shape dissimilarity between the natural and regenerated DRCs and the subsequent age underestimation. It is therefore of interest to investigate how laboratory regenerated DRCs of the used grain sizes grow at very high doses. The DRCs for both grain size fractions have been constructed for doses up to ~6000 Gy. Contrary to what was observed earlier in section 4.3.1, different growth patterns were observed for the silt- and sand-sized quartz; the sand-sized fraction reaches saturation with negligible growth for doses above ~2000 Gy, while the silt-sized fraction shows a continued growth (Fig. 4.4a). Moreover, it can be seen that the saturation characteristics of the two grain sizes are very different. The D_0 value of silt-sized quartz is 1295±125 Gy, while the sand-sized quartz saturates much earlier with a D_0 of 828±93 Gy. These results suggest that the DRC needs to be constructed up to saturation for obtaining a meaningful value of the saturation parameters. The DRC reaches full saturation, when the D_0 values also reach a plateau with the maximum given dose (Timar-Gabor et al., 2017). To determine at what given dose the DRC reaches full saturation, the D_0 values of both grain size fractions were calculated with different maximum regenerative doses (Fig. 4.4b). It can be seen that the D_0 values depend on the maximum given dose. For the sand-sized fraction, the D_0 value reached a plateau at ~2000 Gy, while in the case of silt-sized quartz no plateau was obtained and the D_0 value continued to grow with the size of the maximum regenerative dose. However, there is no marked dependence of the obtained D_e on the maximum given dose for both grain size fractions (Fig. S4.2). The VSL dose response behaviour therefore seems similar to the OSL signal (e.g. Anechitei-Deacu et al., 2018), and appears to be an inherent feature in quartz. The continuous growth of regenerative signals at higher doses may be related to the creation of new defects (Chawla et al., 1998), change in the population of the electron trap, the saturation of a competing non-radiative recombination centre (Woda et al., 2002), or a change in the competition of electrons between different recombination centres at high doses (Lowick and Preusser, 2011). Furthermore, a recent study by Peng et al. (2022) that simulated the natural and laboratory OSL signals and DRCs using a kinetic model for quartz developed by Bailey (2001) showed a discrepancy in competition for electrons in the deep electron trap and recombination centres during stimulation between the natural, regenerative, and test dose cycles; the deep electron trap of natural samples and recombination

centres of laboratory-irradiated samples compete more strongly for free electrons during irradiation/stimulation. Their simulation results also showed that the competition for charge during irradiation, preheat, and stimulation in a MAR aliquot is much closer to a natural aliquot, and therefore the MAR protocol can potentially be used to improve the accuracy of D_e values (especially for the larger D_e values in the high dose region).

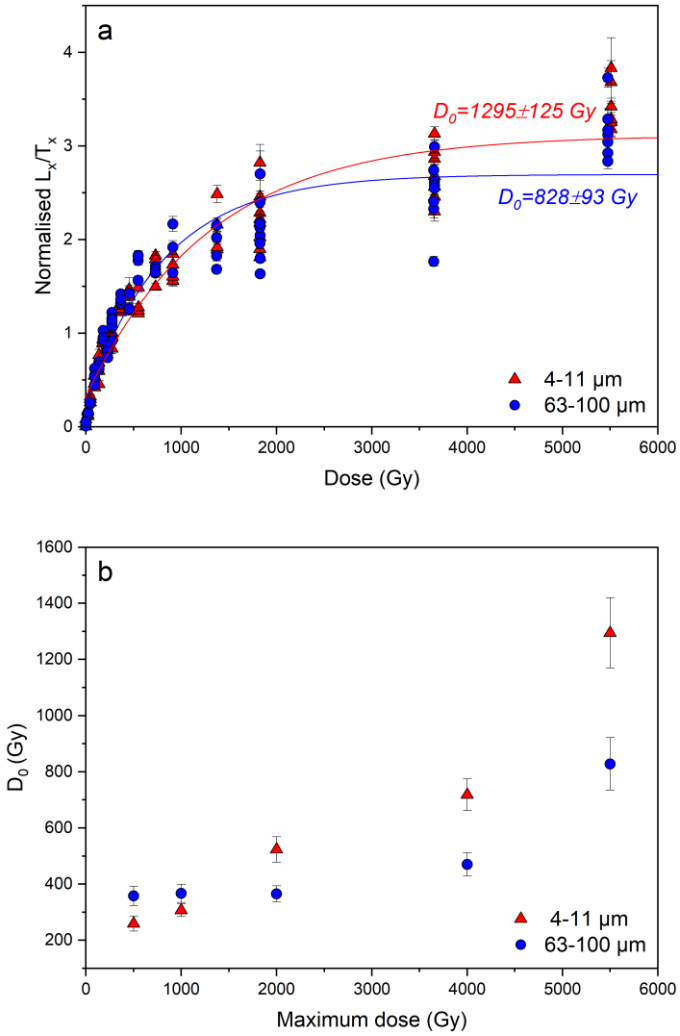

Figure 4.4: (a) Comparison of the extended dose response curve of silt- (triangle) and sand-sized (circle) quartz for doses up to around 6000 Gy; (b) comparison of saturation characteristic values (D_0) of different grain sizes obtained from the data in (a) as a function of the maximum given dose.

4.4 Conclusions

This study compared the VSL dose response patterns of sand- and silt- sized quartz grains from the loess-palaeosol sequence in southern Germany. Our results highlighted the potential of the VSL signal for extending the quartz dating range through its successful application to samples studied in the age range of 20–160 ka. The comparison of VSL MAR SGCs using regeneration doses up to ~1000 Gy for

sand- and silt- sized quartz indicated that they are almost similar in shape with close D_0 values. VSL ages of both grain size fractions were found to be in agreement with reference ages of >50 ka, however, there is a general tendency for the silt-sized quartz to underestimate the reference ages with increasing age. The comparison of the natural and laboratory generated DRCs of each grain size showed that both DRCs broadly overlap in the low dose range for both fractions, while the deviation between natural and laboratory DRCs is higher for the silt-sized fraction in the high dose range (beyond ~300 Gy). This observation is further confirmed by the construction of the DRC for very high doses (up to ~6000 Gy), which showed a continuous growth of the signal up to high doses, especially in the case of silt-sized quartz. Furthermore, a clear dependency between the D_0s and the maximum given dose was observed. This is especially the case for the silt-sized quartz, which showed that the D_0 value increases continuously with the size of the maximum regenerative dose with no sign of a plateau in the saturation data. This linear response in the high dose region of the silt-sized DRC requires caution for dating old samples with expected D_e in the high dose range. However, from data in this study it is not possible to conclude a clearly defined high dose range and further investigations are needed. This linear growth component is much less pronounced for sand-sized quartz and the sand-sized quartz can therefore be regarded as more reliable chronometer in the high dose range.

Acknowledgments

The authors would like to thank Tobias Sprafke for providing samples. Technicians at LIAG are thanked for the sample preparation and gamma spectrometry measurements. Gwynlyn Buchanan is thanked for language corrections. We also wish to thank the anonymous reviewer for very helpful suggestions which greatly improved the manuscript.

References

Aitken, M.J., 1998. An Introduction to Optical Dating: the Dating of Quaternary Sediments by the Use of Photon-Stimulated Luminescence. Oxford University Press.

Anechitei-Deacu, V., Timar-Gabor, A., Constantin, D., Trandafir-Antohi, O., Del Valle, L., Fornós, J.J., Gómez-Pujol, L.L., Wintle, A.G., 2018. Assessing the maximum limit of SAR-OSL dating using quartz of different grain sizes. Geochronometria 45, 146-159.

Ankjærgaard, C., Jain, M., Wallinga, J., 2013. Towards dating quaternary sediments using the quartz violet stimulated luminescence (VSL) signal. Quat. Geochronol. 18, 99-109.

Ankjærgaard, C., Guralnik, B., Porat, N., Heimann, A., Jain, M., Wallinga, J., 2015. Violet stimulated luminescence: geo-or thermochronometer? Radiat. Meas. 81, 78-84.

Ankjærgaard, C., Guralnik, B., Buylaert, J.-P., Reimann, T., Yi, S.W., Wallinga, J., 2016. Violet stimulated luminescence dating of quartz from Luochuan (Chinese loess plateau): agreement with independent chronology up to ~600 ka. Quat. Geochronol. 34, 33-46.

Bailey, R.M., 2001. Towards a general kinetic model for optically and thermally stimulated luminescence of quartz. Radiat. Meas. 33, 17-45.

Chawla, S., Gundu Rao, T.K., Singhvi, A.K., 1998. Quartz thermoluminescence: dose and dose-rate effects and their implications. Radiat. Meas. 29, 53-63.

Colarossi, D., Chapot, M.S., Duller, G.A., Roberts, H.M., 2018. Testing single aliquot regenerative dose (SAR) protocols for violet stimulated luminescence. Radiat. Meas. 120, 104-109.

Constantin, D., Timar-Gabor, A., Veres, D., Begy, R., Cosma, C., 2012. SAR-OSL dating of different grain-sized quartz from a sedimentary section in southern Romania interbedding the Campanian Ignimbrite/Y5 ash layer. Quat. Geochronol. 10, 81-86.

Constantin, D., Camenita, A., Panaiotu, C., Necula, C., Codrea, V., Timar-Gabor, A., 2015. Fine and coarse-quartz SAR-OSL dating of Last Glacial loess in Southern Romania. Quat. Int. 357, 33-43.

Guérin, G., Mercier, N., Adamiec, G., 2011. Dose-rate conversion factors: update. Anc. TL. 29, 5–8.

Huntley, D.J., Lamothe, M., 2001. Ubiquity of anomalous fading in K-feldspars and the measurement and correction for it in optical dating. Can. J. Earth Sci. 38, 1093-1106.

Jain, M., 2009. Extending the dose range: probing deep traps in quartz with 3.06 eV photons. Radiat. Meas. 44, 445-452.

Kars, R.H., Wallinga, J., Cohen, K.M., 2008. A new approach towards anomalous fading correction for feldspar IRSL dating— tests on samples in field saturation. Radiat. Meas. 43, 786–790.

Lapp, T., Kook, M., Murray, A.S., Thomsen, K.J., Buylaert, J.-P., Jain, M., 2015. A new luminescence detection and stimulation head for the Risø TL/OSL reader. Radiat. Meas. 81, 178-184.

Lehmkuhl, F., Nett, J., Pötter, S., Schulte, P., Sprafke, T., Jary, Z., Antoine, P., Wacha, L., Wolf, D., Zerboni, A., Hošek, J., Marković, S., Obreht, I., Sümegi, P., Veres, D., Zeeden, C., Boemke, B., Schaubert, V., Viehweger, J., Hambach, U., 2020. Geodata of European loess, sandy loess and aeolian sand. CRC806-Database.

Li, B., Roberts, R.G., Jacobs, Z., Li, S.H., 2015. Potential of establishing a 'global standardized growth curve' (gSGC) for optical dating of quartz from sediments. Quat. Geochronol. 27, 94-104.

Lowick, S.E., Preusser, F., 2011. Investigating age underestimation in the high dose region of optically stimulated luminescence using fine grain quartz. Quat. Geochronol. 6, 33-41.

Mejdahl, V., 1979. Thermoluminescence dating: beta-dose attenuation in quartz grains. Archaeometry. 21, 63-79.

Morthekai, P., Chauhan, P.R., Jain, M., Shukla, A.D., Rajapara, H.M., Krishnan, K., Sant, D.A., Patnaik, R., Reddy, D.V., Singhvi, A.K., 2015. Thermally re-distributed IRSL (RD-IRSL): A new possibility of dating sediments near B/M boundary. Quat. Geochronol. 30, 154-160.

Murray, A.S., Wintle, A.G., 2000. Luminescence dating of quartz using an improved single-aliquot regenerative-dose protocol. Radiat. Meas. 32, 57-73.

Peng, J., Li, B., 2017. Single-aliquot regenerative-dose (SAR) and standardised growth curve (SGC) equivalent dose determination in a batch model using the R package 'numOSL'. Ancient TL 35, 32–53.

Peng, J., Wang, X., Adamiec, G., 2022. The build-up of the laboratory-generated dose-response curve and underestimation of equivalent dose for quartz OSL in the high dose region: A critical modelling study. Quat. Geochronol. 67, 101231.

Porat, N., Jain, M., Ronen, A., Horwitz, L.K., 2018. A contribution to late middle Paleolithic chronology of the levant: new luminescence ages for the Atlit railway bridge site, Coastal plain, Israel. Quat. Int. 464, 32-42.

Prescott, J.R., Stephan, L.G., 1982. The contribution of cosmic radiation to the environmental dose for thermoluminescent dating- latitude, altitude and depth dependences. PACT. 6, 17-25.

Prescott, J.R., Hutton, J.T., 1994. Cosmic ray contributions to dose rates for luminescence and ESR dating large depths and long-term time variations. Radiat. Meas. 23, 497-500.

Rahimzadeh, N., Tsukamoto, S., Zhang, J., Long, H., 2021a. Natural and laboratory dose response curves of quartz violet stimulated luminescence (VSL): Exploring the multiple aliquot regenerative-dose (MAR) protocol. Quat. Geochronol. 65, 101194.

Rahimzadeh, N., Sprafke, T., Thiel, C., Terhorst, B., Frechen, M., 2021b. A comparison of polymineral and K-feldspar post-IR IRSL ages of loess from Franconia, southern Germany. E&G Quaternary Sci. J. 70, 53-71.

Rees-Jones, J., Tite, M.S., 1997. Optical dating results for British archaeological sediments. Archaeometry 36, 177-187.

Sontag-González, M., Frouin, M., Li, B., Schwenninger, J.-L., 2020. Assessing the dating potential of violet stimulated luminescence protocols. Geochronometria.

Timar-Gabor, A., Vandenberghe, D.A., Vasiliniuc, S., Panaiotu, C.E., Panaiotu, C.G., Dimofte, D., Cosma, C., 2011. Optical dating of Romanian loess: a comparison between sand-sized and silt-sized quartz. Quat. Int. 240, 62-70.

Timar-Gabor, A., Wintle, A.G., 2013. On natural and laboratory generated dose response curves for quartz of different grain sizes from Romanian loess. Quat. Geochronol. 18, 34-40.

Timar-Gabor, A., Constantin, D., Marković, S.B., Jain, M., 2015. Extending the area of investigation of fine versus coarse quartz optical ages from the Lower Danube to the Carpathian Basin. Quat. Int. 388, 168-176.

Timar-Gabor, A., Buylaert, J.-P., Guralnik, B., Trandafir-Antohi, O., Constantin, D., Anechitei-Deacu, V., Jain, M., Murray, A.S., Porat, N., Hao, Q., Wintle, A.G., 2017. On the importance of grain size in luminescence dating using quartz. Radiat. Meas. 106, 464-471.

Woda, C., Schilles, T., Rieser, U., Mangini, A., Wagner, G.A., 2002. Point defects and the blue emission in fired quartz at high doses: a comparative luminescence and EPR study. Radiat. Prot. Dosimetry 100, 261-264.

Supplementary Material- A comparative study of sand- and silt-sized quartz fractions for MAR-VSL dating using loess-palaeosol deposits in southern Germany

Rahimzadeh, N., Tsukamoto, S., Zhang, J.

Published on *Quaternary Geochronology*

https://doi.org/10.1016/j.quageo.2022.101276

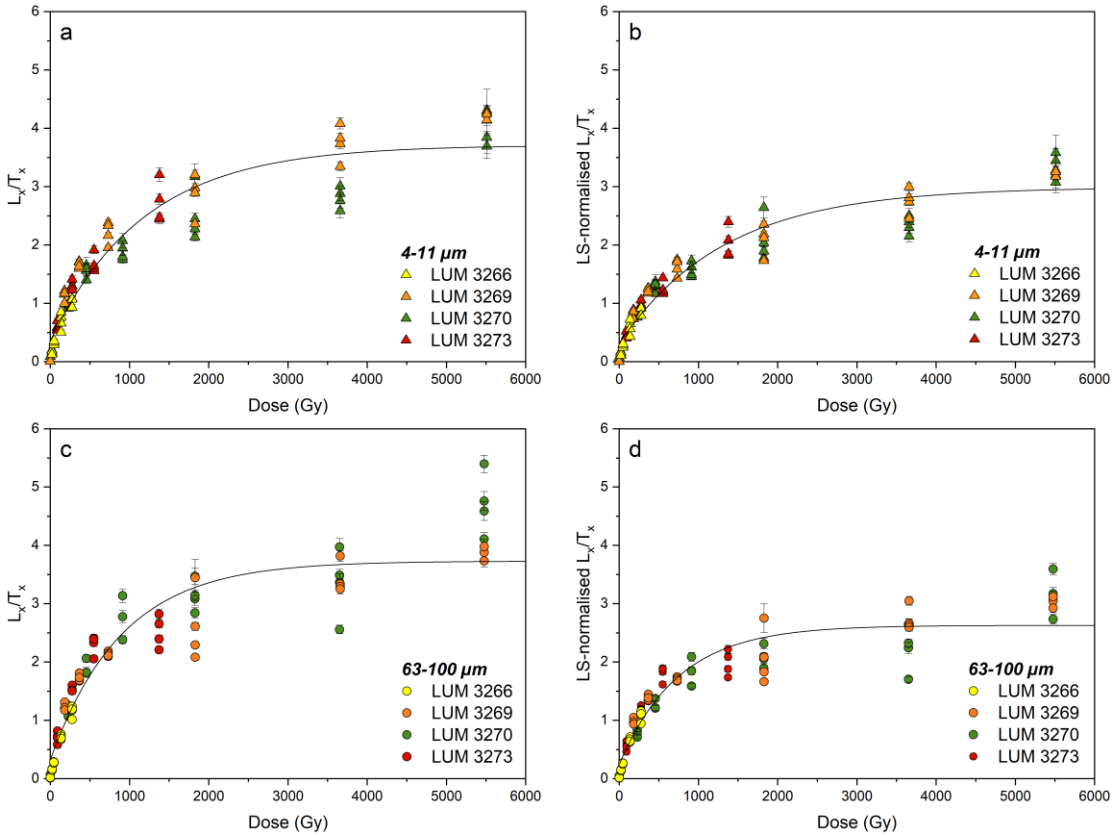

Figure S4. 1*:* MAR L_x/T_x ratios of the (a) silt- and (c) sand-sized quartz for the four samples (LUM 3266, 3269, 3270, and 3273) plotted as a function of laboratory dose, and their re-normalised counterparts (b and d).

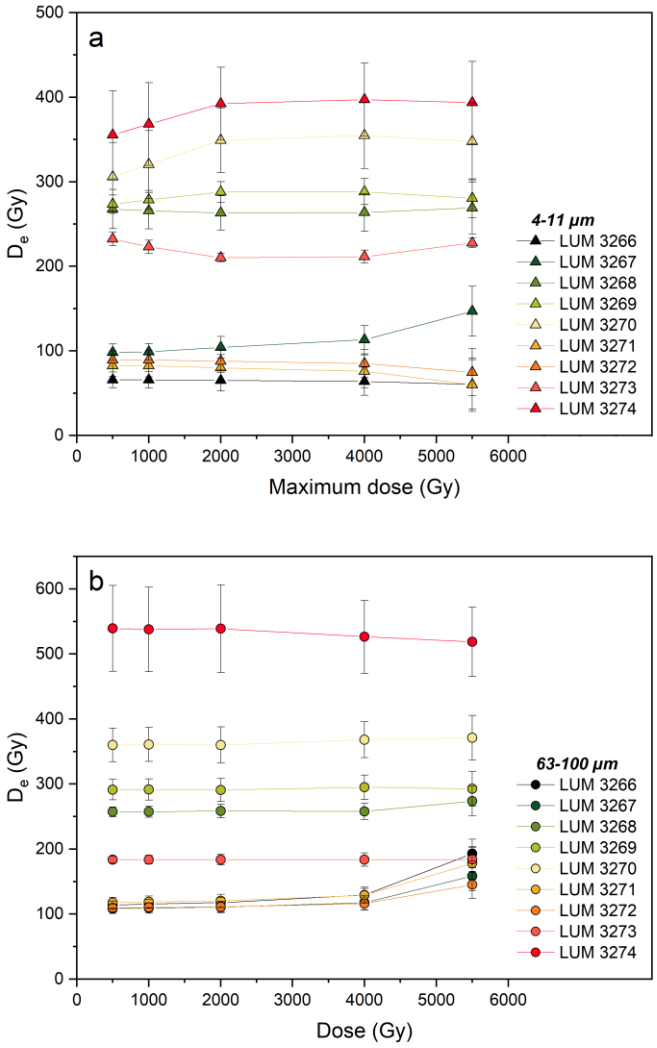

Figure S4.2: Comparison of D_e values obtained for (a) silt- and (b) sand-sized quartz as a function of the maximum given dose.

Table S4.1: Equivalent doses (Gy) and ages (ka) for quartz OSL, K-feldspar CG (K-fsp) and polymineral FG (poly.) $pIRIR_{225}$.

LUM No.	D_e (Gy)			Fading uncorr. age (ka)		Age (ka)		
	OSL	$pIRIR_{225}$ (K-fsp)	$pIRIR_{225}$ (poly.)	$pIRIR_{225}$ (K-fsp)	$pIRIR_{225}$ (poly.)	Quartz	$pIRIR_{225}$ (K-fsp)	$pIRIR_{225}$ (poly.)
3266	64.5±2.6	58.7±0.5	71.6±1.0	15.1±0.7	17.9±1.1	21.8±1.8	18.2±1.3	20.5±1.7
3267	78.7±3.3	69.5±1.7	83.1±2.1	18.0±0.9	20.8±1.4	26.8±2.2	20.1±1.5	23.7±2.2
3268	166±19	173±4	196±6	44.8±2.2	49.5±3.4	> 56[a]	66.7±6.7	69.8±7.3
3269	-	282±12	295±41	69.6±4.0	69.4±10.5	-	110±13	102±21
3270	-	353±13	389±11	94.4±5.3	103±7	-	160±17	154±18
3271	66.5±5.3	68.0±0.8	81.8±1.0	19.0±0.9	22.6±1.5	24.8±2.7	22.6±1.6	27.5±2.4
3272	84.0±6.1	79.5±1.1	97.6±1.3	22.3±1.1	26.9±1.8	31.5±3.2	26.0±1.9	30.1±2.7
3273	163±12	166±5	204±6	42.3±2.2	50.0±3.3	> 55[a]	59.7±7.7	69.5±8.7
3274	-	357±10	393±12	99.8±5.2	110±7	-	149±16	163±21

[a] minimum ages due to saturation of the quartz OSL signal

CHAPTER 5

Characteristics of the quartz isothermal thermoluminescence (ITL) signal from the 375 °C peak and its potential for extending the age limit of quartz dating

Rahimzadeh, N., Zhang, J., Tsukamoto, S., Long, H.

Published on *Radiation Measurements*

https://doi.org/10.1016/j.radmeas.2022.106899

Author contributions

Rahimzadeh, N. Conceptualization, Methodology, Data curation, Formal analysis, Visualization, Writing- original draft, Writing- review and editing; Zhang. J. Conceptualization, Methodology, Validation, Writing- review and editing; Tsukamoto, S. Conceptualization, Methodology, Validation, Writing- review and editing, Supervision; Long, H. Resources, Partly funding acquisition, Writing- review and editing.

ABSTRACT

The quartz isothermal thermoluminescence (ITL) signal measured at 330°C (ITL_{330}) has been proposed as a method to measure deep traps in quartz, i.e., 375 °C TL peak, therefore offering the potential to extend the dating limit of quartz. However, little is known about the applicability of this signal for dating. We therefore investigate the characteristics of the ITL_{330} signal, in terms of the origin of the signal, thermal stability, and bleachability. Since the trapping sensitivity changes induced by high temperature treatments undermine the application of the single aliquot regenerative dose (SAR) protocol, here we evaluate the reliability and applicability of the multiple aliquot methods, i.e., multiple aliquot additive dose (MAAD) and multiple aliquot regenerative dose (MAR) protocols, using samples from the Luochuan section on the Chinese Loess Plateau with the independent age control. Results indicate that the ITL_{330} signal is closely associated with the 375 °C peak of the glow curve, originating from a deep trap at about 1.8 eV with a thermal lifetime of $\sim 10^{10}$ years at 10 °C. The natural ITL_{330} dose response curve (DRC) indicates the signal has a theoretical dating range up to ~800 Gy, equivalent to ~230 ka. When the natural DRC is compared with the laboratory generated DRCs using MAR and MAAD protocols, they start to diverge in shape after ~200 Gy, resulting in significant ITL_{330} age underestimation beyond ~70 ka. However, application of the pulsed-irradiation (PI) method for the MAAD protocol reveals that the shape of the natural DRC can mostly be reproduced with the PI-MAAD protocol and thus it can provide reliable ages up to natural saturation at ~230 ka. While further investigations are required to assess the impact of the repeated pulse irradiation and heating on the signal and determine the optimal pulsed irradiation conditions, it appears that this approach can be a promising step forward to provide a better simulation of the trapping conditions in nature.

5.1 Introduction

The optically stimulated luminescence (OSL) dating of quartz is widely used to obtain the depositional ages of sedimentary deposits. This method is mainly based on the measurement of the fast component of the OSL signal (Wintle and Murray, 2006). However, this component is known to saturate at a low dose. For instance, the signal saturates doses around 120-150 Gy at Luochuan section on the Chinese Loess Plateau, thus allowing reliable dating limit only up to ~50-70 ka at this site (Buylaert et al., 2007; Lu et al., 2007; Lai, 2010; Chapot et al., 2012). Extending the range of luminescence dating beyond the current limitation is therefore a key challenge. In an attempt to extend this limitation, other luminescence signals from

quartz have been proposed, such as the slow OSL component (Singarayer et al., 2000), the isothermal thermoluminescence (ITL; Jain et al., 2005), the thermally transferred OSL (TT-OSL; Wang et al., 2006), and the violet stimulated luminescence (VSL; Jain, 2009).

The thermoluminescence (TL) signal from quartz saturates more slowly than the OSL, thereby allowing dating of older sediments. Two high temperatures and stable glow peaks have been used in quartz dating; these two peaks are the rapidly bleaching TL peak at 325 °C and the slowly bleaching TL peak at 375 °C, respectively (Aitken, 1985). However, this method has some drawbacks such as releasing trap charges associated with both light-sensitive and light-insensitive components, poor separation of signal from different traps, and unwanted signal due to black body radiation caused by high temperature heating (i.e., 450 °C) (Aitken, 1992; Stokes, 1999). A modification of the conventional TL method is the ITL approach, in which TL is recorded while the sample is held at a constant temperature (e.g., Murray and Wintle, 2000; Jain et al., 2005). The potential advantage of the ITL measurement over the conventional TL approach is a better separation of signal from overlapping TL peaks (Buylaert et al., 2006). The quartz ITL signal measured at 310 °C originates from the 325 °C TL trap, and has a dose saturation level about an order of magnitude higher compared to the fast component OSL signal (Jain et al., 2005; Choi et al., 2006). Although these pioneering studies showed promising results, subsequent investigation identified several problems such as age overestimation, which is a result of the initial sensitivity change in the single aliquot regenerative dose (SAR) protocol (Buylaert et al., 2006; Huot et al., 2006). Vandenberghe et al., (2009) reduced the thermal treatments (i.e., preheat and ITL stimulation temperatures) to avoid large sensitivity changes that could not be corrected using the SAR protocol. Regarding the 375 °C TL peak, the quartz ITL signal measured at 330 °C (hereafter ITL_{330}) was proposed by Murray and Wintle (2000) as a method to measure deeper traps in quartz, therefore has the potential to extend the quartz dating range. However, little systematic work has been carried out so far to investigate the physical and dosimetric properties of this signal.

In this study, we propose a modified ITL_{330} dose measurement protocol and use it to provide new information on the characteristics of the ITL_{330} signal, in terms of the origin of the signal, thermal stability, bleachability, and dose response. We then investigate the applicability of this signal by comparing ITL_{330} ages against independent chronology for nine fine-grained quartz samples from the

Luochuan section on the Chinese Loess Plateau with ages up to ~700 ka. Since the SAR protocol can be compromised by trapping sensitivity changes induced by high temperature preheating, this study tests the multiple aliquot methods, i.e., multiple aliquot additive dose (MAAD) and multiple aliquot regenerative dose (MAR) protocols. Since a considerable portion of the VSL signal originates from the 375 °C TL peak (Ankjærgaard et al., 2013; Hernandez and Mercier, 2015), we also take the opportunity to compare this signal to the VSL signal, as both signals originate from the same TL peak in quartz.

5.2 Samples and instrumentation

Experiments presented in the current study have been conducted on archived fine-grained quartz extracts from our previous investigation on the Luochuan Potou section of the Chinese Loess Plateau (cf. Rahimzadeh et al., 2021). Of the 13 investigated samples in Rahimzadeh et al. (2021), nine uppermost samples from unit L1 (10-72 ka; Zhang et al., 2022) to unit L6 (621-684 ka; Ding et al., 2002) were used in this study (Table 5.1). Sample preparation was carried out under subdued red light. The material was treated by hydrochloric acid (HCl; 10%), sodium oxalate ($Na_2C_2O_4$; 0.1 N), and hydrogen peroxide (H_2O_2; 30%) to remove carbonate, mineral aggregates, and organic matter, respectively. The material was then separated according to Frechen et al. (1996) to obtain the fine-grained (4-11 μm) fraction. The separated fine grain material was further etched using hydrofluorosilicic acid (H_2SiF_6) for 5 days to extract the quartz grains from the polymineral fine grains. The absence of feldspar contamination was confirmed by measuring infrared stimulated luminescence (IRSL) signal of sample LUM 3704 which was irradiated with ~100 Gy; no significant IRSL signal was observed and the IR depletion ratio (Duller, 2003) was within 10% of unity (1.03±0.01). For luminescence measurement, the quartz extracts were settled on aluminum discs from suspension in distilled water (2 mg per disc).

Luminescence measurements were undertaken using an automated Risø TL/OSL reader (DA-15), equipped with blue (470±30 nm; ~45 mW cm^{-2}) and infrared (870±40 nm; ~135 mW cm^{-2}) LEDs and calibrated $^{90}Sr/^{90}Y$ beta source with a dose rate of 0.097 Gy s^{-1} for fine grains. All signals were detected through a 7.5 mm Hoya U-340 filter. The ITL signals were analysed using the initial signal integrated over the first 12.5 s minus a background calculated from the last 50 s of stimulation.

Table 5.1: Summary of calculated dose rates, expected natural equivalent doses and dating results using different protocols. The reference ages were calculated following Zhang et al. (2022) and Ding et al. (2002).

LUM No.	Unit	Depth (m)	Dose rate (Gy/ka)	Expected age (ka)	Expected dose (Gy)	MAR D_e[b] (Gy)	MAAD D_e (Gy)	PI-MAAD D_e (Gy)	MAR age (ka)	MAAD age (ka)	PI-MAAD age (ka)
3703[a]	S0	1.0	3.29±0.19	*7.8±0.9*	25.8±3.2		19.9±5.2			6.0±1.6	
3704	L1	3.5	3.56±0.18	*32.4±2.1*	115±9	-	128±31	143±23	-	36.0±9.0	40.1±6.9
4163	L1	7.9	3.33±0.18	*62.5±2.8*	208±14	192±6 (38.8±10.9)	205±6	242±9	57.7±3.5	61.4±3.8	72.6±4.8
4164	S1	10.9	3.65±0.18	*111±16*	405±28	293±16 (44.1±11.6)	290±16	375±26	80.2±5.9	79.6±5.9	103±9
4165	L2	13.9	3.37±0.18	*146±3*	493±28	378±28 (59.9±29.9)	344±28	468±52	112±10	102±10	139±17
3707	S2	18.3	3.63±0.18	*196±8*	711±45	-	350±46	479±86	-	96.4±13.4	132±25
4168	L3	23.1	3.15±0.17	*268±9*	845±52	-	490±25	806±77	-	155±11	255±28
3710	L4	26.6	3.36±0.17	346±35	1161±131	-	517±63	896±266	-	154±20	267±80
4172	L5	34.9	3.30±0.17	470±47	1553±176	633±44 (66.3±22.4)	561±47	1092±315	192±17	170±17	331±97
3712	L6	42.6	3.20±0.17	646±65	2069±233	-	563±81	1101±360	-	176±27	344±114

The expected ages presented in italic font (LUM 3703-4168) were derived from Bacon age-depth model of Zhang et al. (2022). The expected ages from the remaining samples (LUM 3710-3712) were calculated using the Chiloparts record of Ding et al. (2002). See main text for details.

[a] Coarse-grained fraction (63-100 µm) was used for sample LUM 3703.

[b] This column presents the residual corrected MAR Des. The residual values are shown in brackets.

The environmental dose rate was estimated by the radionuclide concentrations of U, Th, and K that were determined using high resolution gamma spectrometry. The same parameters, such as water content, attenuation and conversion factors, as in Rahimzadeh et al. (2021) were used for dose rate calculation.

5.3 The ITL_{330} protocol

The ITL_{330} protocol used in this study builds on the original sequence proposed by Murray and Wintle (2000; Table 5.2a). In the protocol of Murray and Wintle (2000), a preheat to 340 °C for 0 s followed by 5 s blue light stimulation at 330 °C was undertaken to completely remove the OSL signal from the 325 °C TL peak. The samples were then stimulated with a linearly increasing blue light stimulation (from 0 to 1000 s) at 125 °C to obtain the ramped OSL. However, they did not further discuss the implications of this signal. Finally, ITL measurements were performed by holding the samples at 330 °C for 1000 s.

For the present study, a series of experiments were conducted on sample LUM 4163 and subsequently several steps and parameters were modified to improve the performance of the protocol. The heating in all experiments was performed at a rate of 5 °C s^{-1} unless stated otherwise. Firstly, we omitted the 5 s blue stimulation at 330 °C in the initial pretreatment of the original sequence (step 2 of Table 5.2a), as it results in a significant depletion of the ITL signal. Fig. 5.1a shows the ITL_{330} decay curves for an aliquot of sample LUM 4163 following an irradiation of ~100 Gy with and without the 5 s OSL at 330°C before the ITL_{330}. It shows that the intensity of the ITL_{330} signal is ~70% lower when the 5 s blue stimulation at 330 °C is added after the preheat (Fig. 5.1a). The inset to Fig. 5.1a shows a 5 s OSL decay, suggesting that this treatment can be considered as a short ITL signal. Subsequently, to reduce any contribution from the 325 °C TL trap, a blue stimulation at 125 °C for 40 s was included after the preheat (steps 3 and 7 of Table 5.2b). In order to investigate the efficiency of this procedure, an aliquot of sample LUM 4163 was sensitised through repeated cycles of irradiation and annealing. The TL response to a ~350 Gy regenerative dose was then measured after either preheating at 340 °C only, or after the same preheat followed by a blue stimulation (125 °C for 40 s). As shown by Fig. 5.1b, adding a blue stimulation clearly depletes a portion of the lower temperature TL peak. Moreover, in order to reduce the instrument time, the holding duration for the ITL measurement was reduced to 500 s (rather than 1000 s). Fig. 5.1c shows the ITL_{330} decay curves for different

duration of ITL, and it can be seen that the signal has reached a low level after ~400 s.

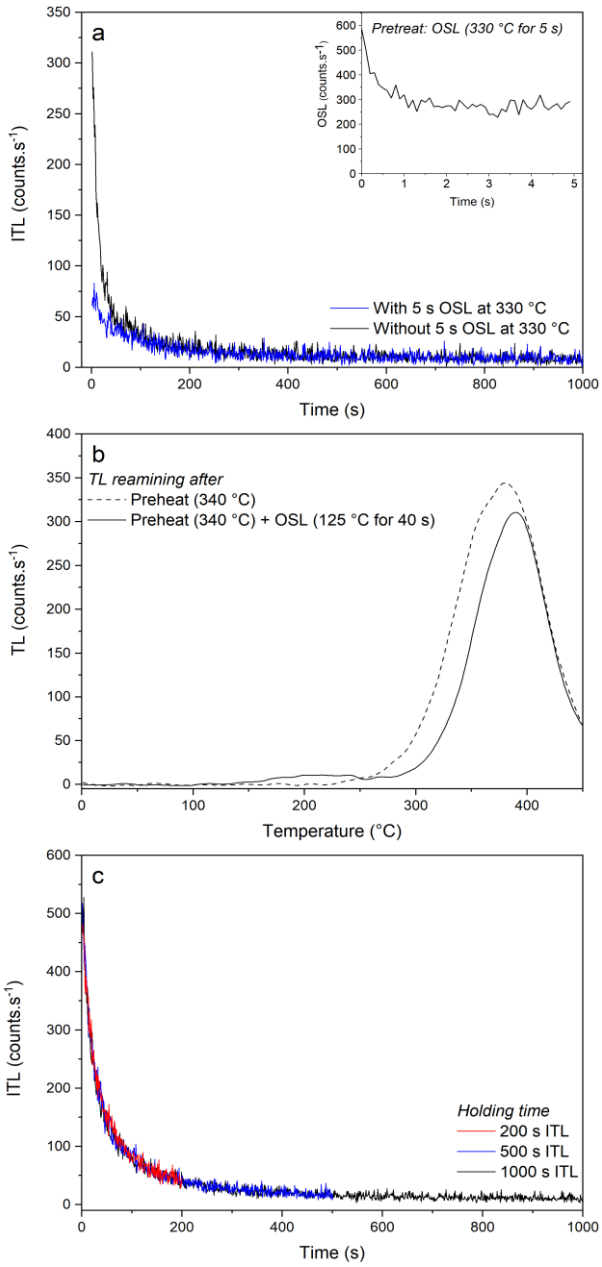

Figure 5.1: Comparison of the (a) ITL_{330} decay curves measured using protocol 5.1a (without ramp OSL step) with (blue curve) and without (black curve) 5 s blue stimulation at 330 °C for an aliquot of sample LUM 4163. Inset: decay curve measured for 5 s blue stimulation at 330 °C, (b) TL remaining after the preheat at 340 °C (dashed curve) and the preheat at 340 °C with blue OSL followed (125 °C for 40 s) (solid curve), and (c) ITL_{330} decay curves for various holding duration for an aliquot of sample LUM 4163 following a regenerative dose of 350 Gy. For all the above experiments, the aliquot was sensitised first by several cycles of irradiation and heating.

Table 5.2: ITL_{330} protocol from Murray and Wintle (2000) and the proposed ITL_{330} protocol used in this study.

Step	a) Original protocol (Murray and Wintle, 2000)	b) Proposed protocol
1	Given dose	Given dose
2	Pretreat (340 °C, then 5 s OSL at 330 °C)	Preheat (340 °C for 0 s)
3	Ramp OSL (0-100% in 1000 s at 125 °C)	Blue OSL (40 s at 125 °C)
4	Heat to 330 °C and hold for 1000 s	Heat to 330 °C and hold for 500 s
5	Test dose	Test dose
6	Pretreat (340 °C, then 5 s OSL at 330 °C)	Preheat (340 °C for 0 s)
7	Ramp OSL (0-100% in 1000 s at 125 °C)	Blue OSL (40 s at 125 °C)
8	Heat to 330 °C and hold for 1000 s	Heat to 330 °C and hold for 500 s

5.4 Characteristics of the ITL_{330} signal

5.4.1 Origin of the signal

To investigate the origin of the ITL_{330} signal measured by the proposed protocol (Table 5.2b), the TL signal loss after the ITL measurement at 330 °C for various holding durations was examined for sample LUM 4163. An aliquot was first sensitised through repeated cycles of irradiation and heating. The TL response to a ~350 Gy regenerative dose was then measured after a preheat at 340 °C and blue stimulation at 125 °C for 40 s (no isothermal TL) and after the same preheating and blue stimulation followed by holding at 330 °C for 200 s, 500 s, and 1000 s, during which time the ITL signal was observed. The loss of TL resulting from the ITL measurement was then obtained by subtracting the TL curve without ITL measurement from that after ITL measurement (Fig. 5.2a). The main depletion in TL due to ITL centered at a temperature of ~380 °C, therefore could correspond to the well-known 375 °C TL peak in quartz. It is noteworthy that the amount of TL that is lost during different holding durations is almost similar.

To further test whether the ITL_{330} signal originates from the 375 °C TL peak, the pulse annealing curve was measured using the proposed protocol in Table 5.2b. An aliquot of LUM 4163 was given a dose of ~500 Gy and preheated to 340 °C followed by a blue stimulation at 125 °C for 40 s. The aliquot was subsequently heated to an annealing temperature between 200 °C and 450 °C using a heating rate of 5 °C s^{-1} in 10 °C intervals before ITL measurement at 330 °C. Any sensitivity change was monitored by the response of the corresponding signal to a test dose of ~200 Gy. The pulse annealing curve demonstrates that there is no ITL_{330} signal

left when the annealing temperature is above ~390 °C, confirming its likely origin with the 375 °C TL peak of quartz (Fig. 5.2b).

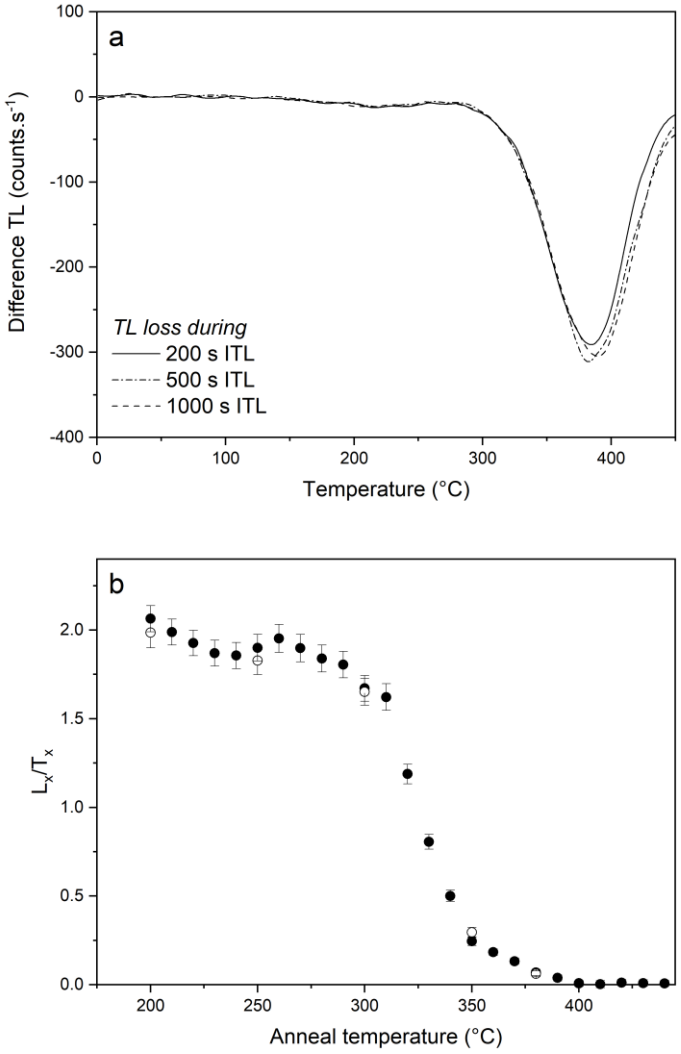

Figure 5.2: (a) TL signal loss showing the charge depletion as a result of the isothermal TL measurements at 330 °C with different holding times, and (b) pulse annealing curve for the ITL_{330} signal for sample LUM 4163. Open circles are the repeated measurements at the end of the experiment to test the reproducibility of the measurement. The heating was performed at a rate of 5 °C s^{-1}.

5.4.2 Thermal stability

Determining the thermal stability of the ITL signal is important for evaluating whether the proposed protocol probes stable electron traps. The thermal stability of the ITL_{330} signal was investigated using an aliquot of samples LUM 4163, and 3707. The latter sample was also used for the investigation of the thermal stability of the VSL signal (Rahimzadeh et al., 2021). The kinetic parameters of the ITL_{330} trap were assessed using the isothermal decay technique. The thermal holding experiments were conducted following a dose of 400 Gy, preheat at 340 °C, and blue stimulation at 125 °C for 40 s. The aliquots were then held at 260, 280, 300,

and 320 °C for time periods of 10 s up to 10000 s before the ITL measurement at 330 °C. The ITL response to a test dose of 200 Gy was used for sensitivity correction. Previous studies showed that the decay of the slowly bleaching peak (SBP), which is commonly referred to as the 375 °C TL peak, does not follow first order kinetics (e.g., Hornyak et al., 1992; Spooner and Franklin, 2002). Therefore, the thermal lifetime of the ITL_{330} signal was estimated using the stretched hyperbolic function, which also has been used in fitting the VSL signal (Ankjærgaard et al., 2013, 2015; Rahimzadeh et al., 2021):

$$I(t) = (1 + ct/\tau_{eff})^{-1/c}, \qquad c > 0 \tag{5.1}$$

where $I(t)$ is the intensity of the signal at time t, $\tau eff(s)$ is the effective lifetime, and the stretching factor c is a dimensionless parameter accounting for deviation from first order kinetics (where c=0). The average calculated stretching factor (c) is 0.60±0.02 for LUM 4163 and 0.65±0.01 for sample 3707. The isothermal decay curves of sample LUM 3707 are shown in Fig. 5.3. E and s values can be calculated by plotting the lifetimes derived from the data sets in Fig. 5.3 as a function of $1/kT$ (inset Fig. 5.3). The calculated kinetic parameters are E = 1.84±0.12 eV and s = 4.3×10^{14} s^{-1} for sample LUM 4163, and E = 1.88±0.10 eV and s = 7.0×10^{14} s^{-1} for sample LUM 3707. Similar results were obtained by Gong et al. (2010), who studied the TL thermochronometry of quartz from boreholes in Eastern China, and calculated E and s values of 1.87 eV and 5×10^{14} s^{-1}, respectively, for the 375 °C quartz TL peak, although the method used for kinetic parameters determination was not mentioned. However, a lower trap depth (E value of 1.66 eV) was reported for the 375 °C quartz TL peak using the initial rise method (Aitken, 1985; Appendix E).

The thermal lifetime of the ITL_{330} signal at a mean annual temperature of 10 °C at Luochuan (Hu et al., 2015) was calculated as 4.0×10^{10} and 1.1×10^{11} years for sample LUM 4163 and 3707, respectively.

The ITL_{330} kinetic parameters (E and s) of sample LUM 3707 are comparable to previously reported values for the VSL signal of the same sample (E ~2.0 eV and s ~8×10^{15} s^{-1}, from Rahimzadeh et al., 2021), suggesting that both signals originate from the same trap. In comparison, the E values of the ITL signal associated with the 325 °C TL peak are ~1.5-1.6 eV (e.g., Jain et al., 2007; Vandenberghe et al.,

2009), confirming that the ITL_{330} signal originates from a deeper and thus more stable trap.

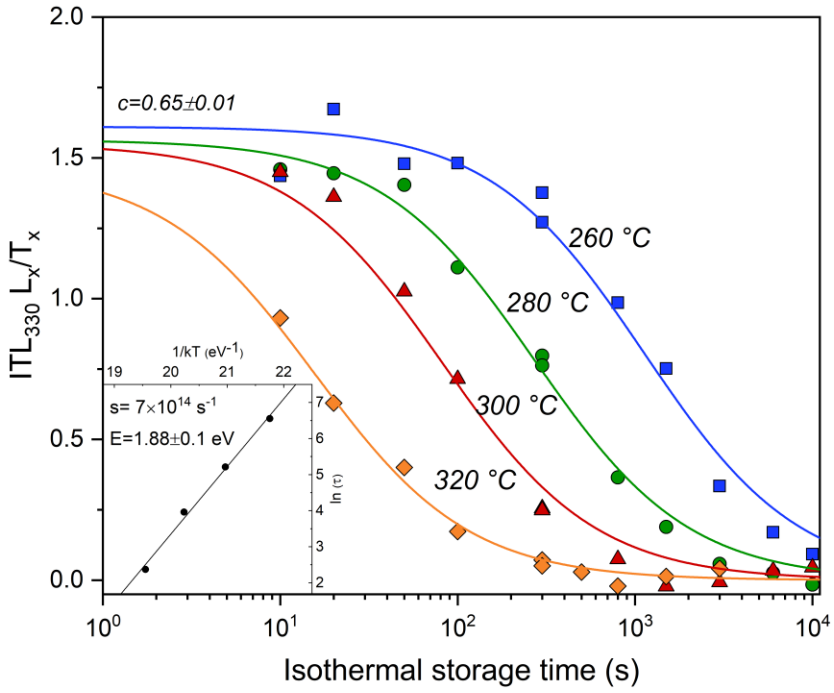

Figure 5.3: Isothermal holding of sample LUM 3707 at temperatures between 260 and 320 °C for different durations prior to the ITL signal measured at 330 °C. The data was fitted using stretched hyperbolic equation. Inset shows the kinetic parameters (E and s) of the ITL_{330} signal derived from the Arrhenius plot.

5.4.3 Bleachability

One of the most important prerequisites of luminescence dating for sediments is resetting the studied signal to a negligible level at the burial time. The slowly bleaching nature of the 375 °C TL peak (e.g., Franklin, 1997, 1998; Franklin et al., 2000) suggests that there is greater chance for insufficient signal zeroing (compared to the 325 °C TL peak). Therefore, two experiments were undertaken to investigate the resetting of the ITL_{330} signal.

In the first experiment, the equivalent dose (D_e) of the youngest available sample (LUM 3703) with an expected natural dose of 26±3 Gy (Table 5.1) was measured using the proposed protocol outlined in Table 5.2b, to evaluate the bleachability of the ITL_{330} signal in natural conditions. Note that the 63-100 µm fraction was used for this experiment, because of the lack of fine grain quartz. The D_e value was measured using MAAD protocol and obtained by extrapolation of the DRC back to where it intercepts the dose axis (Fig. 5.4a). The D_e measured using

the ITL_{330} signal was 20±5 Gy (Fig. 5.4a), consistent with the expected dose, implying that the residual dose for the ITL_{330} signal is insignificant.

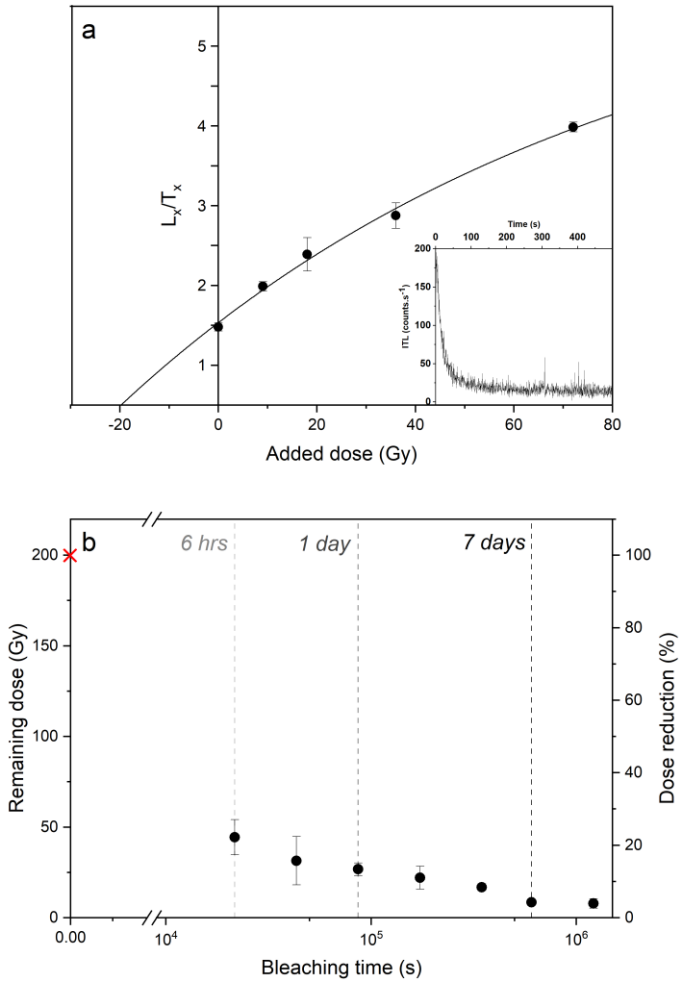

Figure 5.4: (a) MAAD dose response curve and decay curve (inset) of sample LUM 3703 with an expected dose of 26 Gy. Three aliquots were used per dose point and the data is fitted with a single saturating exponential function, and (b) bleaching curve of the ITL_{330} signal by exposure to the Hönle SOL2 solar simulator. 105 aliquots of sample LUM 3712 were heated to 450 °C and irradiated with 200 Gy, bleached in the solar simulator for different bleaching duration, and measured using MAAD protocol in Table 5.2b. Note that no measurement was done for 0 s bleach and it was assumed that the amount of dose prior to the bleaching test (i.e., 0 s bleaching) is equal to the 200 Gy given dose (red cross).

The second experiment was the solar simulator (Hönle SOL2) bleaching test using the oldest sample LUM 3712 with an expected dose of 2069±233 Gy. Laboratory zeroing of the signal by heating to 450 °C followed by administering a regeneration dose of 200 Gy was first carried out to remove the natural signal and also eliminate the possible effect of the variation in natural dose among subsamples. Seven groups with 15 aliquots in each were bleached for up to 14 days (6 h, 12 h, 1 day, 2 days, 4 days, 7 days, and 14 days) by the SOL2, and D_e values were measured using MAAD protocol (Table 5.2b), and range between 44.4±9.8 Gy (6 hours bleaching) and 7.9±2.7 Gy (14 days bleaching). It can be seen from Fig.

5.4b, that the dose depleted to about 22% within 6 hours. After 7 days of bleaching, the remaining dose of ITL_{330} signal reduced to about 4% (8.5±1.1 Gy); however it appears that the signal stabilised at this level and further exposure to the SOL2 for 14 days did not significantly reduce the remaining dose. However, it should be noted that during exposure in the solar simulator the sample has been heated above ambient temperature (stabilised at ~45 °C after 1 hour of SOL2 exposure), and therefore cannot have mimicked the natural sunlight bleaching.

5.5 Natural and laboratory dose response curves

In the previous section, the main physical characteristics of the ITL_{330} signal, in terms of the origin of the signal, thermal stability, and the bleaching properties were investigated. This section evaluates the dosimetric response and the applicability of the multiple aliquot approaches to this signal for extending the dating limit of quartz.

5.5.1 Natural dose response curve

The natural DRC of the ITL_{330} signal was constructed using reference ages of the Luochuan loess section. For the six uppermost samples from L1 to L3, the reference ages were obtained from the luminescence age model of Zhang et al. (2022) for the Luochuan section, which is constructed by performing age-depth modelling with the Bacon software (Blaauw and Christen, 2011) with high resolution quartz OSL and multi-elevated temperature post-IR IRSL (MET-pIRIR) ages. To calculate the expected ages for each sample, the depth of the samples was first adjusted based on the relative position of each sample within its unit, then correlated to the depth in Zhang et al. (2022). The mean Bacon model age was taken as reference age and the half of the difference between the maximum and minimum model ages was used as the uncertainty. The expected ages from the remaining samples (i.e., L4, L5 and L6) were derived from a linear interpolation of two boundary ages of the Chiloparts record (Ding et al., 2002), with an assumed 10% uncertainty. The expected natural doses were then obtained by multiplying the measured dose rates by reference ages.

To construct a natural DRC, the natural signals (L_n/T_n, 200 Gy test dose) were measured for six aliquots from each sample and plotted against the expected natural doses (Fig. 5.5). The data is fitted with a single saturating exponential (SSE) function plus a constant offset, yielding a characteristic saturation dose (D_0) of 396±68 Gy, and the constant offset of 0.53±0.21, implying that the natural DRC does not go through the origin which suggests the difficult-to-bleach part of the

ITL_{330} signal. This unbleachable residual signal can be calculated from the fitted natural curve, giving a value of ~80 Gy; this is much larger than the residual dose obtained from the coarse grain fraction (see section 5.4.3). Alternatively, this offset may be due to insufficient data points in the low dose region of the DRC (i.e., with only two samples with an expected dose <200 Gy). With the average dose rate of 3.5 Gy/ka from the Luochuan section, the upper dating limit of the ITL_{330} signal at this site was estimated to be ~230 ka (by considering two times D_0 is the upper dating limit).

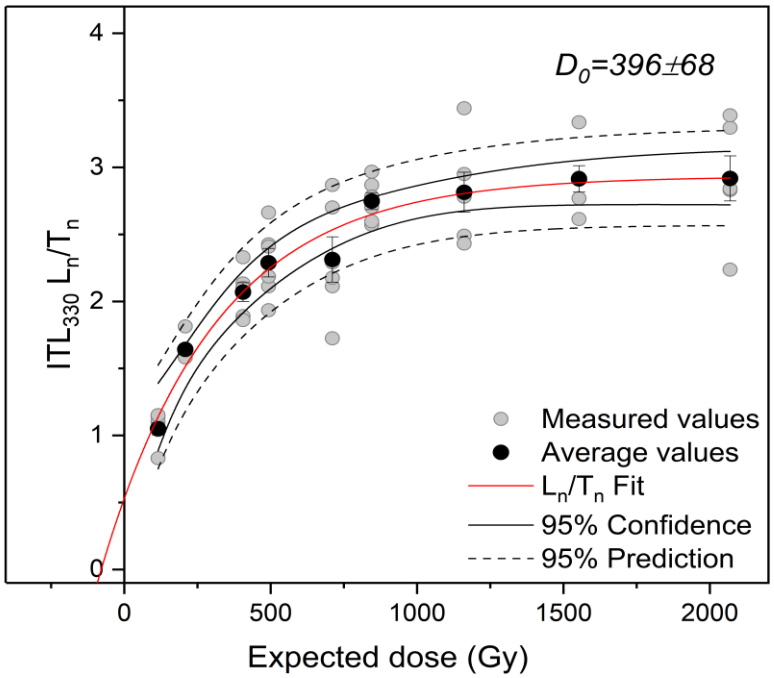

Figure 5.5: Natural ITL_{330} dose response curve. Each point represents the mean L_n/T_n and error from six aliquots plotted against the corresponding expected dose. The data is fitted (adjusted R^2=0.97) with a single saturating exponential function plus a constant offset.

5.5.2 MAR dose response curve

Four samples (LUM 4163, 4164, 4165, and 4172) were used to test the MAR protocol, where the natural signals were reset prior to irradiation. From Fig. 5.4b, it can be seen that the depletion of the ITL_{330} signal after 7 days and 14 days are similar, therefore 7 days bleaching was chosen as it is practically more feasible to carry out. A total of 78 aliquots (21 from LUM 4163, 21 from LUM 4164, 21 from LUM 4165, and 15 from LUM 4172) were bleached in the solar simulator for 7 days. Bleached aliquots were divided into several groups with 3 aliquots in each, exposed to different radiation doses ranging from 0 to ~2000 Gy. The same test dose (200 Gy) as employed to construct the natural DRC was used. The MAR DRCs were built from L_x/T_x ratios fitted with a SSE function. The average L_x/T_x value of 0.42±0.04 for 0 Gy regenerative dose demonstrated that 7 days of bleaching might

not be sufficient to completely remove the natural signal, which is in contrast to the result of SOL2 bleaching test in Section 5.4.3. Indeed, in the bleaching experiment the sample was heated prior to radiation to completely remove the signal, whereas in actual sediments the residual could accumulate over many cycles. Therefore, the residual dose of each sample was calculated by extrapolation of their MAR DRC back to where it intercepts the dose axis. The obtained residual dose values range between 38.8±10.9 Gy (LUM 4163) to 66.3±22.4 Gy (LUM 4172). The obtained residual doses were each added to the regenerative dose points of the corresponding MAR DRCs to take into account that the natural signal of samples is not completely removed prior to irradiation in the MAR protocol; (residual corrected) MAR DRCs of all samples are presented in supplementary Fig. S5.1.

The MAR DRCs together with the natural L_n/T_n fit from Fig. 5.5 are shown in Fig. 5.6. For each individual MAR DRC the D_0 value range between 297±49 Gy (LUM 4163) to 479±34 Gy (LUM 4172), giving a D_0 value of 397±32 Gy for the averaged MAR DRC (fit to all the data). Although the comparison of the natural and MAR DRC is not simple, due to a small number of data points in the low dose region of the natural DRC, it can be seen from Fig. 5.6, that the natural and MAR DRCs are markedly dissimilar in shape, and overlay each other only for doses up to ~200 Gy. Beyond 200 Gy, the natural DRC lies below the MAR DRC.

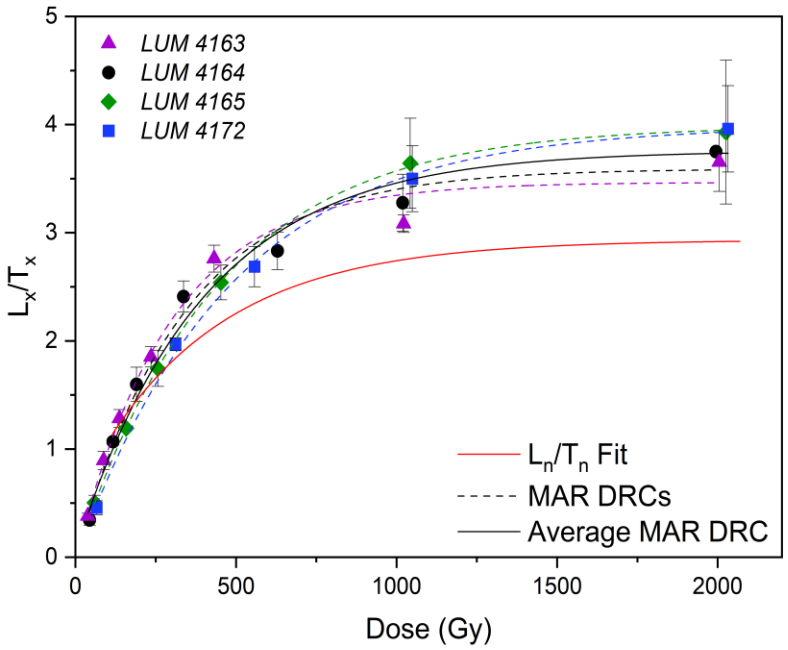

Figure 5.6: MAR DRCs for four samples (LUM 4163, 4164, 4165, and 4172) in dashed lines are plotted together with the natural L_n/T_n fit from Fig. 5.5 (red line). 3 aliquots were measured for each regenerative dose and data is fitted with a single saturating exponential function. Note that all MAR DRCs are after residual correction (see text for further details).

5.5.3 MAAD dose response curve

The data presented in section 5.5.2 demonstrated that all studied samples for the MAR approach yielded large residual doses even after 7 days of SOL2 exposure, which can thus hamper the applicability of the MAR protocol. It is therefore of interest to investigate the MAAD protocol, with which doses were added directly on top of the natural dose. Sample LUM 3704 with an expected natural dose of 115±9 Gy (Table 5.1) was used to test the MAAD protocol. 24 aliquots of sample LUM 3704 containing the natural dose (N) were split into several batches with 3 aliquots in each (except the natural batch which contains 6 aliquots), exposed to different additive radiation doses, and measured using the protocol in Table 5.2b with the same test dose (200 Gy) as used previously in the MAR measurements. The MAAD DRC with N+0, N+50 Gy, N+100 Gy, N+200 Gy, N+400 Gy, N+800 Gy, and N+1600 Gy dose points was built and fitted with a SSE function plus a constant offset. A D_0 value of 366±36 Gy and a constant offset of 0.24±0.14 are obtained (Fig. 5.7, dash dotted black line). The comparison between natural and MAAD DRCs reveals that the natural DRC is considerably below the MAAD DRC; they deviate from each other at very low doses (~200 Gy; Fig. 5.7), similar to the MAR DRC.

One possible explanation for the observed difference in the natural and laboratory DRCs could be related to the significantly different irradiation rates the samples received in nature and in the laboratory. At natural dose rates, the concentration of electrons in thermally unstable traps always remains consistently low, while the thermally stable traps are filled steadily over time. In contrast, under a high dose rate of beta irradiation in the laboratory (~10^8 times higher than that in nature), those thermally unstable traps will be occupied by electrons as the trapping rate is much higher than the decay rate. As the thermally unstable traps start to be occupied under laboratory irradiation, the free unstable traps become less and a higher portion of the evicted electrons will be captured by the thermally stable traps. Consequently, the trapping efficiency for the thermally stable traps under laboratory irradiation is higher than under the natural irradiation (Bailey, 2004). To overcome the issue related to different laboratory and natural dose rates, some studies proposed to administer each laboratory dose in small pulses separated by heat treatments (i.e., pulsed-irradiation procedure) rather than by the conventional continuous irradiation (Bailey et al., 2005; Qin and Zhou, 2009). With the heat treatment between the pulsed irradiations, the thermally unstable traps can be emptied, which can mimic the situation under

natural irradiation. We therefore applied the pulsed-irradiation procedure to investigate whether this approach would resolve or reduce the differences between the natural and laboratory DRCs.

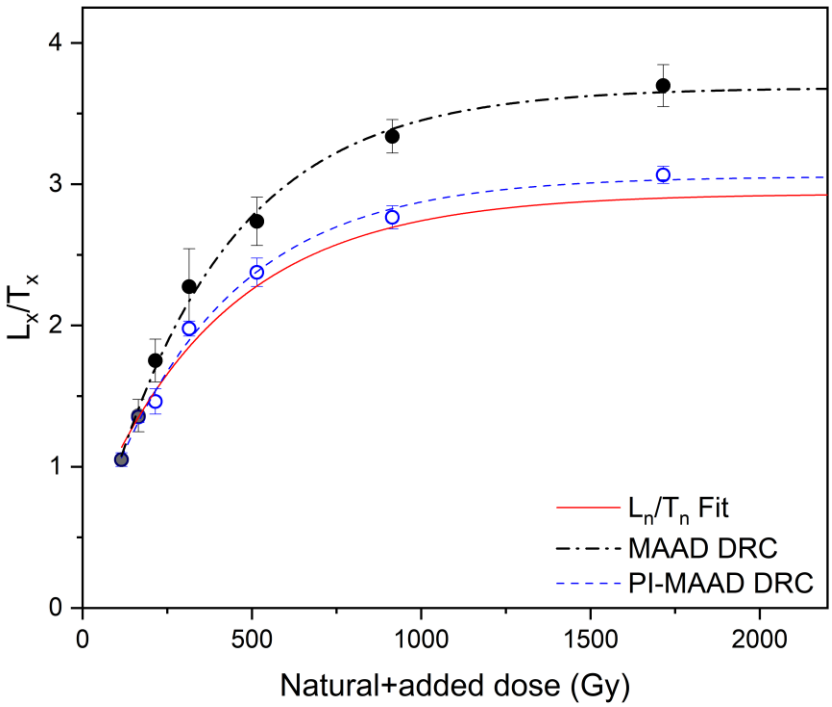

Figure 5.7: MAAD (dash dotted black line) and PI-MAAD (dashed blue line) DRCs using sample LUM 3704 are plotted together with the natural L_n/T_n fit from Fig. 5.5 (solid red line). The (PI-)MAAD was measured by adding doses on top of the natural expected dose of 115 Gy, after which L_x and T_x signals were measured. The mean L_x/T_x and standard error from 3 aliquots are plotted as a function of the total (natural+added) dose data and fitted with a single saturating exponential function. For a PI-MAAD, a pulsed irradiation approach was used with a unit dose of 10 Gy and 200 °C cutheat in between.

Pulsed-irradiation MAAD (PI-MAAD) DRC was constructed for sample LUM 3704 using the same additive doses and test dose as employed to construct MAAD DRC. 3 aliquots were used for each additive dose. A pulsed-irradiation with 10 Gy dose was given for each step separated by a 200 °C cutheat. It should be noted that the size of pulse dose and the cutheat temperature might influence the D_e estimation (e.g., Bailey, 2004; Qin and Zhou, 2009). To mimic the radiation dose rates in nature, we selected a small unit dose of 10 Gy. Furthermore, inter-pulse cutheat temperature of 200 °C was selected to reduce the potential effect of partial annealing of higher temperature TL peak while still removing low temperature TL peak. Note that continuous irradiation was used for the test dose signal. All other measurement conditions were the same as used for MAAD so that any differences observed in the resultant DRC could correspond to the difference in the way of irradiation.

When PI-MAAD DRC (Fig. 5.7, dashed blue line) is compared against the MAAD DRC (dash dotted black line), the L_x/T_x ratios are in agreement up to ~160 Gy dose, but lower L_x/T_x ratios were obtained for PI-MAAD at higher dose. One would expect that the repeated inter-pulse thermal treatments might cause thermal depletion of the ITL_{330} signal. To check whether this is the case, the loss of the signal due to the repeated inter-pulse cutheat steps was investigated. The sample was irradiated with 1000 Gy in a single irradiation step and then given different numbers of thermal treatments (0 and 100 repeated 200 °C cutheat steps) before the ITL_{330} measurement (Table 5.2b; steps 2-8). Comparison of the L_x/T_x values with and without repeated cutheat treatments indicating that the signal loss after 100 times cutheat at 200 °C is about 5%. However, a comparison of MAAD and PI-MAAD datasets for 900 Gy irradiation (with 80 times cutheat at 200 °C for the PI-MAAD) shows that the signal intensity reduced to ~17% after pulsed irradiation. Therefore it can be concluded that the thermal depletion of the signal due to the repeated cutheat steps is not significant. Furthermore, although a marked change is observed between the MAAD and PI-MAAD DRCs, there is virtually no difference in their D_0 value; i.e. D_0 of 366±36 Gy and 370±40 Gy for MAAD and PI-MAAD, respectively. Finally, when the PI-MAAD DRC (dashed blue line) is compared with the natural ITL_{330} DRC (Fig. 5.7, solid red line) it can be observed that the shape of the natural DRC can mostly be reproduced with a PI-MAAD approach. This suggests that pulsed-irradiation can provide a better simulation of the trapping conditions in the natural environment. Although pulsed-irradiation protocol appears to be a promising step forward in reducing the shape dissimilarity between the natural and regenerated DRCs, further systematic investigations are required for optimal pulsed irradiation conditions in terms of thermal treatment and pulse dose (e.g., Qin and Zhou, 2009). For example, Chapot et al. (2014) showed that the percentage of TT-OSL signal loss per inter-pulse thermal treatment in the pulsed irradiation protocol is significant, especially for the high temperature cutheat (i.e. higher than 240 °C). Therefore more research is needed to evaluate and account for the degree of signal reduction by the repeated inter-pulse thermal treatments.

5.6 Age comparison

To evaluate the performance of different ITL_{330} protocols, natural L_n/T_n values are interpolated onto the laboratory DRCs to estimate the D_es. For the MAR protocol, the L_n/T_n values of 4 samples (LUM 4163, 4164, 4165, and 4172) are interpolated to their corresponding DRCs. Note that the residual corrected MAR DRCs were

used to estimate the equivalent doses (see section 5.5.2). For the (PI-)MAAD protocol, all natural L_n/T_n values (except LUM 3704) are interpolated onto (PI-)MAAD DRC, following the approach of Ankjærgaard et al. (2016), though they obtained D_es by projecting the natural signals onto a piecewise linear interpolation of the DRC data points. Note that the (PI-)MAAD DRC was constructed assuming that the natural dose of sample LUM 3704 was 115 Gy (Table 5.1), and that the additional doses were added on top of this dose. For sample LUM 3704, which was used to construct the (PI-)MAAD DRC, the D_e was obtained by extrapolation of theDRC to the dose axis. A summary of all the information relevant to the D_es and estimated ages is given in Table 5.1. The estimated ages by different protocols together with the expected ages are plotted against the sampling depths in Fig. 5.8.

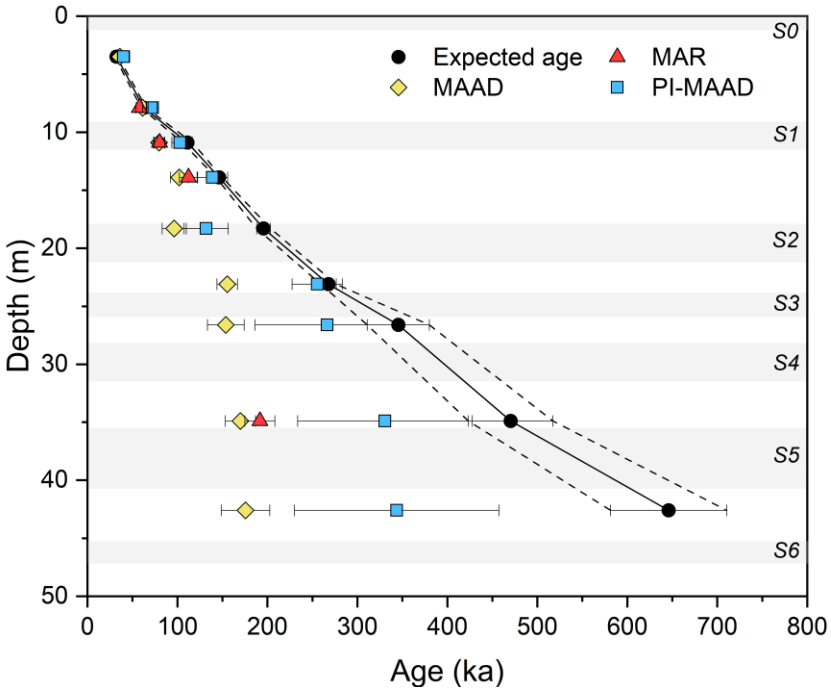

Figure 5.8: Calculated ITL_{330} ages using MAR, MAAD, and PI-MAAD protocols (values in Table 5.1) compared with expected ages from Zhang et al. (2022) and Ding et al. (2002).

As shown in Fig. 5.8, the estimated ITL_{330} ages using MAR and MAAD protocols agree with each other, as would be expected as both have similar dose response curves (Fig. S5.2). However, both MAR and MAAD ages underestimated the expected ages beyond ~70 ka (corresponding to about 200 Gy), which is in agreement with our observation from the DRCs comparison that the natural and laboratory DRCs deviate after ~200 Gy. This indicates that the maximum dating limit for the ITL_{330} signal using MAR and MAAD protocol at Luochuan section is ~70 ka, slightly higher than the upper limit of quartz blue OSL at Luochuan (i.e., ~40-50 ka; Buylaert et al., 2007; Lai, 2010; Chapot et al., 2012). For the PI-MAAD protocol, obtained ages are consistent with expected ages up to 290 ka, except

sample LUM 3707, which is still in agreement with its independent age within 2 sigma uncertainties. The large uncertainty for the three oldest samples (i.e. LUM 3710, 4172, and 3712) is mainly due to the saturation of the signal ($2D_0$ ~740 Gy). Furthermore, a relative steady age increase beyond ~250 ka suggests that the ITL_{330} signal reached its field saturation, which is in line with our previous observation from the natural DRC, for which an upper dating range limit ($2D_0$) was 792±136 Gy, equivalent to ~230 ka (233±40 ka) based on the average environmental dose rate of 3.4±0.06 Gy/ka for the 9 studied samples. Therefore, all estimated ages beyond about 230 ka should be treated as minimum ages.

5.7 Can ITL_{330} be an alternative to VSL for extending the age range?

Both ITL_{330} and VSL signals are thought to have considerable potential for extending the age range of quartz. These signals originate from what is commonly referred to the quartz 375 °C TL peak; a deeper and more stable trap than that of the OSL signal. It is therefore of great interest to investigate whether the ITL_{330} signal can be used as an alternative to the VSL signal, since measuring the VSL signal required a special instrumental facility, which might not be readily available in all luminescence laboratories. The VSL dataset of the same samples from Rahimzadeh et al. (2021) was used for this comparison. The VSL signal was measured using the protocol of Rahimzadeh et al. (2021) (Table S5.1), with the first 2.5 s of stimulation minus an early background taken from the following 15 s being used in the calculations. The fixed test dose of 200 Gy was employed in both ITL_{330} and VSL measurements. The natural DRC of each signal was normalised to its highest value to enable comparison of their shapes.

Fig. 5.9a shows the normalised natural DRCs of both signals. The shape of natural growth curves, characterised by the D_0, are very similar (both with D_0 of ~400 Gy). It is also obvious from Fig. 5.9a that the DRCs of both signals do not pass through the origin at 0 Gy, suggesting the difficult-to-bleach part of the signals. From the fitted curves, an identical residual dose of 80 Gy was calculated for both signals. However, as mentioned earlier in section 5.5.1, this offset can be due to the limited number of young samples with low natural doses; therefore the magnitude of this residual dose needs to be evaluated further by additional measurements of younger samples. Note that the ITL_{330} D_e for the youngest sand-sized sample (LUM 3703, with an expected dose of 26±3 Gy) is 20±5 Gy, suggesting no large residual dose for the ITL signal (see section 5.4.3). Overall, the D_0 of ~400 Gy for both signals suggests an identical theoretically measurable dose range of ~800 Gy, which would correspond to a dating range of ~230 ka (for a dose rate of 3.5 Gy/ka

measured from the Luochuan samples).To further evaluate how similar these two signals are, the VSL D_es are compared with those obtained using the ITL_{330} signal. All VSL D_es were measured using MAR standardised growth curve method (MAR-SGC; Rahimzadeh et al., 2021). With the exception of one sample (LUM 4168), the ITL_{330} D_e values (determined using MAR and MAAD protocols) were consistent with the VSL D_es (Fig. 5.9b), and both largely underestimate their expected D_e values beyond ~200 Gy (Fig. S5.3). Although further investigation is needed to understand how these two signals are related, the observations here indicate that both signals have similar characteristics, in terms of kinetic parameters (see section 5.4.2), DRCs and estimated burial doses, and therefore the ITL_{330} signal could be an alternative to the VSL signal.

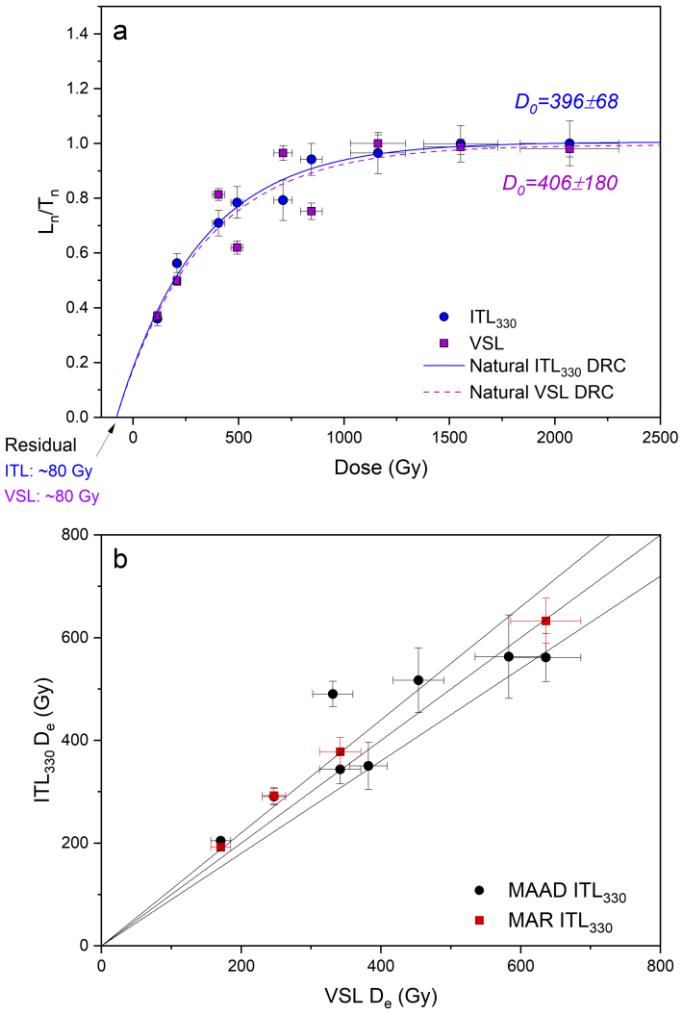

Figure 5.9: Comparison of the (a) normalised natural DRCs of the VSL (dashed violet line) and ITL_{330} (solid blue line) signals. Note that for each sample 6 and 12 natural aliquots were measured for the ITL_{330} and VSL signal, respectively. The data is fitted with a single saturating exponential function plus a constant offset, and (b) measured ITL_{330} D_e values using a MAR (red squares) and a MAAD (black circles) protocols and measured VSL D_e values using MAR-SGC from Rahimzadeh et al. (2021).

5.8 Summary and conclusions

In this study, a comprehensive investigation of the physical and dosimetric properties of the quartz ITL signal measured at 330 °C was conducted using fine-grained quartz samples with ages up to ~700 ka from the Luochuan section of the Chinese Loess Plateau. Measurements using the proposed protocol in this study showed that the origin of the ITL_{330} signal is closely associated with a TL peak at 375°C in quartz and it originates from a deep trap at about 1.8 eV with a thermal lifetime of $\sim 10^{10}$ years at 10 °C. The residual dose measured using the youngest available sample indicates that there is a negligible residual dose for the ITL_{330} signal. Furthermore, the SOL2 bleaching experiment showed that the ITL_{330} signal can be depleted to about 4% of the initial dose after 7 days of SOL2 exposure. The natural ITL_{330} dose response curve saturates at ~800 Gy, suggesting that ITL_{330} would enable dating at the Luochuan section up to about 230 ka.

Comparison of the natural and laboratory regenerated DRCs (for both MAR and MAAD protocols), reveals that they deviate from one another at about ~200 Gy, resulting in significant ITL_{330} age underestimation beyond ~70 ka. Application of the pulsed laboratory irradiation appears as a promising method to reduce the differences between the natural and laboratory DRCs; the PI-MAAD DRC produces ITL_{330} ages in agreement with the expected ages up until ~290 ka. However, the obtained ages beyond 230 ka should be considered as minimum ages, since they reach their natural saturation. Despite the encouraging results showing success in reproducing the shapes of the natural signal, it should be highlighted that more studies are needed to evaluate the impact of the repeated pulse irradiation and heating on the signal. Regarding the MAR protocol, it should be noted that the signal bleachability undermines the straightforward application of the MAR protocol for the ITL_{330} signal, even if the pulsed irradiation approach can reduce the differences between the natural and laboratory DRCs. Furthermore, a comparison of the VSL and ITL_{330} demonstrated that both signals have similar characteristics, in terms of kinetic parameters, DRCs and estimated burial doses, suggesting that both signals might originate from the same trap in quartz, and therefore the ITL_{330} signal can be used as an alternative signal in cases where the violet laser facility is not available. However further investigation is needed to confirm these observations and to draw firm conclusions about the precise origin of these two signals and how they are related to each other.

Acknowledgments

We thank Petra Posimowski and Sabine Mogwitz for sample preparation and gamma spectrometry measurements. Jingran Zhang, Zhong He and Linhai Yang are thanked for their assistance in the fieldwork and sample collection. We thank Mayank Jain, an anonymous reviewer, and the Associate Editor, Geoff Duller for their helpful and constructive comments which helped improve the paper. This work was partially supported by the National Natural Science Foundation of China (No. 41977381).

References

Aitken, M.J., 1985. Thermoluminescence Dating. Academic Press, ISBN 0-12-046380-6, 359 p.

Aitken, M.J., 1992. Optical dating. Quat. Sci. Rev. 11, 127-131.

Ankjærgaard, C., Jain, M., Wallinga, J., 2013. Towards dating quaternary sediments using the quartz violet stimulated luminescence (VSL) signal. Quat. Geochronol. 18, 99-109.

Ankjærgaard, C., Guralnik, B., Porat, N., Heimann, A., Jain, M., Wallinga, J., 2015. Violet stimulated luminescence: geo-or thermochronometer? Radiat. Meas. 81, 78-84.

Ankjærgaard, C., Guralnik, B., Buylaert, J.-P., Reimann, T., Yi, S.W., Wallinga, J., 2016. Violet stimulated luminescence dating of quartz from Luochuan (Chinese loess plateau): agreement with independent chronology up to ~600 ka. Quat. Geochronol. 34, 33-46.

Bailey, R.M., 2004. Paper I–simulation of dose absorption in quartz over geological timescales and its implications for the precision and accuracy of optical dating. Radiat. Meas. 38, 299-310.

Bailey, R.M., Armitage, S.J., Stokes, S., 2005. An investigation of pulsed-irradiation regeneration of quartz OSL and its implications for the precision and accuracy of optical dating (Paper II). Radiat. Meas. 39, 347-359.

Blaauw, M., Christen, J.A., 2011. Flexible paleoclimate age-depth models using an autoregressive gamma process. Bayesian Anal. 6, 457-474.

Buylaert, J.P., Murray, A.S., Huot, S., Vriend, M.G.A., Vandenberghe, D., De Corte, F., Van den haute, P., 2006. A comparison of quartz OSL and isothermal TL measurements on Chinese loess. Radiat. Prot. Dosimetry 119, 474-478.

Buylaert, J.P., Vandenberghe, D., Murray, A.S., Huot, S., De Corte, F., Van den Haute, P., 2007. Luminescence dating of old (> 70 ka) Chinese loess: a comparison of single aliquot OSL and IRSL techniques. Quat. Geochronol. 2, 9-14.

Chapot, M.S., Duller, G.A.T., Roberts, H.M., 2014. Assessing the impact of pulsed-irradiation procedures on the thermally transferred OSL signal in quartz. Radiat. Meas. 65, 1-7.

Chapot, M.S., Roberts, H.M., Duller, G.A.T., Lai, Z.P., 2012. A comparison of natural- and laboratory-generated dose response curves for quartz optically stimulated luminescence signals from Chinese Loess. Radiat. Meas. 47, 1045–1052.

Choi, J.H., Murray, A.S., Cheong, C.S., Hong, D.W., Chang, H.W., 2006. Estimation of equivalent dose using quartz isothermal TL and the SAR procedure. Quat. Geochronol. 1, 101-108.

Ding, Z.L., Derbyshire, E., Yang, S.L., Yu, Z.W., Xiong, S.F., Liu, T.S., 2002. Stacked 2.6-Ma grain size record from the Chinese loess based on five sections and correlation with the deep-sea δ18O record. Paleoceanography 17, 5-1-5-21.

Duller, G.A:T., 2003. Distinguishing quartz and feldspar in single grain luminescence measurements. Radiat. Meas. 37, 161-165.

Franklin, A.D., 1997. On the interaction between the rapidly and slowly bleaching peaks in the TL glow curve of quartz. J. Lumin. 75, 71-76.

Franklin, A.D., 1998. A kinetic model of the rapidly bleaching peak in quartz thermoluminescence. Radiat. Meas. 29, 209-221.

Franklin, A.D., Prescott, J.R., Robertson, G.B., 2000. Comparison of blue and red thermoluminescence from quartz. Radiat. Meas. 32, 633-639.

Frechen, M., Schweitzer, U., Zander, A., 1996. Improvements in sample preparation for the fine grain technique. Ancient TL 14, 15-17.

Gong, G.L., Li, S.H., Sun, W.D., Guo, F., Xia, B., Lu, B.F., 2010. Quartz thermoluminescence- another potential paleo-thermometer for studies of sedimentary basin thermal history. Chin. J. Geophys. 53, 103-112.

Hernandez, M., Mercier, N., 2015. Characteristics of the post-blue VSL signal from sedimentary quartz. Radiat. Meas. 78, 1-8.

Hornyak, W.F., Chen, R., Franklin, A., 1992. Thermoluminescence characteristics of the 375 °C electron trap in quartz. Phys. Rev. B 46, 8036-8049.

Hu, P., Liu, Q., Heslop, D., Roberts, A.P., Jin, C., 2015. Soil moisture balance and magnetic enhancement in loessepaleosol sequences from the Tibetan Plateau and Chinese Loess Plateau. Earth Planet. Sci. Lett. 409, 120-132.

Huot, S., Buylaert, J.P., Murray, A.S., 2006. Isothermal thermoluminescence signals from quartz. Radiat. Meas. 41, 796-802.

Jain, M., Bøtter-Jensen, L., Murray, A.S., Denby, P.M., Tsukamoto, S., Gibling, M.R., 2005. Revisiting TL: dose measurement beyond the OSL range using SAR. Ancient TL 23, 9-24.

Jain, M., Duller, G.A.T., Wintle, A.G., 2007. Dose response, thermal stability and optical bleaching of the 310 °C isothermal TL signal in quartz. Radiat. Meas. 42, 1285–1293.

Jain, M., 2009. Extending the dose range: probing deep traps in quartz with 3.06 eV photons. Radiat. Meas. 44, 445-452.

Lai, Z., 2010. Chronology and the upper dating limit for loess samples from Luochuan section in the Chinese Loess Plateau using quartz OSL SAR protocol. J. Asian Earth Sci. 37, 176-185.

Lu, Y.C., Wang, X.L., Wintle, A.G., 2007. A new OSL chronology for dust accumulation in the last 130,000 yr for the Chinese Loess Plateau. Quat. Res. 67, 152-160.

Murray, A.S., Wintle, A.G., 2000. Application of the single-aliquot regenerative dose protocol to the 375 °C quartz TL signal. Radiat. Meas. 32, 579-583.

Qin, J.T., Zhou, L.P., 2009. Stepped-irradiation SAR: a viable approach to circumvent OSL equivalent dose underestimation in last glacial loess of northwestern China. Radiat. Meas. 44, 417-422.

Rahimzadeh, N., Tsukamoto, S., Zhang, J., Long, H., 2021. Natural and laboratory dose response curves of quartz violet stimulated luminescence (VSL): Exploring the multiple aliquot regenerative-dose (MAR) protocol. Quat. Geochronol. 65, 101194.

Singarayer, J.S., Bailey, R.M., Rhodes, E.J., 2000. Potential of the slow component of quartz OSL for age determination of sedimentary samples. Radiat. Meas. 32, 873-880.

Spooner, N.A., Franklin, A.D., 2002. Effect of the heating rate on the red TL of quartz. Radiat. Meas. 35, 59-66.

Stokes, S., 1999. Luminescence dating applications in geomorphological research. Geomorphology. 29, 153-171.

Vandenberghe, D.A.G., Jain, M., Murray, A.S., 2009. Equivalent dose determination using a quartz isothermal TL signal. Radiat. Meas. 44, 439-444.

Wang, X.L., Lu, Y.C., Wintle, A.G., 2006. Recuperated OSL dating of fine-grained quartz in Chinese loess. Quat. Geochronol. 1, 89-100.

Wintle, A.G., Murray, A.S., 2006. A review of quartz optically stimulated luminescence characteristics and their relevance in single-aliquot regeneration dating protocols. Radiat. Meas. 41, 369-391.

Zhang, J., Hao, Q., Li, S.H., 2022. An absolutely dated record of climate change over the last three glacial-interglacial cycles from Chinese loess deposits. Geology. 50, 1116-1120.

Supplementary Material- Characteristics of the quartz isothermal thermoluminescence (ITL) signal from the 375 °C peak and its potential for extending the age limit of quartz dating

Rahimzadeh, N., Zhang, J., Tsukamoto, S., Long, H.

Published on *Radiation Measurements*

https://doi.org/10.1016/j.radmeas.2022.106899

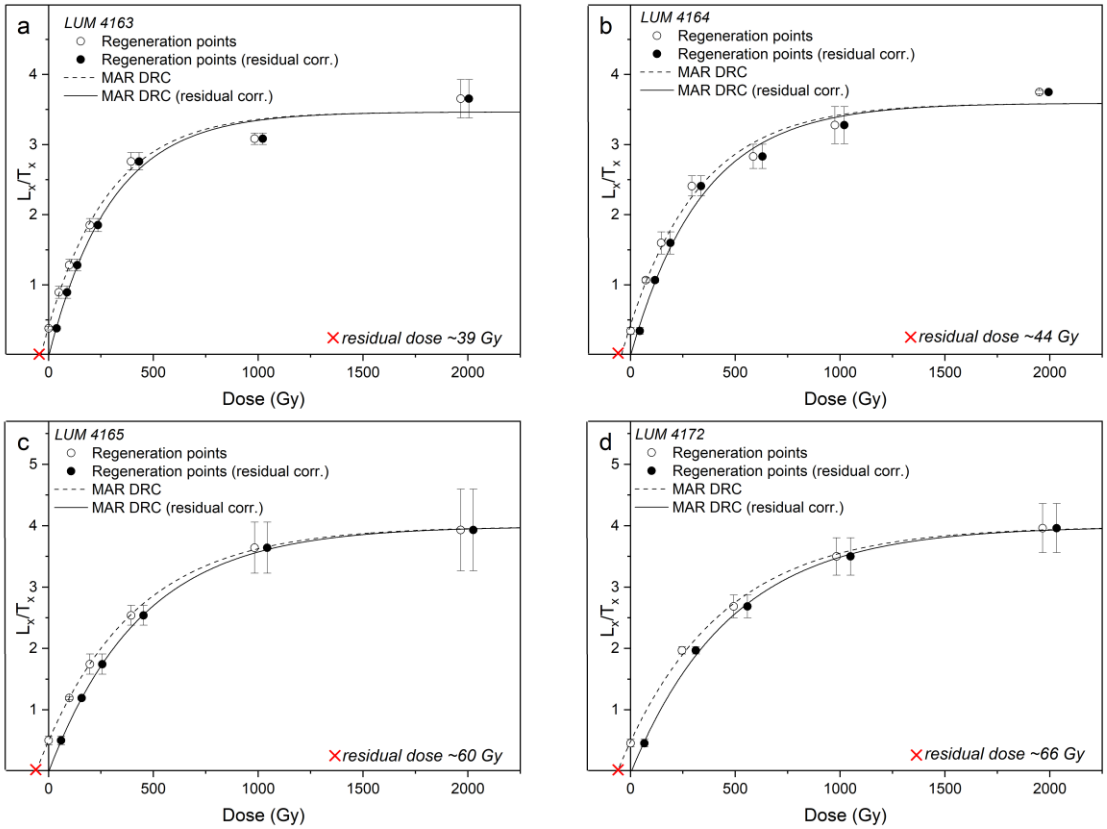

Figure S5.1: MAR DRCs measured for 4 samples are shown as dashed lines with regeneration points represented by open circles. The residual dose (red cross), which is determined by extrapolation of the DRC back to the dose axis, is added to the regenerative dose points to take into account that the natural signal is not completely removed prior to adding doses. The residual corrected regeneration points (filled circles) were then used to construct the residual corrected MAR DRCs (solid black lines) to estimate the equivalent dose.

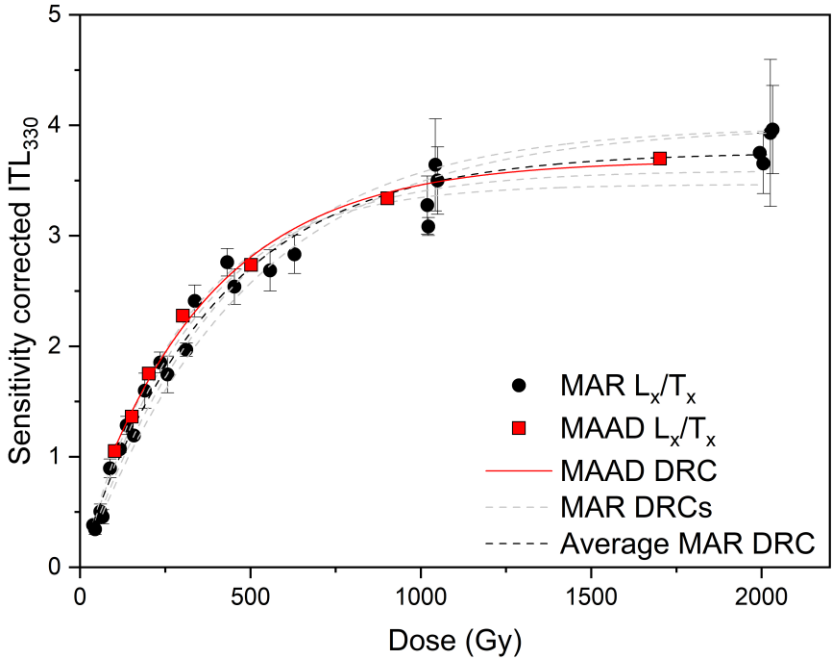

Figure S5.2: Comparison between the average MAR DRC (dashed black line) and MAAD DRC (solid red line). The grey dashed lines represent the individual MAR DRCs for 4 samples.

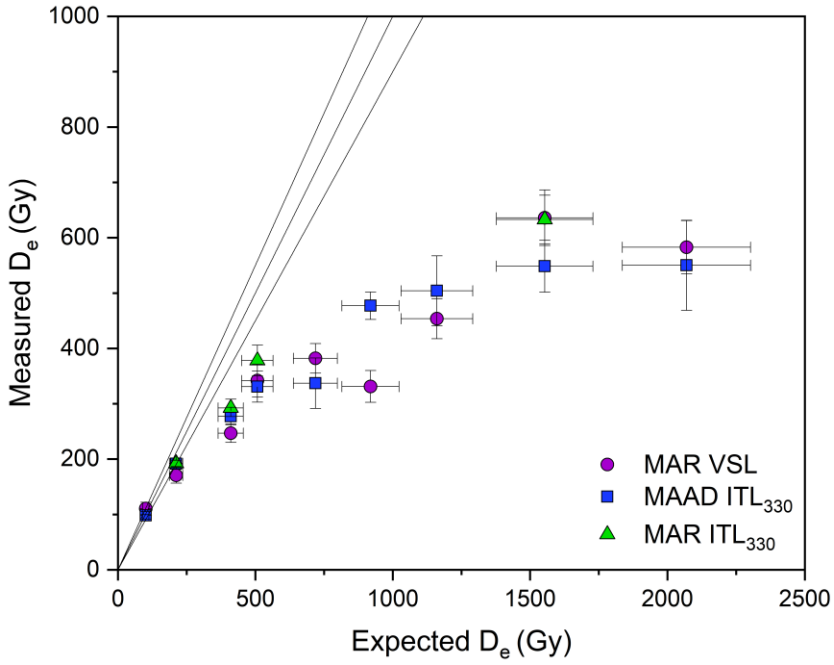

Figure S5.1: Measured MAR (green triangles), MAAD (blue squares) ITL_{330}, and MAR VSL (violet circles) D_e values as a function of the expected D_e values for each sample.

Table S5.1: VSL protocol used in Rahimzadeh et al. (2021).

Step	VSL protocol	Observed
1	Given dose (x Gy)	
2	Preheat (280 °C, 10 s)	
3	Blue bleach (125 °C, 40 s)	
4	VSL (125 °C, 500 s)	L_x
5	Violet bleach (240 °C, 500 s)	
6	Test dose	
7	Preheat (280°C, 10 s)	
8	Blue bleach (125 °C, 40 s)	
9	VSL (125 °C, 500 s)	T_x
10	Violet bleach (240 °C, 500 s)	

CHAPTER 6

Summary and conclusions

6.1 Summary and overall conclusions

The overall aim of this doctoral thesis was to develop and test the applicability of VSL dating to extend the age range of conventional OSL dating to cover the full Quaternary. This research focused on coastal and marine deposits from Sardinia as well as loess deposits from China and Germany. Here the findings of each chapter are summerised.

Since previous attempts (e.g. Ankjærgaard et al., 2016; Colarossi et al., 2018, Ataee et al., 2022) to use the VSL signal with a SAR protocol have had limited success, the first part of this thesis (Chapter 2) aimed to explore SAR VSL protocols and assess the behaviour of the VSL signal under different measurement conditions to establish an optimised SAR protocol. Samples (four coarse-grained quartz) used in this chapter were from the aeolian/foreshore environment of Sardinia, where a comparison of VSL and blue OSL ages is possible due to the low dose rate of carbonate-rich environment. In a first step, dose recovery experiments were conducted on one sample following different protocols used in previous studies (i.e. Ankjærgaard et al., 2013, 2015, 2016; Colarossi et al., 2018) in order to select a suitable SAR protocol. Only the protocol of Colarossi et al. (2018) was successful in recovering dose, however large recuperation of ~15% was observed. Therefore, further experiments on parameters such as violet stimulation temperature, preheat temperature, and violet bleach temperature were carried out to improve the SAR VSL protocol. Laboratory tests of the SAR protocol, i.e., recycling ratio, recuperation, and dose recovery, showed satisfactory performance of the proposed SAR VSL protocol. When the SAR VSL ages compared with reference ages (i.e. blue OSL and pIRIR), it was observed that all measured SAR VSL ages are in agreement with reference ages, except one sample with the largest expected dose of ~320 Gy, for which significant VSL underestimation (~50%) was observed. This underestimation is most likely related to trapping sensitivity change between natural and regenerated VSL signals due to the first preheating in the SAR protocol, which is likely dose dependent. To test whether sensitivity change in the SAR protocol was the reason for this VSL underestimation, the sensitivity corrected MAR protocol was carried out. The MAR VSL ages were in agreement with reference ages in two out of four samples; the other two samples showed overestimation. This overestimation of MAR VSL ages can be explained by incomplete bleaching of the natural VSL signal after 7 days of SOL2 exposure used for the MAR protocol. This was later confirmed by bleaching experiments, which showed that the bleaching behaviour of the VSL signal is

sample dependent for the deposits under investigation. However no definite explanation can yet be given, whether the variations in mineralogical composition as well as the different bleaching histories, or different VSL source trap properties are the source of the different bleaching behaviour amongst samples.

It appears that a SAR-type protocol for VSL is not straightforward to extend the quartz age range (Chapter 2). Making use of an optimised VSL dating protocol, which was established in Chapter 2, thirteen fine-grained quartz samples from the Luochuan section on the Chinese Loess Plateau with depositional ages in the range of 25-1400 ka were dated by MAR procedure (Chapter 3). The homogenous and well-bleached sediments from the Chinese Loess Plateau with the framework of independent age control provide the opportunity to investigate the applicability and reliability of the MAR VSL protocol. In addition, the Luochuan section offers a continuous record of deposition throughout last 2.6 Ma and can therefore be used to construct the natural DRC. The natural DRC indicated that the VSL signal has a theoretical dating range up to ~900 Gy at the Luochuan section, equivalent to ~300 ka. However, the application of the MAR protocol resulted in significant age underestimation beyond ~100 ka. This observed age underestimation cannot attributed to either thermal instability of the VSL signal or bleaching treatment in the MAR protocol, but is related to the different shapes of the natural and laboratory DRCs; they start to diverge in shape after ~250 Gy. Comparison of the natural and laboratory DRCs suggested that there is additional linear growth in the laboratory DRC, which is artificial and does not exist in nature. This result was, however, contradicting the previous study by Ankjærgaard (2019), who showed that the MAR DRC using coarse-grained quartz from the same region (Luochuan) can reproduce the shape of the natural DRC. Based on these observations it was concluded that the grain size can also plays an important role in obtaining reliable ages.

To further confirm these observations from Chapter 3, a direct comparison study between different grain size fractions from the same set of samples was carried out (Chapter 4). Nine fine- (4-11 μm) and coarse-grained (63-100 μm) quartz samples from a loess-palaeosol sequence in southern Germany for the last 160 ka were used for MAR VSL dating. For these samples a luminescence chronology based on blue OSL and fading-corrected $pIRIR_{225}$ ages is available, which was used to test the reliability of the VSL ages and also construct the natural DRC. The comparison of MAR DRCs using regeneration doses up to ~1000 Gy for both grain size fractions showed that they are almost similar in shape with close

characteristic saturation dose values. The estimated VSL ages from both grain size fractions were found to be in agreement with reference ages of >50 ka. However, there was a systematic tendency for the fine-grained VSL ages towards underestimation with increasing age. It was shown that the fine-grained MAR DRC starts to deviate from the natural DRC at ~300 Gy and therefore tends to underestimate the reference ages beyond ~100 ka. The constructed laboratory DRCs to very high doses (~ 6000 Gy) for both grain size fractions confirmed this observation; a continuous growth of the regenerative signal up to high doses was observed, especially for fine-grained quartz. This linear growth component was, however, much less pronounced for coarse-grained quartz, and therefore the coarse-grained quartz can be regarded as more reliable chronometer, especially for dating old samples.

Whilst the previous three chapters focused on the VSL signal, Chapter 5 explored the characteristics of the quartz ITL signal measured at 330 °C and its potential for extending the dating range of quartz. As initially demonstrated by Murray and Wintle (2000), the ITL signal measured at 330 °C (ITL_{330}) can probe deep traps in quartz, i.e. 375 °C TL peak, therefore has the potential to be developed into a dating method that can extend the quartz age range. Chapter 5 aimed at providing additional data on the characteristics of the ITL_{330} signal and investigate the dosimetric usability of the multiple aliquot approaches (e.g. MAR and MAAD) to this signal by using nine fine-grained quartz with ages up to ~700 ka from the Luochuan section. It was demonstrated that the ITL_{330} signal originates from a deep tap at ~1.8 eV with a thermal lifetime of $\sim 10^{10}$ years at 10 °C, and is bleachable by sunlight. The natural ITL_{330} saturates at ~800 Gy, corresponding to an upper age limit of ~230 ka, using a mean dose rate of 3.5 Gy/ka. A comparison of the natural and laboratory generated DRCs (for both MAR and MAAD protocols) demonstrated that they do not overlap, causing large age underestimation beyond ~70 ka. To overcome the issue related to the shape dissimilarity between the natural and laboratory regenerated DRCs, the pulsed-irradiation approach, in which the laboratory irradiation is administered in small pulses with preheat in between, was carried out for MAAD protocol. Application of the pulsed laboratory irradiation appears as a promising method to reduce the differences between the natural and laboratory DRCs; the PI-MAAD protocol can provide reliable ages up to natural saturation at ~230 ka. Furthermore, since both ITL_{330} and VSL signals originate from the same TL peak in quartz, the ITL_{330} data was compared with the VSL dataset of the same samples from Chapter 3 to

investigate whether the ITL_{330} signal can be used as an alternative to the VSL signal. It was demonstrated that both signals have similar characteristics, in terms of kinetic parameters, DRCs, and estimated burial doses; suggesting that both signals might originate from the same trap in quartz, and therefore the ITL_{330} signal can be used as an alternative signal in cases where the especial instrumental facility of violet laser is not available.

The outcome of the four presented research papers enables to make the following main conclusions:

a) Attempts to validate the SAR VSL protocol were not straightforward, despite the improvements achieved in terms of passing the procedural tests of the SAR protocol. It is therefore important to acknowledge the alarming observation that passing all laboratory tests do not guarantee the ability of the SAR protocol to successfully convert natural signals into equivalent doses. The result presented here is in line with previous studies which suggest that the range of applicability for the SAR protocol is dose dependent; the maximum limit has been suggested to be ~200 Gy. Indeed, the main challenge in obtaining correct VSL D_e values lies in the fact that the first high preheating in the SAR VSL procedure induces trapping sensitivity change between the natural and regenerated signals, thereby causing dissimilarity between natural and laboratory SAR DRCs. However, adopting a low preheat is also not possible due to the contribution of other thermally unstable and early saturating traps, i.e. the fast OSL component. Since identifying the optimal preheat temperature which can make a balance between these two phenomena, i.e. isolating a sufficiently stable signal and not affecting the trapping sensitivity of the signal, is difficult, it therefore appears that the application of the SAR procedure for the VSL signal is quite problematic.
b) The multiple aliquot approaches offer a way to circumvent the trapping sensitivity change problem. However the application of the MAR VSL protocol on fine-grained quartz from the Luochuan section also failed to improve burial dose estimation. It was demonstrated that the measurement protocols do not produce a laboratory dose response curve with a similar shape to that of the natural growth, thereby causing age underestimations. Similar observations were also made for the ITL_{330} MAR and MAAD DRCs. Here one would expect that the dissimilarity between natural and regenerated DRCs and subsequently age underestimation is an

inherent feature in quartz, regardless of the measurement protocol applied, and therefore the different shape of natural and SAR VSL DRCs does not caused by trapping sensitivity change induced by high preheating. However, the study of Ankjærgaard (2019), who tested multiple aliquot methods on coarse-grained quartz from the same region, demonstrated that it is possible to reproduce the shape of the natural DRC with multiple aliquot methods. Therefore, the growth pattern of laboratory generated DRC seems to be linked to the used grain size. Further investigation of the VSL dose response patterns of different grain sizes of quartz confirmed these observations; for the fine-grained quartz there is an additional linear component in the high dose region, which does not exist in nature. Therefore for dating old samples with equivalent doses falling on the high dose region of the DRC, preference should be given to the coarse-grained quartz as a dosimeter.

c) Despite the unsuccessful application of the multiple aliquot methods on fine-grained quartz, it is encouraging that the natural DRC of both VSL and ITL_{330} signals saturate at ~800 Gy when fitting the DRCs with a single saturating exponential function. This growth suggests that both signals would enable dating up to ~230 ka at the Luochuan section, and possibly even older samples in other low dose rate environments. This natural growth can be reproduced by a pulsed-irradiation approach; thus it appears to be a promising step forward in our attempts to extend the dating range of quartz.

d) In luminescence laboratories where the violet laser facility is not available, the ITL_{330} signal can be used as an alternative to the VSL signal. It was demonstrated that both signals have similar characteristics, In terms of kinetic parameters, natural DRCs, and estimated burial doses, suggesting that both signals might originate from the same trap in quartz. Therefore, the ITL_{330} signal can become a promising alternative to the VSL signal, which does not need special instrumental facility for measurement.

6.2 Potential future directions

As summarised in the previous section (6.1), the result of this thesis further improves our current understanding of the dosimetric potential of other luminescence signals from quartz, i.e. VSL and ITL_{330}, as a means to extend the dating range of quartz. However, open or new questions still remain for further investigations. In the following, the most important of these questions are addressed.

Further investigations on the bleaching behaviour of the VSL signal

As shown in Chapter 2, attempts to use the SAR-type protocol for VSL were not successful, therefore the multiple aliquot methods, i.e. MAAD and MAR, seem to be a promising approach in VSL dating. Since the MAAD method requires a modern sample that should be analogue to the environmental conditions of the older one, which might not be always available, the MAR approach appears to be the most applicable method. However, in the MAR protocol, it is necessary to remove the dosimetric signal before the irradiation. It, therefore, becomes important to consider what an appropriate bleaching treatment and duration is. This thesis however has shown that the bleaching behaviour of the VSL signal is sample dependent, and therefore the application of the MAR method is quite complicated in heterogeneous environments. The question arises if variable bleaching behaviour among different samples is related to measuring samples with different bleaching histories, mineralogical compositions, or VSL source trap properties. A full explanation of the mechanisms behind it requires detailed investigations in terms of bleaching behaviour and mineralogical composition.

The upper applicability limit of fine-grained quartz for accurate VSL dating

The continuous growth of regenerative signals at higher doses for the fine-grained quartz (Chapters 3 and 4) resulted in the suggestion that the fine-grained quartz cannot be considered as reliable chronometer for dating old samples with expected D_e in the high dose range. However, further detailed investigation is needed to conclude a clearly defined high dose range. This is of great importance for dating loess deposits where the fine grains have been (and will be) the preferred material.

Further investigations on the pulsed-irradiation procedure

It has been shown that the shape of the natural ITL_{330} dose response curve can be reproduced with a pulsed-irradiation MAAD approach up to the limit of the natural saturation, which subsequently resulted in providing reliable ages up to ~230 ka (Chapter 5). However, in this thesis no detailed investigation was carried out to evaluate different pulsed irradiation conditions (i.e. thermal treatment and pulse dose). Of great importance in future studies will be investigations to further explore the impact of the repeated pulsed irradiation and heating upon the signal and also determine the optimal pulsed irradiation conditions. Furthermore, the application of the pulsed-irradiation procedure was only tested here for the ITL_{330} MAAD DRC. This would be particularly interesting to test the performance of this method on different signals of quartz (i.e. OSL and VSL) and measurement protocols.

References

Ankjærgaard, C., Jain, M., Wallinga, J., 2013. Towards dating Quaternary sediments using the quartz Violet Stimulated Luminescence (VSL) signal. Quat. Geochronol. 18, 99–109.

Ankjærgaard, C., Guralnik, B., Porat, N., Heimann, A., Jain, M., Wallinga, J., 2015. Violet stimulated luminescence: geo-or thermochronometer? Radiat. Meas. 81, 78-84.

Ankjærgaard, C., Guralnik, B., Buylaert, J.-P., Reimann, T., Yi, S.W., Wallinga, J., 2016. Violet stimulated luminescence dating of quartz from Luochuan (Chinese loess plateau): agreement with independent chronology up to ~600 ka. Quat. Geochronol. 34, 33-46.

Ankjærgaard, C., 2019. Exploring multiple-aliquot methods for quartz violet stimulated luminescence dating. Quat. Geochronol. 51, 99-109.

Ataee, N., Roberts, H.M., Duller, G.A.T., 2022. Isolating a violet stimulated luminescence (VSL) signal in quartz suitable for dating: Investigating different thermal treatments and signal integration limits. Radiat. Meas. 156, 106810.

Colarossi, D., Chapot, M.S., Duller, G.A., Roberts, H.M., 2018. Testing single aliquot regenerative dose (SAR) protocols for violet stimulated luminescence. Radiat. Meas. 120, 104-109.

Murray, A.S., Wintle, A.G., 2000. Application of the single-aliquot regenerative dose protocol to the 375 °C quartz TL signal. Radiat. Meas. 32, 579-583.